Varian User Meeting, Taichung, June 13, 2006

Some Recent Progress of Solid State NMR Spectroscopy (and Micro-Imaging)：Methodologies and Applications

國立中山大學化學系
丁尚武
Shangwu Ding
Department of Chemistry,
National Sun Yat-sen University

Contents

- Summary of Technical Development:
  - CPMAS
  - Heteronuclear Decoupling
  - Homonuclear Decoupling
  - Recoupling (CSA and Dipolar)
  - MQMAS, STMAS, SPAM, Exchange etc
- Examples of Applications:
  - Materials
  - Biological Systems
- Micro-Imaging with NMR

The talk may contain contents that are not included in your proceedings. To request a full size ppt file of this lecture, contact the speaker at ding@mail.nsysu.edu.tw.

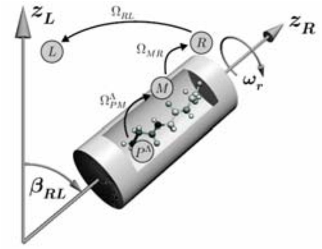

Magic Angle Spinning (MAS)

Andrew

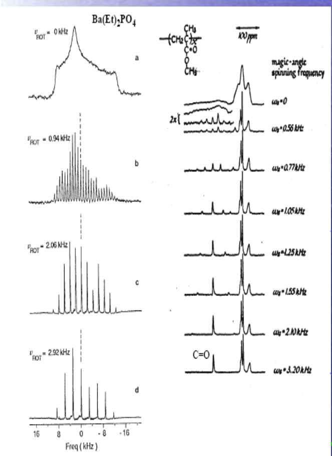

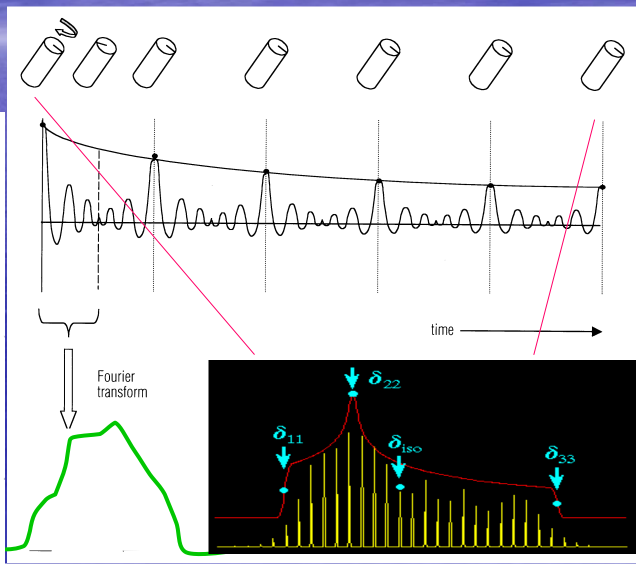

Truly MA ($\Delta\ \theta$ <0.001°)

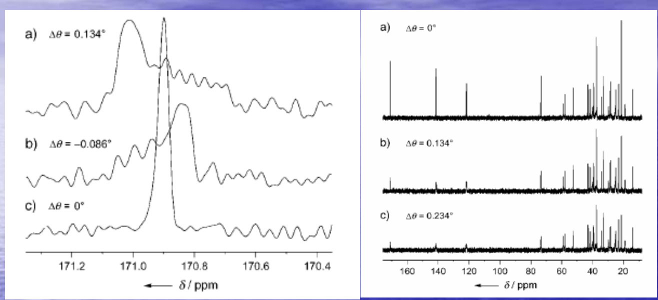

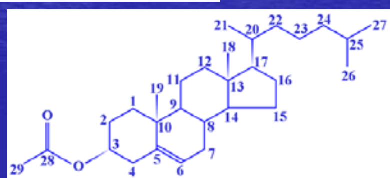

Sasa Antonijevic and Geoffrey Bodenhausen, Angew. Chem. Intl. Ed. 44,2935(2005)

Truly MA

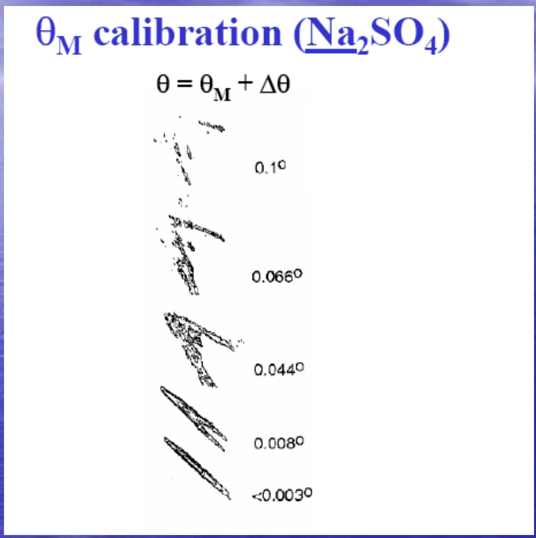

C. Huguenard, F. Taulelle, Z.H. Gan, J. Magn. Reson, 156, 131, **2002**.

Truly Stable Spinning

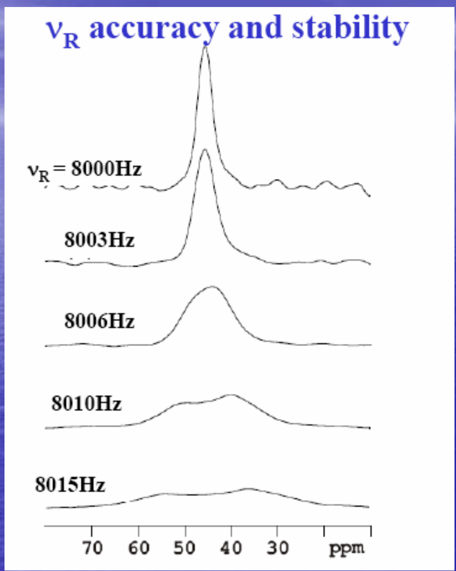

J.P. Amoureux, L. Delevoye, G. Fink, F. Taulelle, A. Flambard, L. Montagne, J. Magn. Reson, 175, 285, **2005**.

Truly (?) High Speed

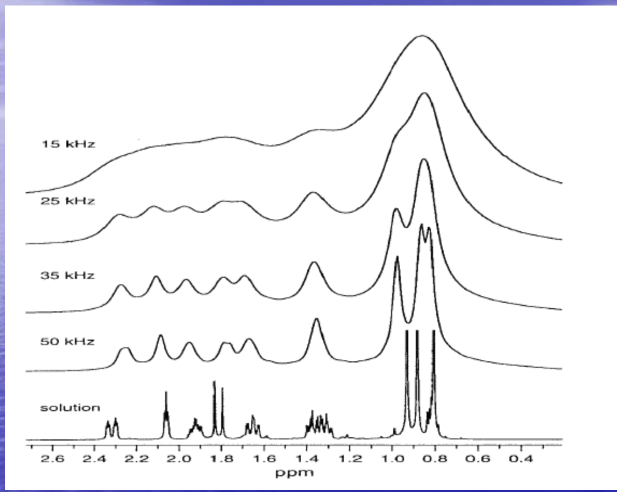

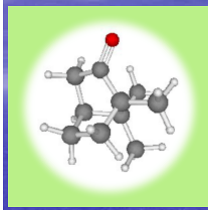

^1H MAS of camphor

A. Samoson, Encyclopedia of NMR, 2ndedition,J. Wiley & Sons, 142,**2002.**

Jakobsen Lab

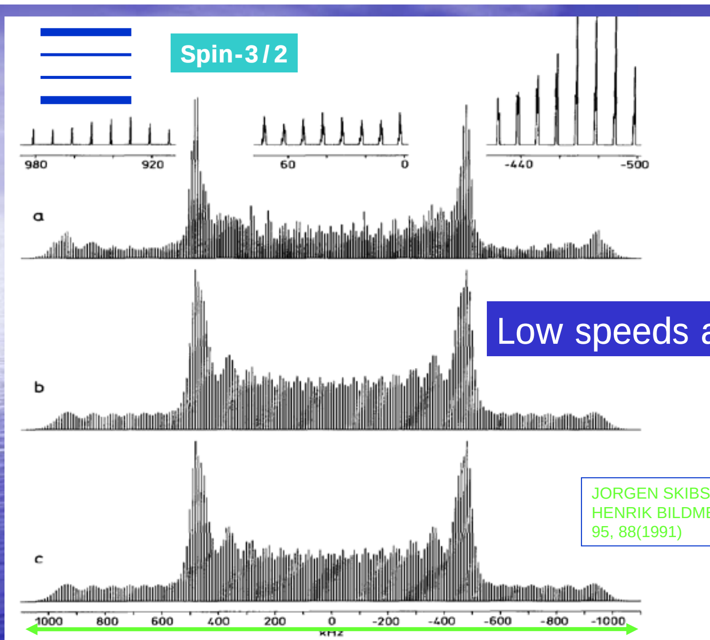

IG. 1. Simulated MAS NMR spectra of the satellite transitions for a spin-$I = \frac{3}{2}$ nucleus using $C_Q = 2.0$ Iz, $\eta = 0.0$, $\nu_r = 10$ kHz, and $\nu_L = 105.8$ MHz (^{23}Na at 9.4 T). The calculations include (a) $\omega_Q^{(1)}(t)$ and erms for $\omega_Q^{(2a)}(t)$, (b) $\omega_Q^{(1)}(t)$ and the time-dependent terms of $\omega_Q^{(2a)}(t)$, and (c) $\omega_Q^{(1)}(t)$ only. The lineshape he individual ssb's in (a), caused by the time-independent terms of $\omega_Q^{(2)}(t)$, is clarified in the expansions.

Low speeds are still useful

JORGEN SKIBSTED, NIELS CHR. NIELSEN, HENRIK BILDME, HANS J. JAKOBSEN, JMR, 95, 88(1991)

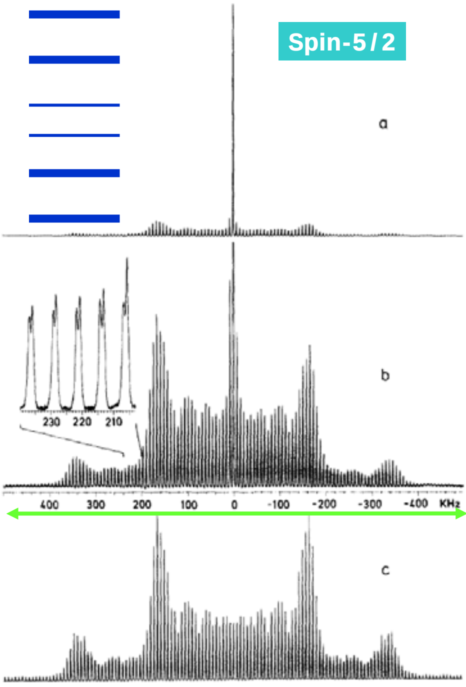

Jakobsen Lab

7AI (104.2 1 MHz) MAS NMR spectra of the entral and satellite transitions for α-Al2O3. The pm scale is referenced to an external sample of .0 M AlCl3, in H2O. (a) Experimental spectrum howing the relative intensities of the central and atellite transitions and observed using a Varian XR-400 S wideline spectrometer; ω_r= 7525 Hz, pectral width SW = 1 .0 MHz, pulse width pw = 1 .0 μ s (π /4 solid pulse), and number of transients t= 5 12. (b) Spectrum in (a) with the vertical scale xpanded by a factor of ten; the inset shows xpansion of a region where the second-order uadrupolar shift between the (±5/2, ±3/2) and the ±3/2, ±1/2) satellite transitions is clearly observed see text). (c) Simulated MAS spectrum for the atellite transitions in (b) obtained using QCC = .38 MHz, η = 0.00, ω_r= 7525 Hz, and Gaussian newidths of 900 and I 175 Hz for the (±3/2, ±1/2) nd (±5/2, ±3/2) transitions. respectively.

HANS J. JAKOBSEN, JORGEN SKIBSTED, HENRIK BILDSBE, ANDNIELS CHR .NIELSEN,JMR 85,173(1989)

^{51}V MAS (H_Q+H_{CSA})

Jakobsen Lab

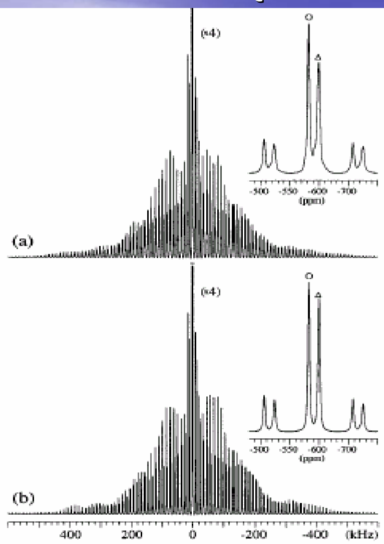

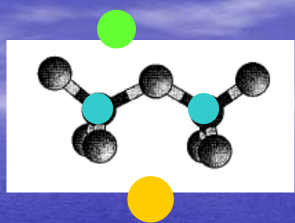

Ulla Gro Nielsen, Hans J. Jakobsen, and Jørgen Skibsted, J Phys Chem B 105,420(2001)

Figure 8. (a) ^{51}V MAS NMR spectrum (14.1 T, ν_r = 12.0 kHz) of the central and satellite transitions for $BaCaV_2O_7$. (b) Optimized simulation of the two manifolds of ssbs in part a using the ^{51}V data for the two ^{51}V sites of $BaCaV_2O_7$ in Table 1 and an intensity ratio of 1:1 for the two manifolds of ssbs. The insets illustrate the spectral region for the central transitions, where the isotropic peaks are indicated by circles (V(1)) and triangles (V(2)).

$BaCaV_2O_7$	V(1)	2.57 ± 0.07	0.32 ± 0.02	100 ± 2	0.65 ± 0.11	82 ± 28	38 ± 7	90^d	−581.6 ± 0.5
	V(2)	3.20 ± 0.06	0.85 ± 0.02	99 ± 3	0.49 ± 0.20	95 ± 28	27 ± 16	90 ± 35	−598.8 ± 0.5

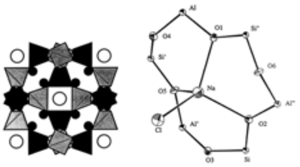

26 January 2001

ELSEVIER

Chemical Physics Letters 333 (2001) 413–418

CHEMICAL PHYSICS LETTERS

www.elsevier.nl/locate/cplett

High resolution ^{23}Na and ^{27}Al NMR satellite transition spectroscopy (SATRAS) of natural sodalite ($Na_8Cl_2(AlSiO_4)_6$) under magic-angle-spinning

Shangwu Ding, Charles A. McDowell *

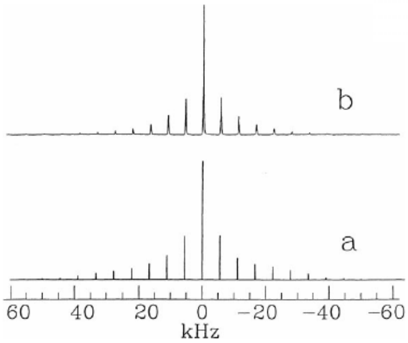

Fig. 2. The experimental (a) and simulated (b) ^{23}Na SATRAS NMR spectra of polycrystalline blue sodalite in a magnetic field of 4.7 T.

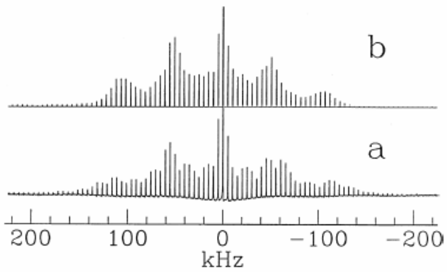

Fig. 3. The experimental (a) and simulated (b) ^{27}Al SATRAS spectra of polycrystalline blue sodalite in a magnetic field of 9.4 T.

The quadrupolar and chemical shift interaction parameters evaluated from simulation of the ^{23}Na and ^{27}Al SATRAS NMR spectra of blue sodalite

Site	C_Q	η_Q	δ_{CS} (ppm)	η_{CS}	α_{CS-Q}	γ_{CS-Q}	β_{CS-Q}
^{23}Na	81 ± 5.0 kHz	0.35 ± 0.05	95 ± 5.0	0.95 ± 0.5	5 ± 12.0	75 ± 30.0	23 ± 10.0
^{27}Al	1.45 ± 0.1 MHz	0.1 ± 0.05	40 ± 5.0	0.7 ± 0.1	30 ± 15.0	50 ± 12.0	10 ± 15.0

Cross polarization (CP) and CPMAS

Pines **Schaefer**

β-carotene

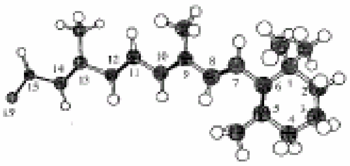

^{13}C CP/MAS NMR

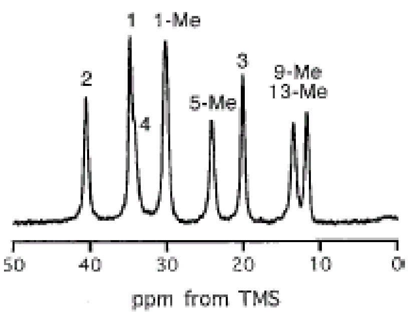

Pulse sequence:

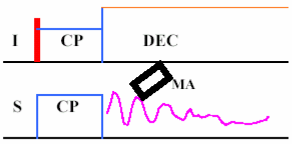

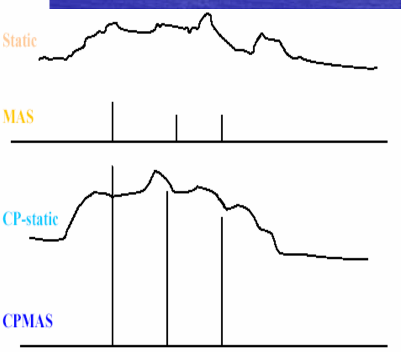

Ramp CP, Adiabatic CP etc (Matching Condition Satisfied at High Speeds)

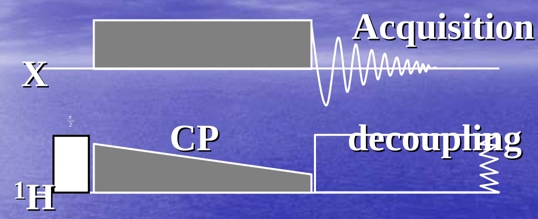

Metz, G., X. Wu, and S.O. Smith. J. Magn. Reson. 1994, 110,219

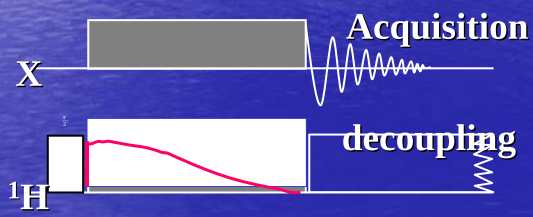

Hediger, S., B.H. Meier, N.D. Kurur, G. Bodenhausen, and R.R. Ernst, Chem Phys Lett, 1994, 223, 283.

Comparison of standard and ramp-CP

Carbonyl-signal of glycine (nat. abundance), ν_{rot} = 20 kHz, as function of ^{1}H-power

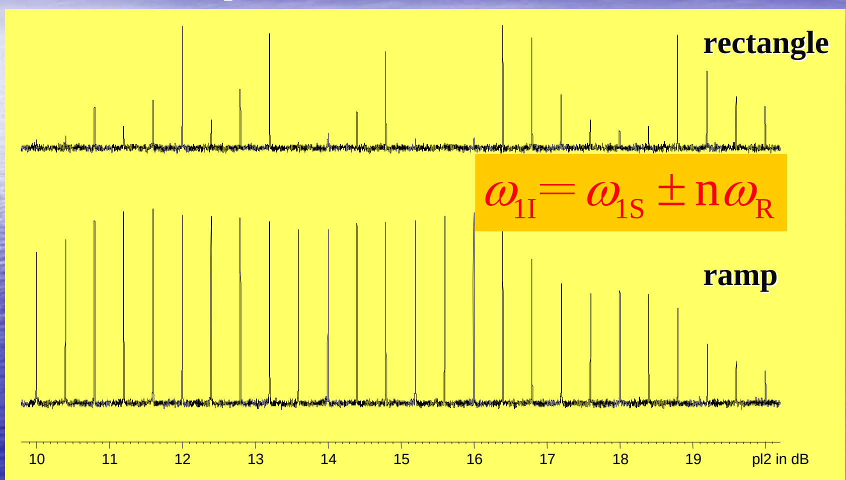

Double-CP

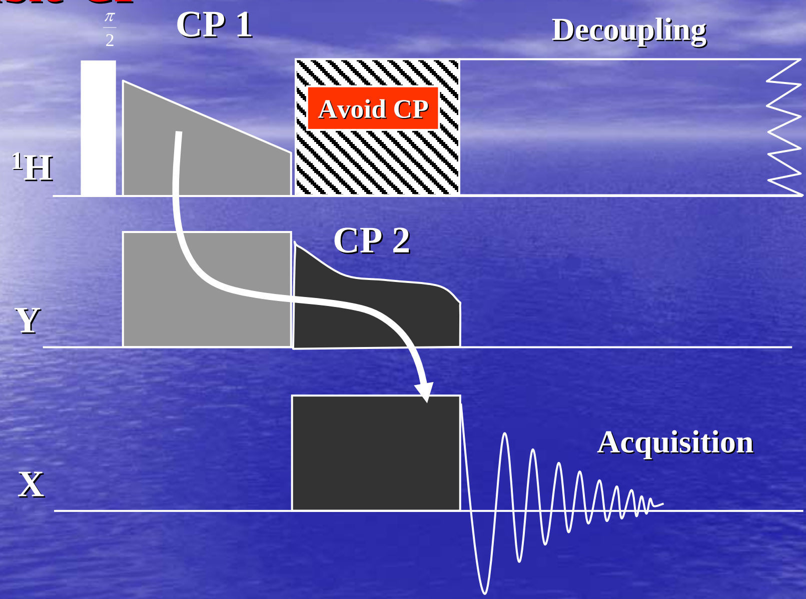

Schaefer, J., Stejskal, E. O., Garbow, J. R., McKay, R. A. *J. Magn. Reson. 59*, 150 (1984).

de Groot Lab

H-N-C Double- CPMAS: Spectral Simplification

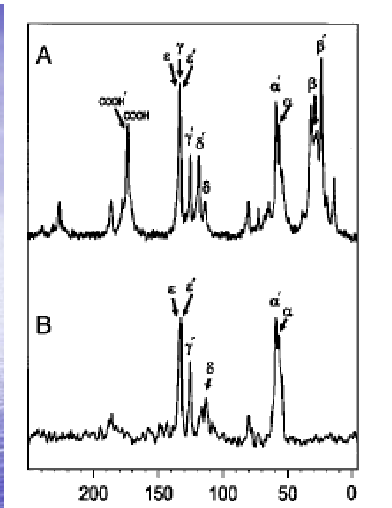

(A) CP-MAS 13C NMR spectrum and (B) 15N-13C double-CP/MAS NMR data of the [13C6,15N3]-His labeled LH2 complex, measured at 220 K by using a wide-bore 750 NMR spectrometer. The spinning rate around the magic angle was kept at 12 kHz. Each spectrum represents about 156 000 scans collected with an acquisition time of 8 ms and a recycle time of 2 s. The spectra are normalized at the α' peaks.

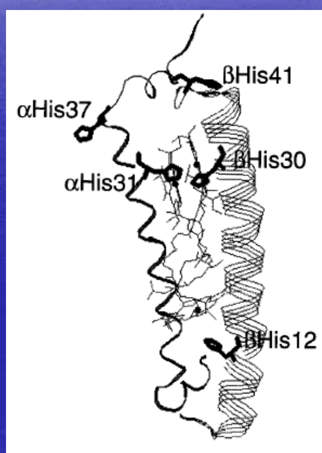

de Groot et al., JACS 123,4203(2001).

CP and HETCOR between Quadrupolar Spins

^{11}B-{^{27}Al} CP-HETCOR NMR spectrum

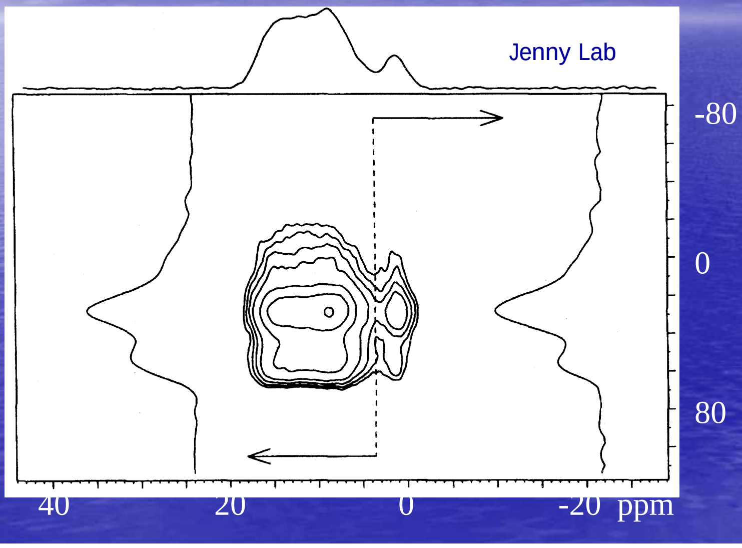

Decoupling Sequences

- Heteronuclear decoupling:
  CW
  TPPM
  XiX
  CM
  COMORO
  SPINAL
  SDROOPY,eDROOPY,DUMBO, eDUMBO, eDUMBO$_{lk}$
- Homonuclear decoupling
  WAHUHA
  Lee-Goldburg (LG and variants: FSLG, PMLG,wPMLG)
  MREV-8
  BR-24
  BLEW-12
  CORY-24
  TREV-8
  MSHOT-3
  DUMBO, eDUMBO, eDUMBO$_{lk}$,
  CNn^{v}, RNn^{v}

Decoupling sequences: TPPM

TPPM = *T*wo *P*ulse *P*hase *M*odulation

Griffin Lab

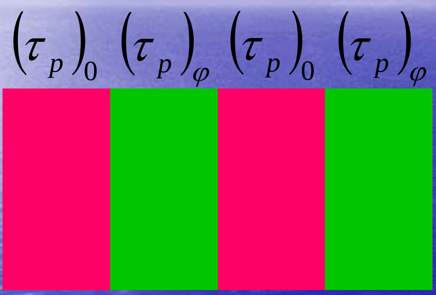

Pulse length: $\tau_p \approx \tau_\pi$ - ε: ε ≈ 0 – 0.6 μs, optimize!

Phaseshift: $\varphi \approx 15^\circ$, evt. optimize!

TPPM- decoupling, optimize t_p

Griffin Lab

C_α-signal in Glycine-2-^{13}C-^{15}N, ν_{rot}= 30 kHz, φ = 15°

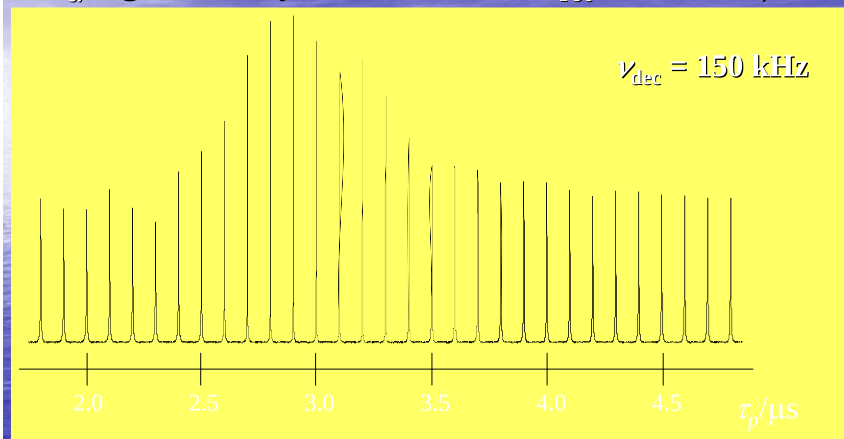

optimum pulse length: τ_p = 2.9 μs, (τ_π= 3.2 μs)

XiX - decoupling

Meier Lab

XiX= X Inverse X

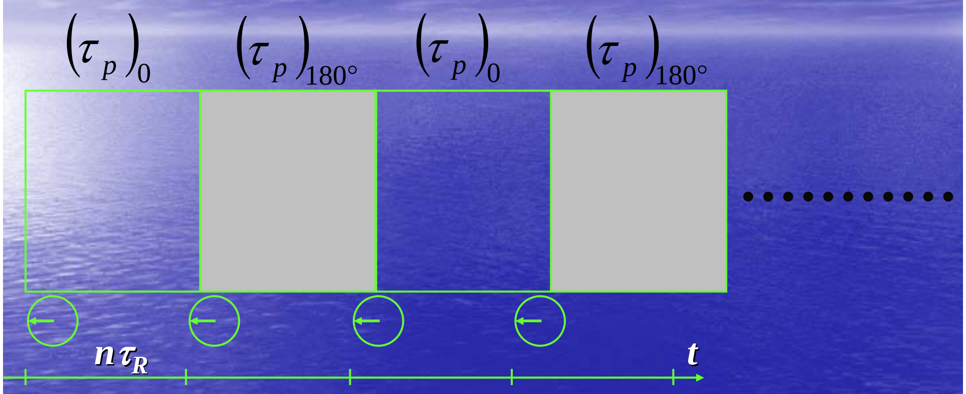

Pulse length: $\tau_p = x \cdot \tau_R$, $x \approx n$, but $x \neq n$, ...
(recoupling at $(n/4)\tau_R$) optimize!

XiX- decoupling, optimize τ_p

Meier Lab

C_α-signal of glycine-2-^{13}C-^{15}N, ν_{rot}= 30 kHz,

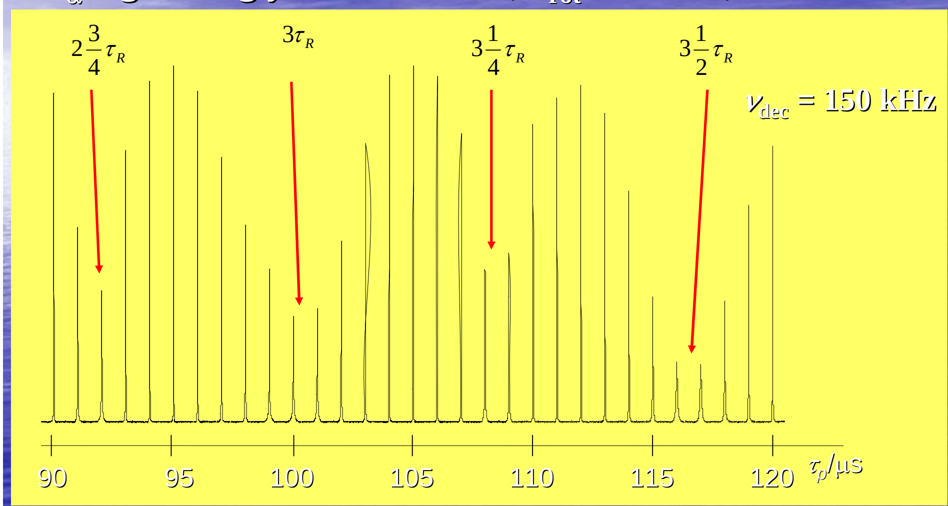

Comparison of decoupling methods

C_α-signal of glycine-2-^{13}C-^{15}N, ν_{dec} = 150 kHz

Meier Lab

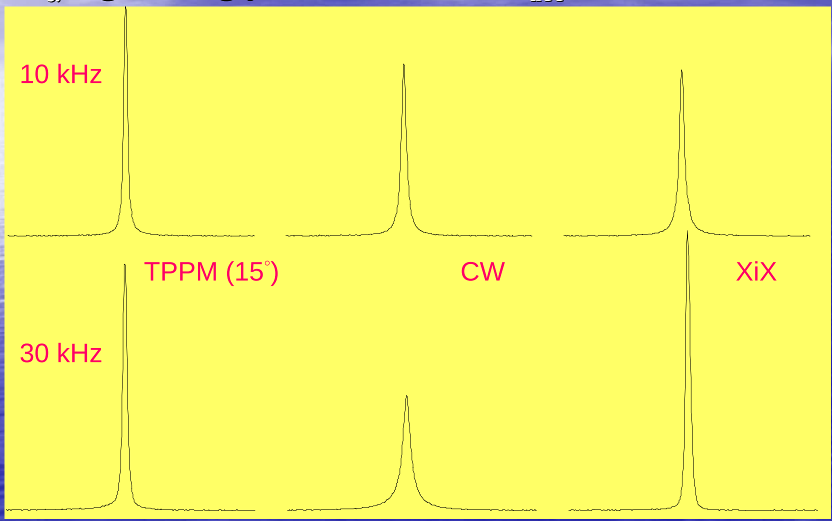

Decoupling methods: π -pulse decoupling

Rotorsynchronised train of 180°-pulses
xy-16-phase cycle for large band width

Meier Lab

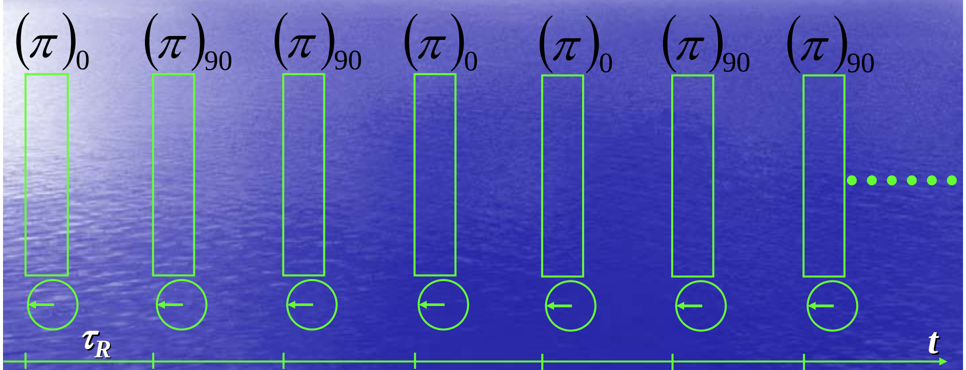

xy-16-phase cycle: 0–90–90–0–0–90–90–0–180–270–270–180–180–270–270–180

π -pulse decoupling for ^{19}F

^{19}F: Dipol-Dipol-coupling spun out at fast rotation
but: large chemical shift anisotropy
⇒ large band width important

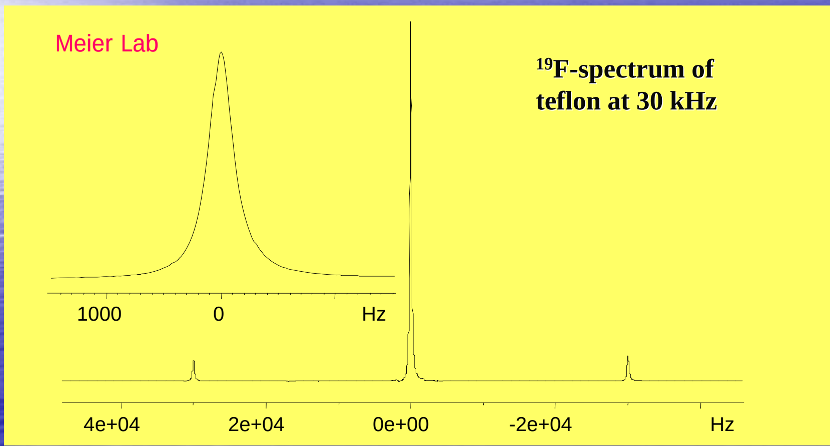

π -pulse-decoupling for ^{19}F

$^{13}C\{^{19}F\}$-CP/MAS-spectrum of Teflon, ν_{rot}= 30 kHz

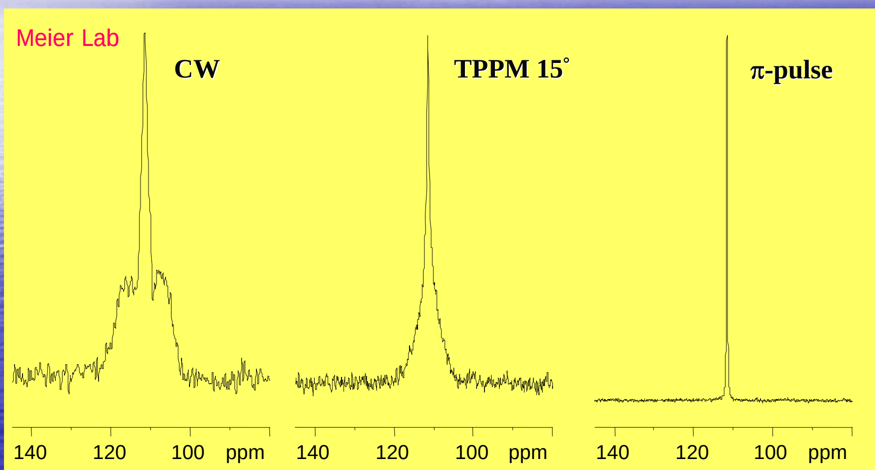

Pulsed (homonuclear) decoupling

WAHUHA
Lee-Goldburg (LG and variants: FSLG, PMLG, wPMLG)
MREV-8
BR-24
BLEW-12
CORY-24
TREV-8
MSHOT-3
DUMBO, eDUMBO, $eDUMBO_{lk}$,
CNn^{v}, RNn^{v}

Lee-Goldburg (LG) Series

LG: Magic-angle-spinning in spin space (Magic Sandwich)

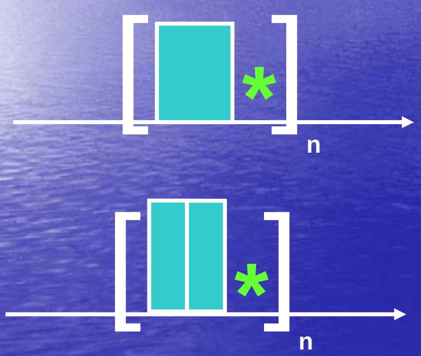

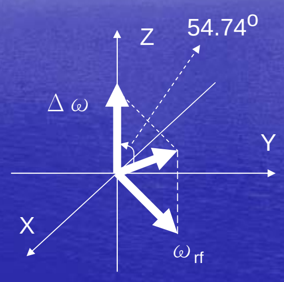

$$\omega_{rf} = \omega_1 \cos(\omega t_p + \varphi)$$

Frequency-Switched LG (windowed) Phase-Modulated LG

TREV-8

Takegoshi & McDowell

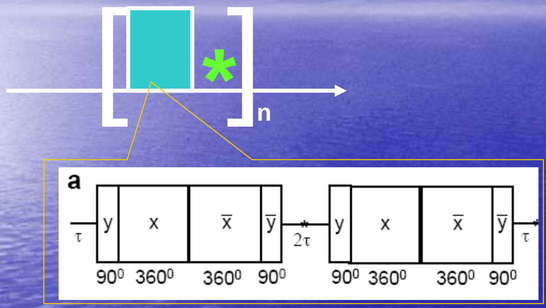

MSHOT

(Magic Sandwich High Order Terms Decoupling)

Nielsen Lab

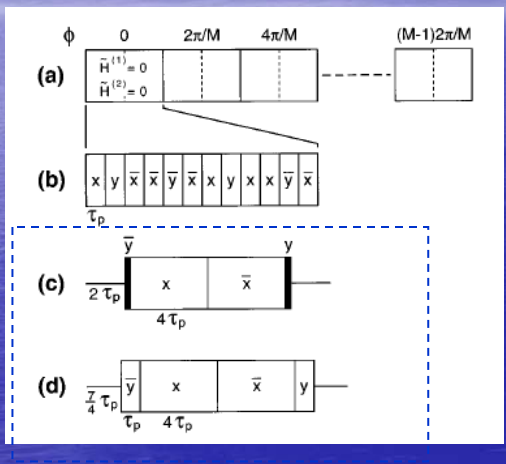

MSHOT

Nielsen Lab

M. Hohwy and N. C. Nielsen, *J. Chem. Phys.* **106**, 7571 (1997).
M. Hohwy, P. V. Bower, H. J. Jakobsen, and N. C. Nielsen, *Chem. Phys. Lett.* **273,** 297 (1997)
M. Hohwy, J. T. Rasmussen, P. V. Bower, H. J. Jakobsen, N. C. Nielsen *J. Magn. Reson.* **133**,374(1998).

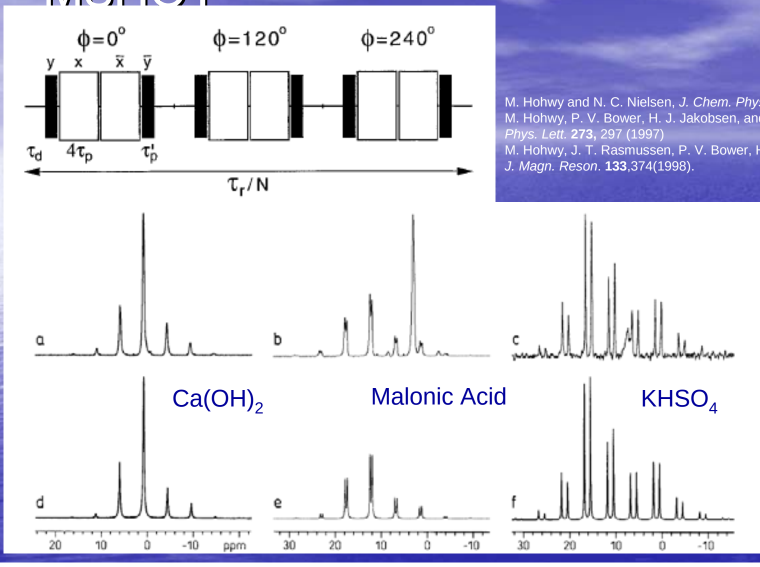

^{1}H CRAMPS (400 MHz) spectra of (a, d) $Ca(OH)_2$ ($\omega_r/2\pi$ = 710 Hz, N = 15, 16-s relaxation delay, 128 scans), (b, e) malonic acid ($\omega_r/2\pi$ = 751 Hz, N = 14, 128-s relaxation delay, 16 scans), and (c, f) $KHSO_4$ ($\omega_r/2\pi$ = 697 Hz, N = 15, 128-s relaxation delay, 16 scans; the low sensitivity in the experimental spectrum is ascribed to extremely long T_1 values). (a–c) Experimental spectra. (d–f) Simulations obtained by iterative fitting of the experimental spectra in (a–c) and corresponding to the chemical shielding parameters in Table 1. The effect of MSHOT-3 decoupling was taken into consideration by scaling the chemical shift terms by a factor of 0.352.

MSHOT-3-CRAMPS (combination of rotation and multi-pulse spectroscopy

Emsley Lab

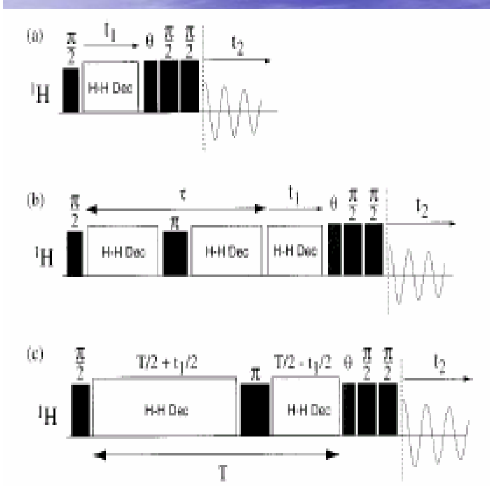

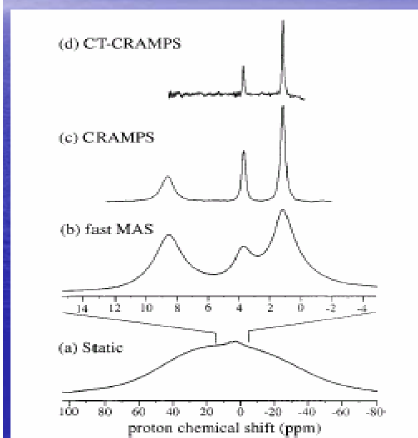

Anne Lesage, Luminita Duma, Dimitris Sakellariou, and Lyndon Emsley *J. Am. Chem. Soc.* **2001**, *123*, 5747−5752

PMLG, wPMLG

Vega Lab

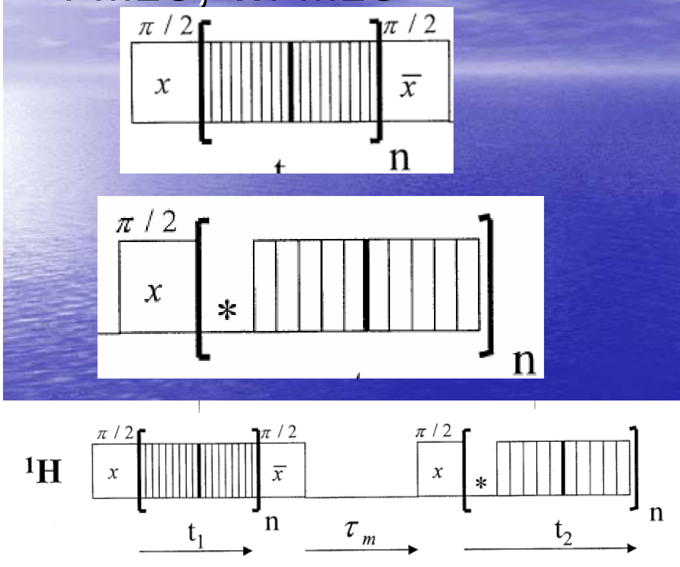

wPMLG: Example

Vega Lab

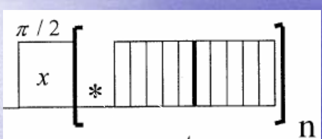

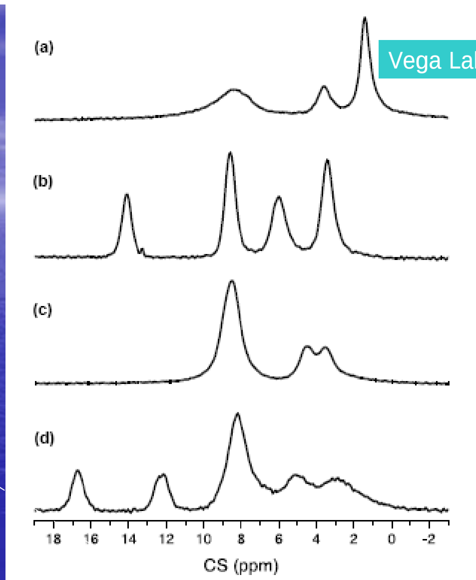

The one-dimensional proton spectra of (a) U–15N–DL-alanine, (b) monoethyl fumarate, (c) glycine and (d) U–13C –15N–histidineHClH$_2$O, detected during wPMLG-5 at a spinning frequency of 14.3 kHz and a Larmor frequency of 300 MHz. The length of the detection windows was 3.2 μs and that of the PMLG pulses was 1.7 μs.

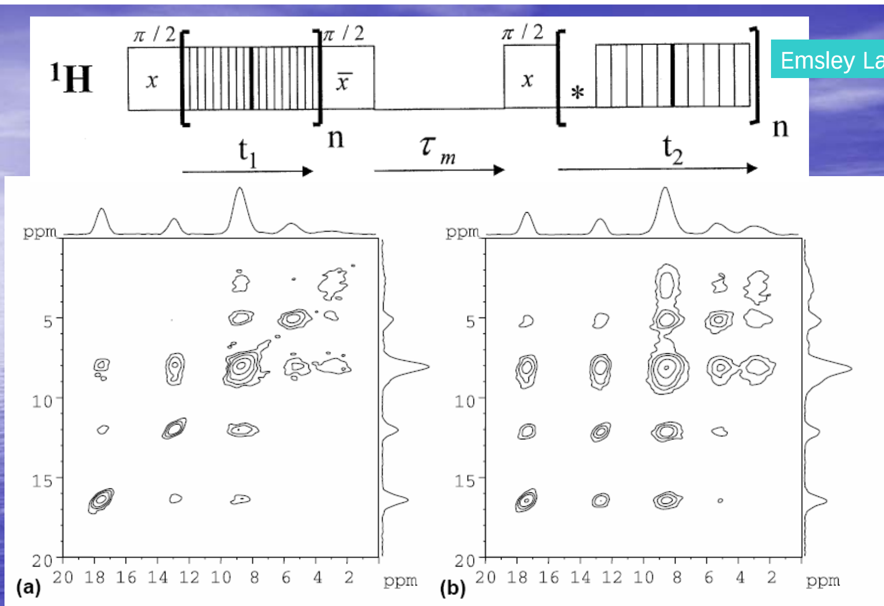

Emsley Lab

2D proton–proton correlation spectra of U–13C–histidineHClH2O, obtained using the pulse sequence shown at the top, with mixing times of (a) 200 μs and (b) 500 μs. The F1 (vertical) and F2 (horizontal) proton spectra are skyline projections of the 2D spectra. These experiments were performed at a spinning frequency of 14.286 kHz and a Larmor frequency of 300 MHz. During the PMLG-9 and wPMLG-5 irradiation the pulse lengths were 1.1 and 1.7 μs, respectively. The length of the detection windows during wPMLG-5 was 3.2 μs.

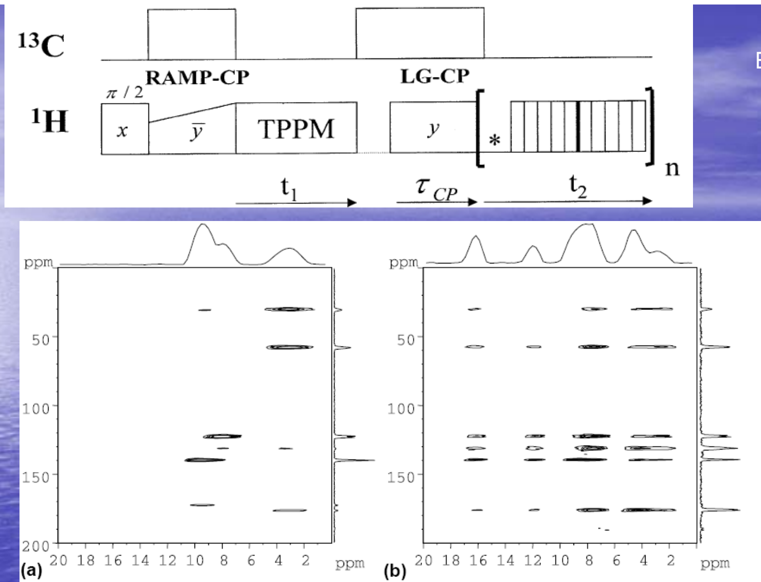

Emsley Lab

2D carbon–proton correlation spectra of U–13C–histidineHClH2O, obtained using the pulse sequence shown at the top, with Lee–Goldburg CP mixing times of (a) 80 μs and (b) 3 ms. The F1 (vertical) carbon and F2 (horizontal) proton spectra are skyline projections of the 2D spectra. These experiments were performed at a spinning frequency of 14.286 kHz and a Larmor frequency of 300 MHz. During the wPMLG-5 irradiation the pulse lengths were 1.7 μs and the length of the detection windows was 5.1 μs.

Pulsed (homonuclear) decoupling (WAHUHA (WHH4), MREV-8)

Waugh Lab

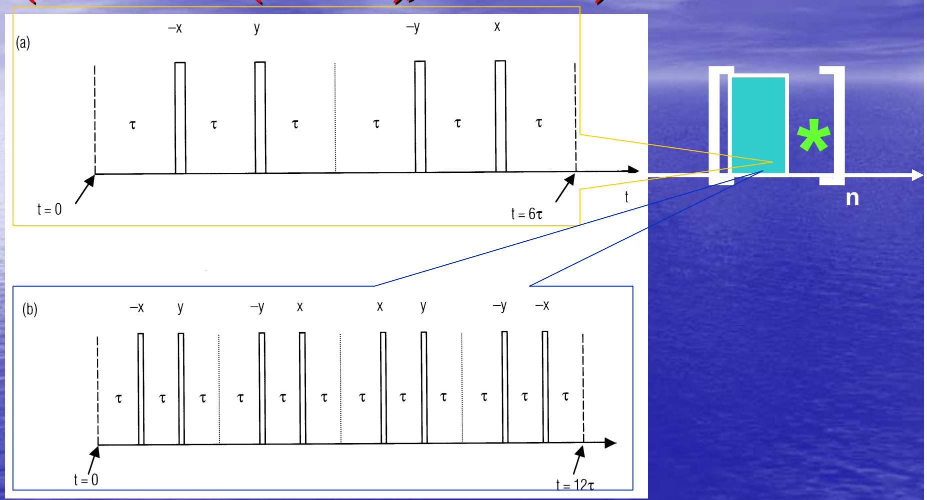

P. MANSFIELD, M. J. ORCHARD, D. C. STALKER, AND K. H. B. RICHARDS, Phys. Rev. B 7, 90 (1973).
W. K. RHIM, D. D. ELLEMAN, AND R. W. VAUGHAN, .I. Chem. Phys. 59, 3740 (1973).
W. K. RHIM, D. D. ELLEMAN, L. B. SCHREIBER, AND R. W. VAUGHAN, J. Chem. Phys. 60, 4595 (1974).

Burum Lab

BR-(24,48,52)

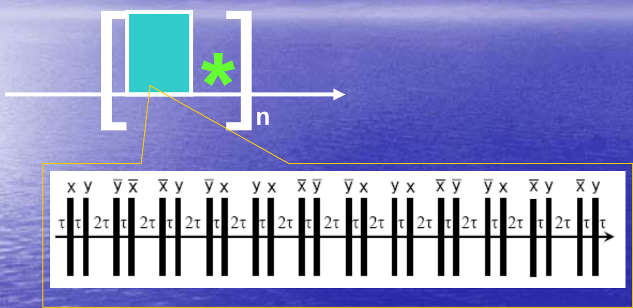

D. P. Burum and W. K. Rhim, J. Chem. Phys. **70**, 3553 (1979); a powder spectrum for ice was also reported using REV-8: L. M. Ryan, R. C. Wilson, and B. C. Genstein, Chem. Phys. Lett. **52**, 341 (1977).
D. P. Burum and W. K. Rhim, J. Magn. Reson. **34**, 241 (1979).
D. P. BURUM AND W. K. RHIM, J. Chem. Phys. 71, 944 (1979).

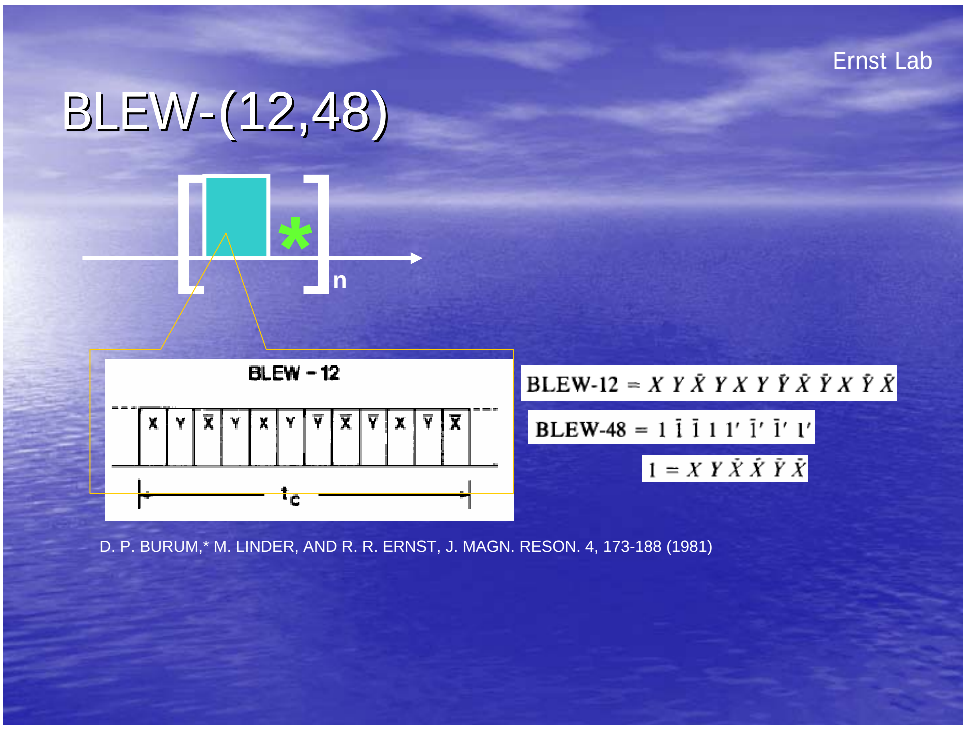
Ernst Lab
BLEW-(12,48)
n
BLEW - 12
X Y X̄ Y X Y Ȳ X̄ Ȳ X Ȳ X̄
t_c
BLEW-12 = X Y X̄ Y X Y Ȳ X̄ Ȳ X Ȳ X̄
BLEW-48 = 1 1̄ 1̄ 1 1′ 1̄′ 1̄′ 1′
1 = X Y X̄ X̄ Ȳ X̄
D. P. BURUM,* M. LINDER, AND R. R. ERNST, J. MAGN. RESON. 4, 173-188 (1981)

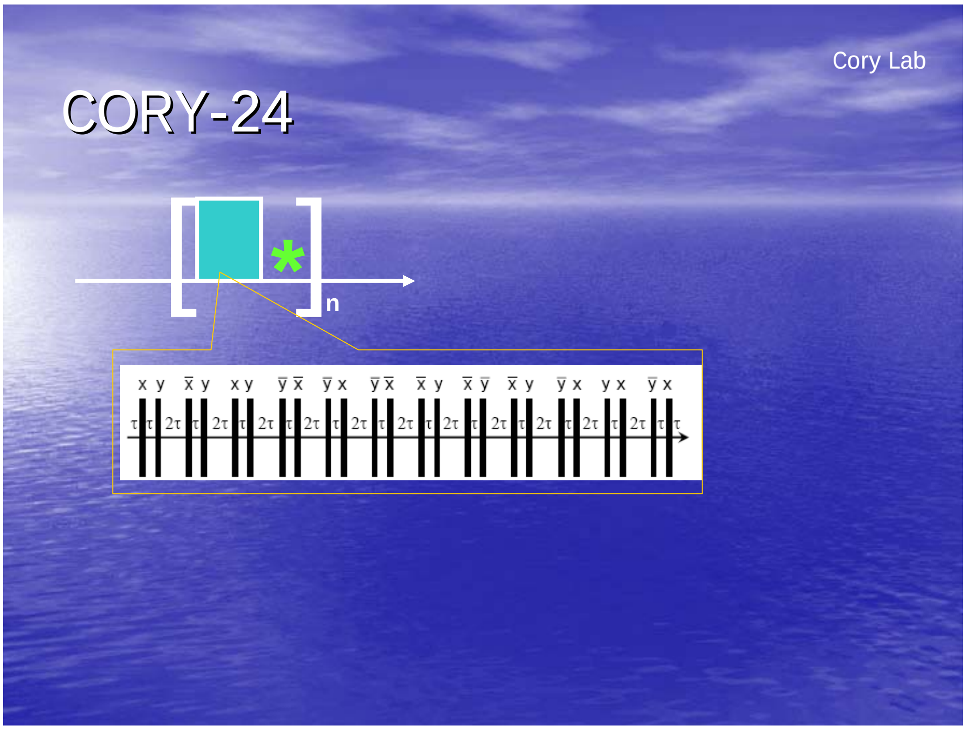
Cory Lab
CORY-24
n
x y x̄ y x y ȳ x̄ ȳ x ȳ x̄ x̄ y x̄ ȳ x̄ y ȳ x y x ȳ x
τ τ 2τ τ 2τ τ 2τ τ 2τ τ 2τ τ 2τ τ 2τ τ 2τ τ 2τ τ 2τ τ 2τ τ

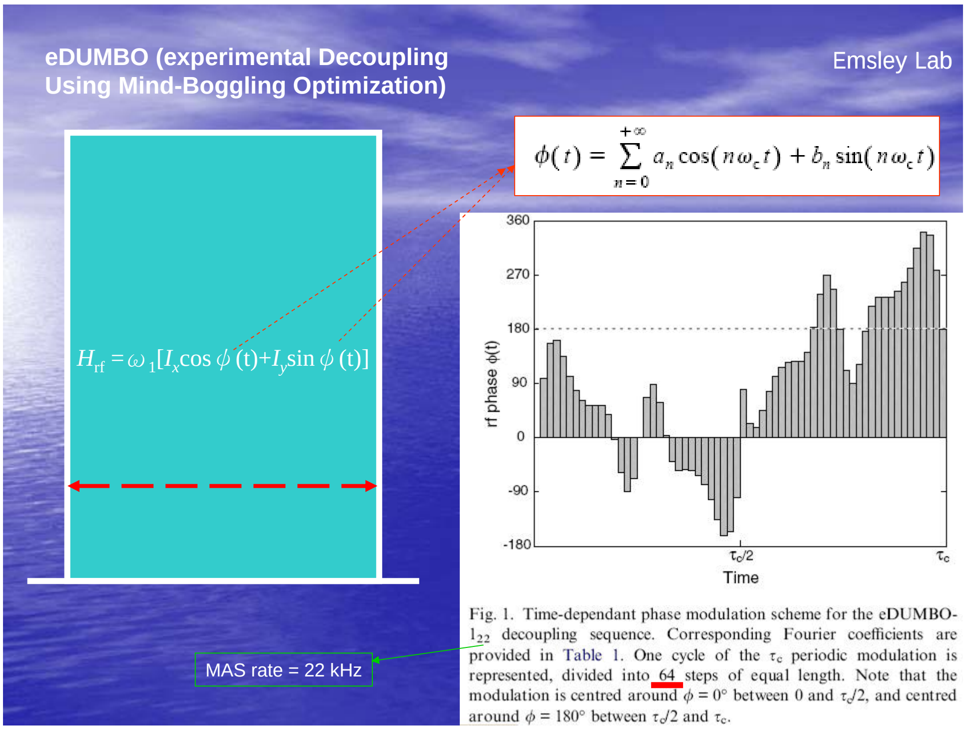
eDUMBO (experimental Decoupling Using Mind-Boggling Optimization)
Emsley Lab
$\phi(t) = \sum_{n=0}^{+\infty} a_n \cos(n\omega_c t) + b_n \sin(n\omega_c t)$
$H_{rf} = \omega_1[I_x \cos\phi(t) + I_y \sin\phi(t)]$
MAS rate = 22 kHz
rf phase φ(t)
360
270
180
90
0
-90
-180
$\tau_c/2$
τ_c
Time
Fig. 1. Time-dependant phase modulation scheme for the eDUMBO-1_{22} decoupling sequence. Corresponding Fourier coefficients are provided in Table 1. One cycle of the τ_c periodic modulation is represented, divided into 64 steps of equal length. Note that the modulation is centred around $\phi = 0°$ between 0 and $\tau_c/2$, and centred around $\phi = 180°$ between $\tau_c/2$ and τ_c.

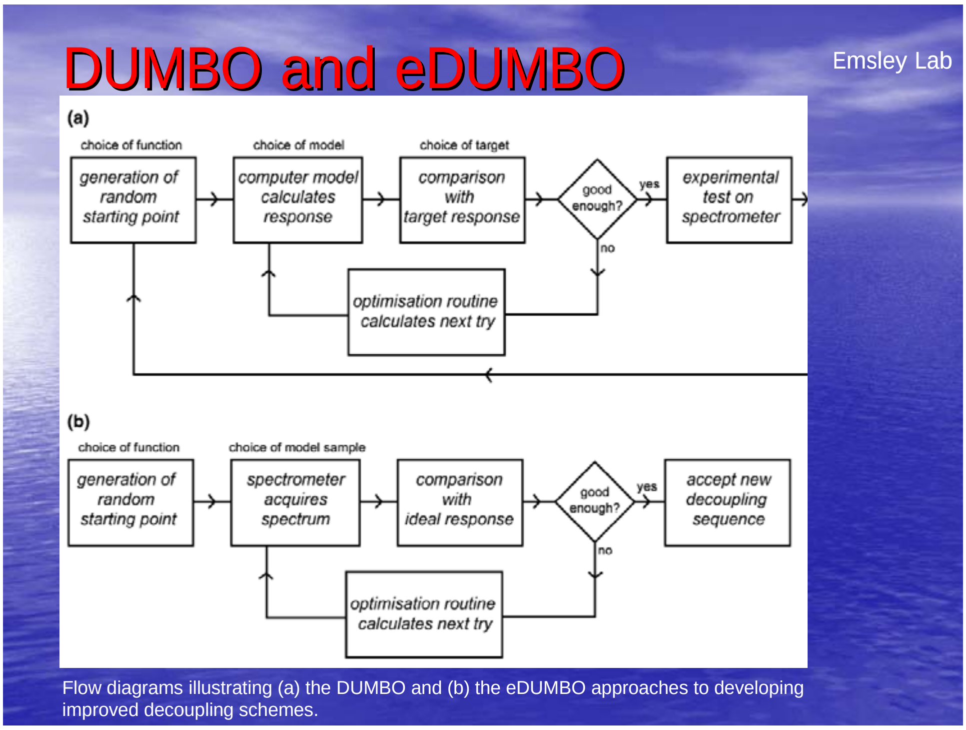
DUMBO and eDUMBO
Emsley Lab
(a)
choice of function
choice of model
choice of target
generation of random starting point
computer model calculates response
comparison with target response
good enough?
yes
no
experimental test on spectrometer
optimisation routine calculates next try
(b)
choice of function
choice of model sample
generation of random starting point
spectrometer acquires spectrum
comparison with ideal response
good enough?
yes
no
accept new decoupling sequence
optimisation routine calculates next try
Flow diagrams illustrating (a) the DUMBO and (b) the eDUMBO approaches to developing improved decoupling schemes.

Symmetry Based Decoupling Pulse Sequences

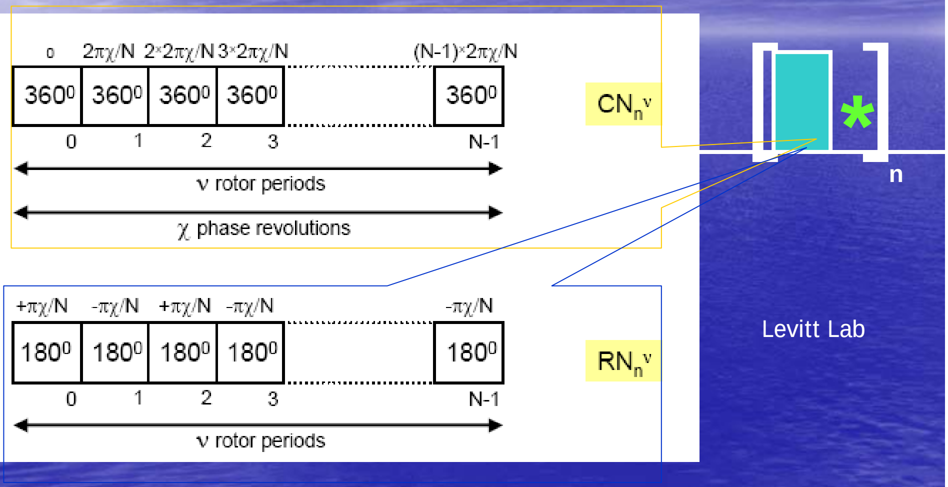

From Decoupling to Recoupling

- High resolution achieved with MAS sacrifices information on anisotropy.
- Anisotropy can be recovered with recoupling
- Selective and broadband recoupling
- CSA recoupling
- Dipolar recoupling
- Quadrupolar coupling

CSA Recoupling

- Off magic angle spinning — Grant and Pugmire
- Stop and go (STAG) — Maciel, Wind
- Magic-angle-hopping (MAH) — Bax & Maciel
- Switching-angle-spinning (SAS) or Dynamic-angle-spinning (DAS) — Pines, Terao
- Magic-angle-turning (MAT) — Grant, Hu
- SPEED etc. — Grant

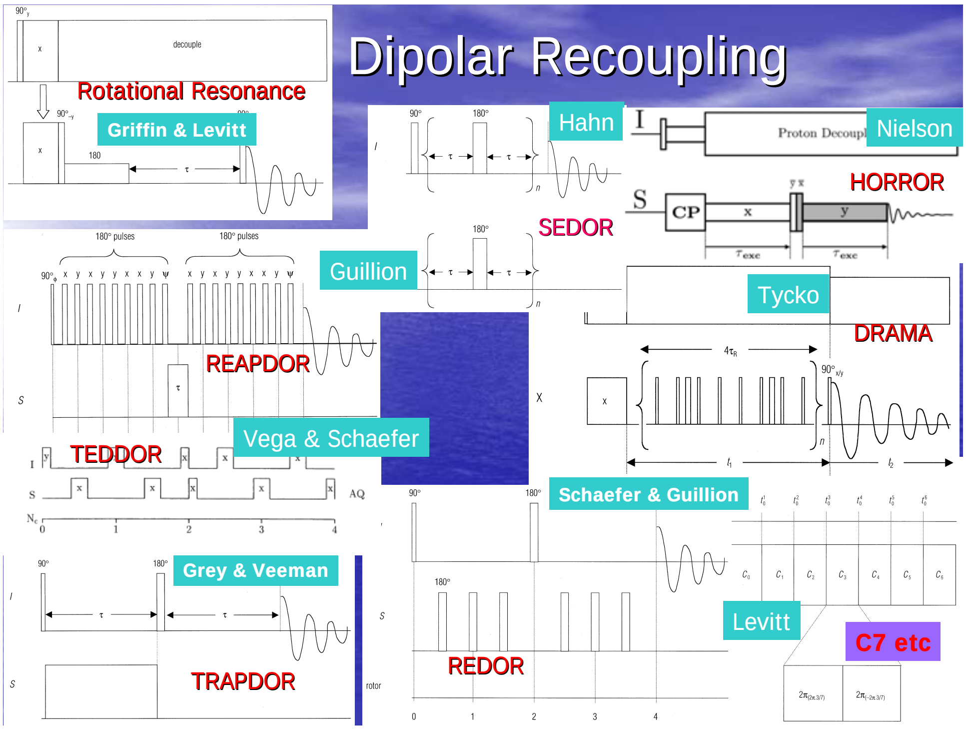

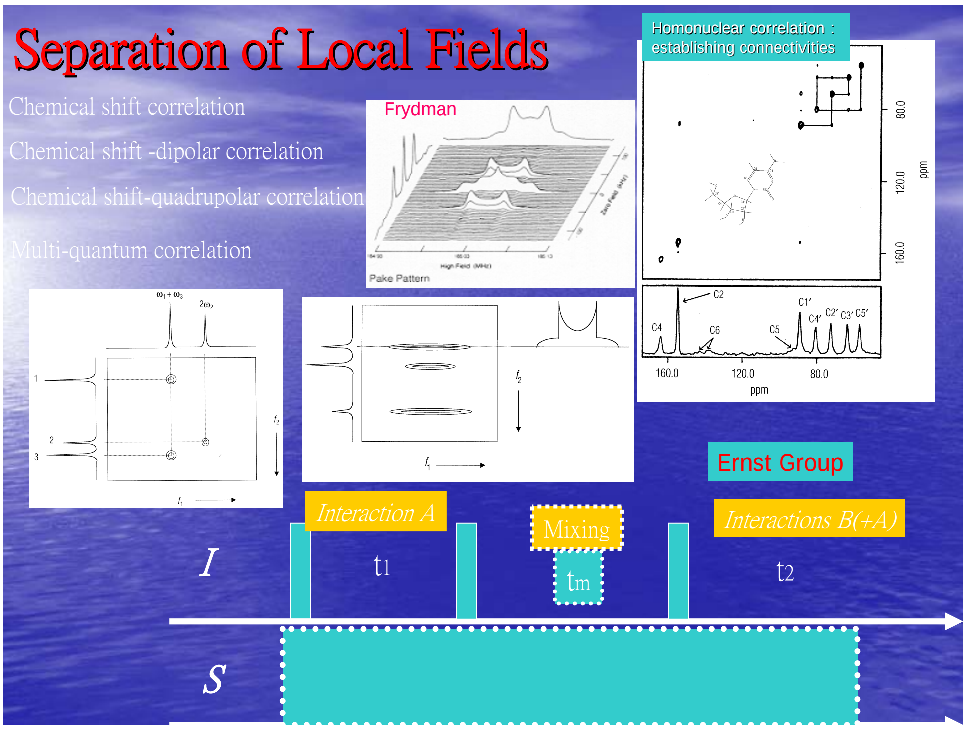
Separation of Local Fields
Chemical shift correlation
Chemical shift -dipolar correlation
Chemical shift-quadrupolar correlation
Multi-quantum correlation
Frydman
Pake Pattern
Homonuclear correlation : establishing connectivities
ppm
C2
C4
C6
C5
C1'
C4'
C2'
C3'
C5'
Ernst Group
Interaction A
Mixing
Interactions B(+A)
I
t1
tm
t2
S

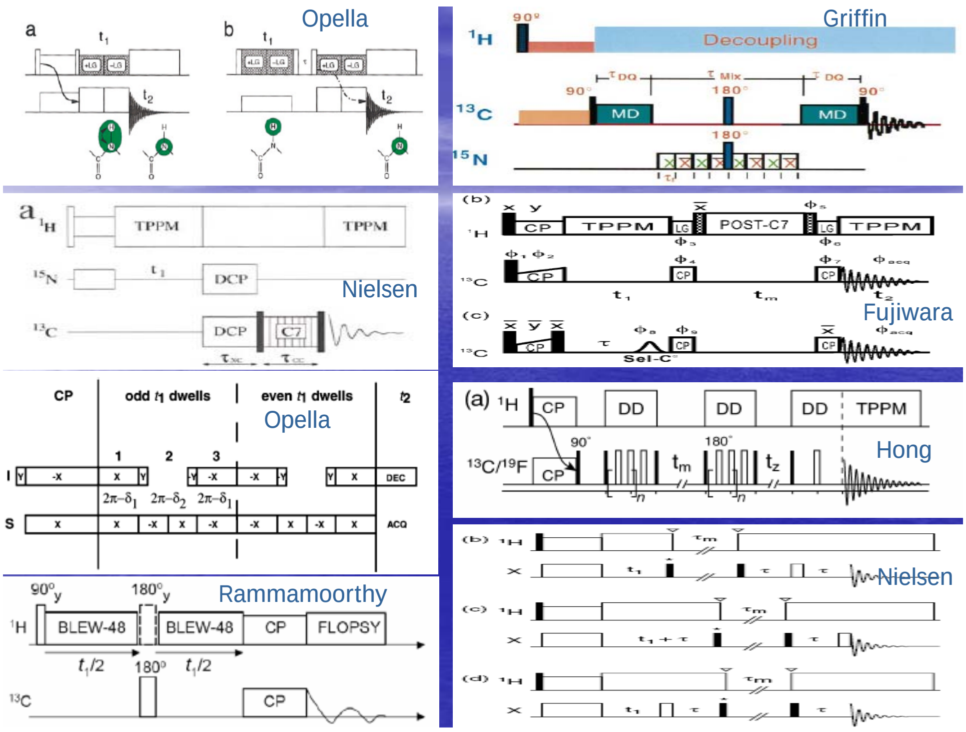
Opella
Griffin
Decoupling
MD
CP
Nielsen
TPPM
DCP
C7
POST-C7
Fujiwara
Sel-C
odd t1 dwells
even t1 dwells
Opella
ACQ
DEC
DD
Hong
Rammamoorthy
BLEW-48
FLOPSY
Nielsen

Multiple Quantum Magic Angle Spinning

Frydman Lab

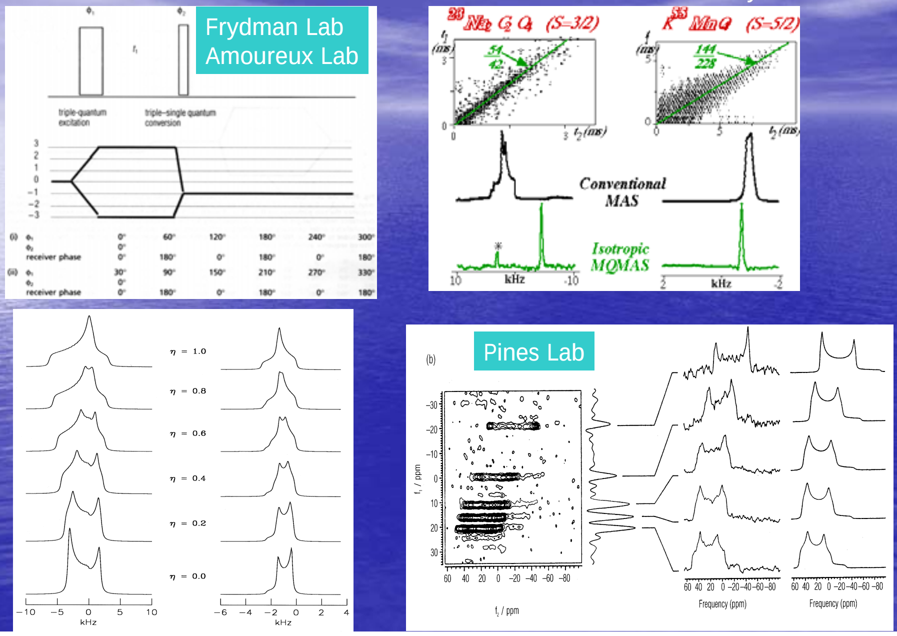

3D CSA-D Correlation (with One Quadrupolar Spin)

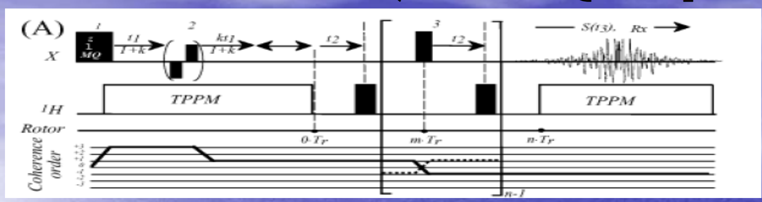

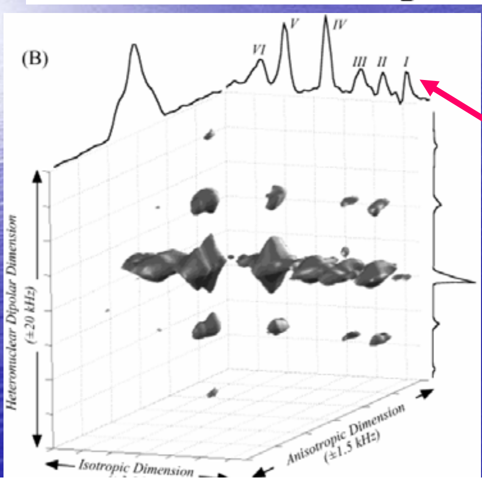

Six nonequivalent Na sites are resolved.

J. Grinshtein, C. V. Grant, L. Frydman, J Am Chem Soc 124,13344(2002).

How Many Magnetically Nonequivalent Sites in Disodium ATP?

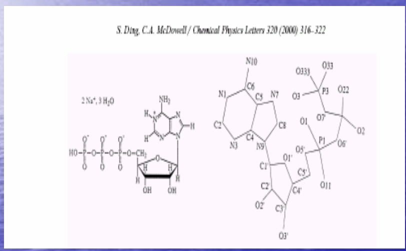

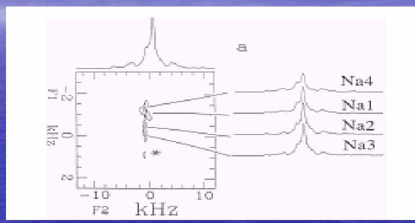

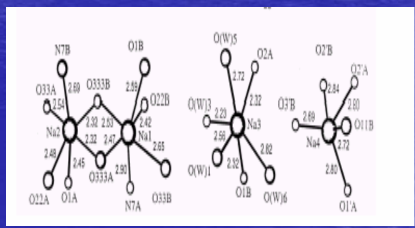

- S. Ding, C.A. McDowell, Chem. Phys. Lett. 2000, 320, 316-322

The Sodium Ions Inside a Lipophilic G-Quadruplex Channel

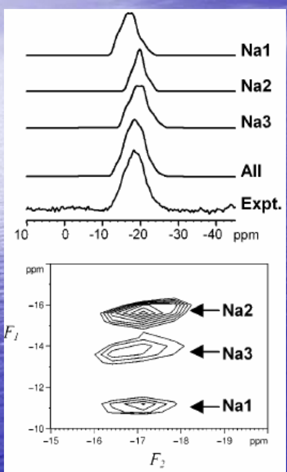

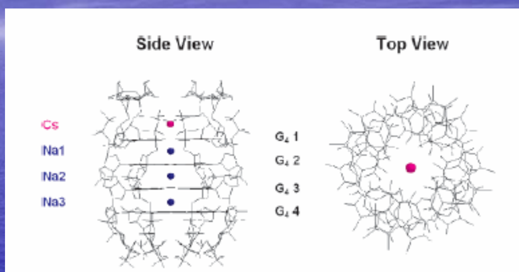

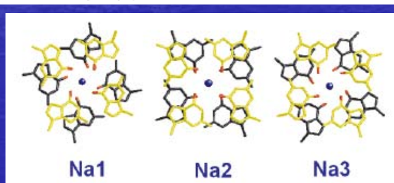

Alan Wong, James C. Fettinger, Scott L. Forman, Jeffery T. Davis, and Gang Wu*, J. Am. Chem. Soc. 2002,124,742.

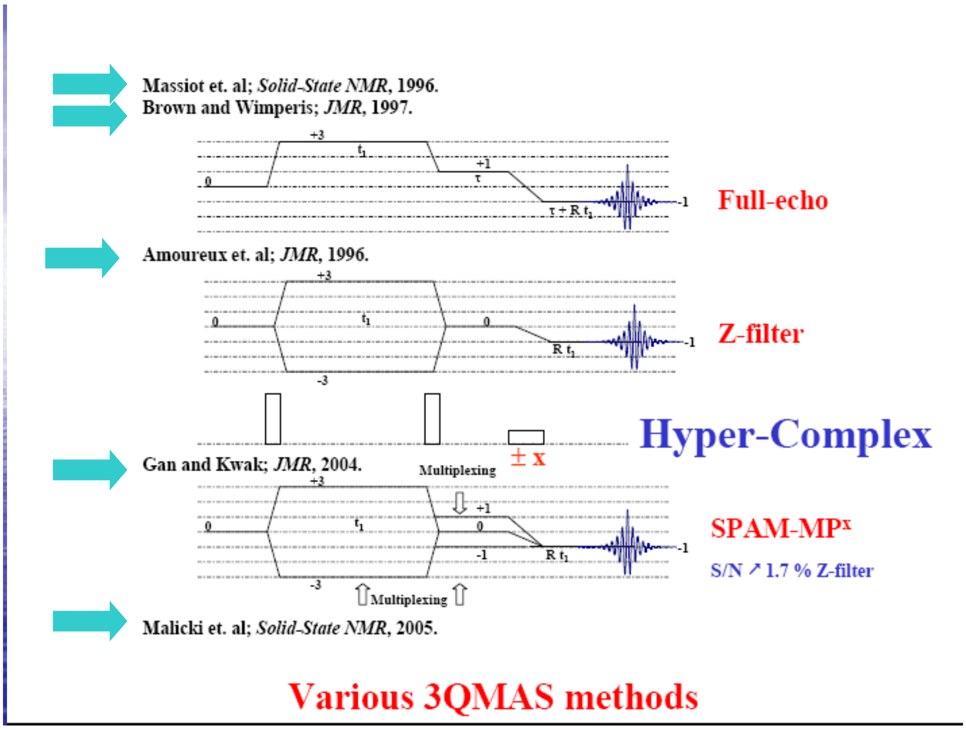

Massiot et. al; Solid-State NMR, 1996.
Brown and Wimperis; JMR, 1997.
Full-echo
Amoureux et. al; JMR, 1996.
Z-filter
Hyper-Complex
Gan and Kwak; JMR, 2004.
Multiplexing
± x
SPAM-MPx
S/N ↗ 1.7 % Z-filter
Multiplexing
Malicki et. al; Solid-State NMR, 2005.
Various 3QMAS methods

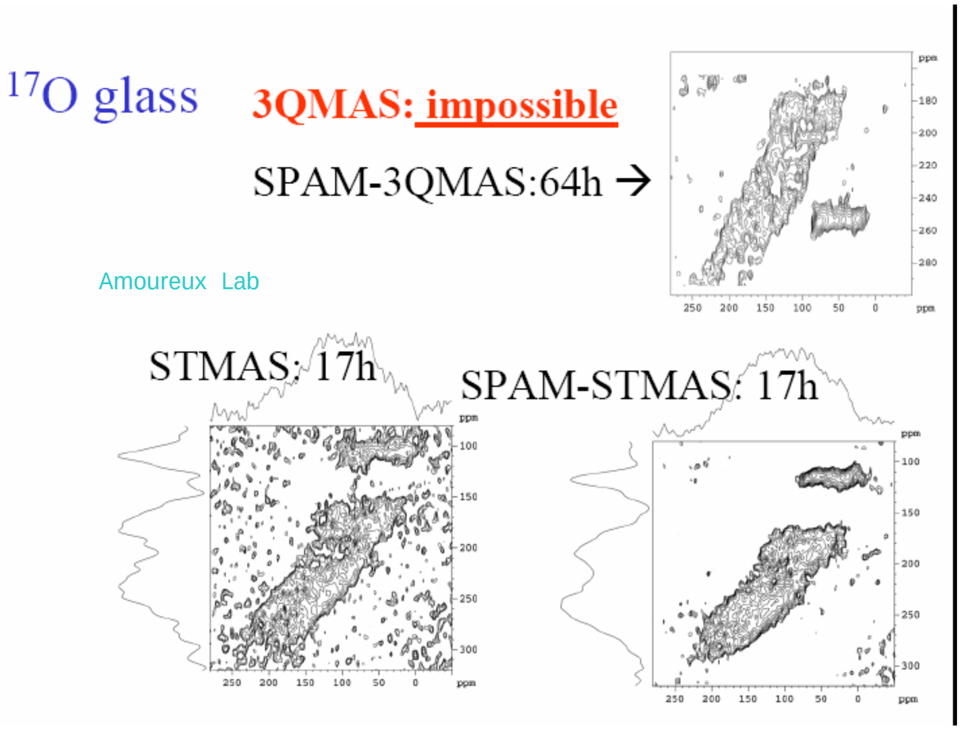

17O glass
3QMAS: impossible
SPAM-3QMAS:64h →
Amoureux Lab
STMAS: 17h
SPAM-STMAS: 17h

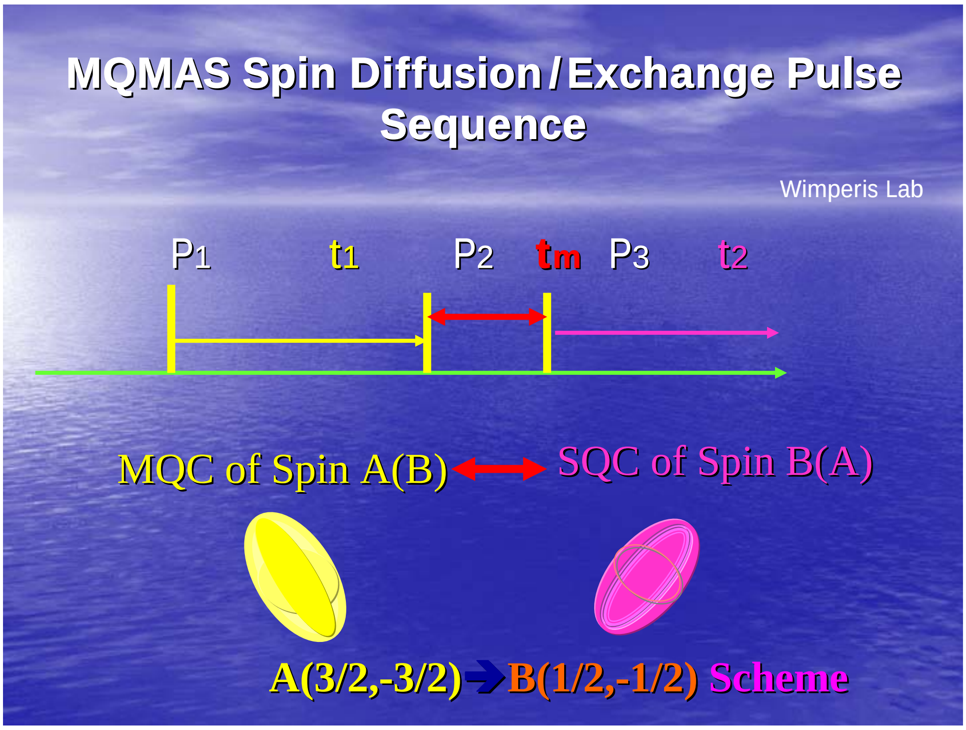
MQMAS Spin Diffusion / Exchange Pulse Sequence
Wimperis Lab
P1 t1 P2 tm P3 t2
MQC of Spin A(B)
SQC of Spin B(A)
A(3/2,-3/2)→B(1/2,-1/2) Scheme

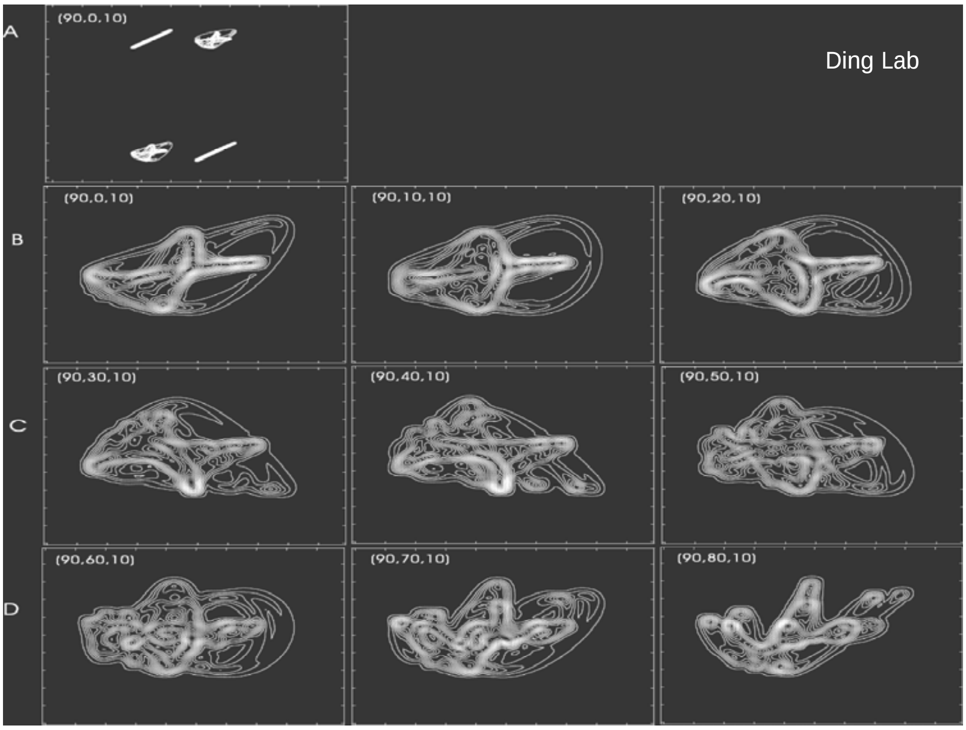
Ding Lab
A
(90,0,10)
B
(90,0,10)
(90,10,10)
(90,20,10)
C
(90,30,10)
(90,40,10)
(90,50,10)
D
(90,60,10)
(90,70,10)
(90,80,10)

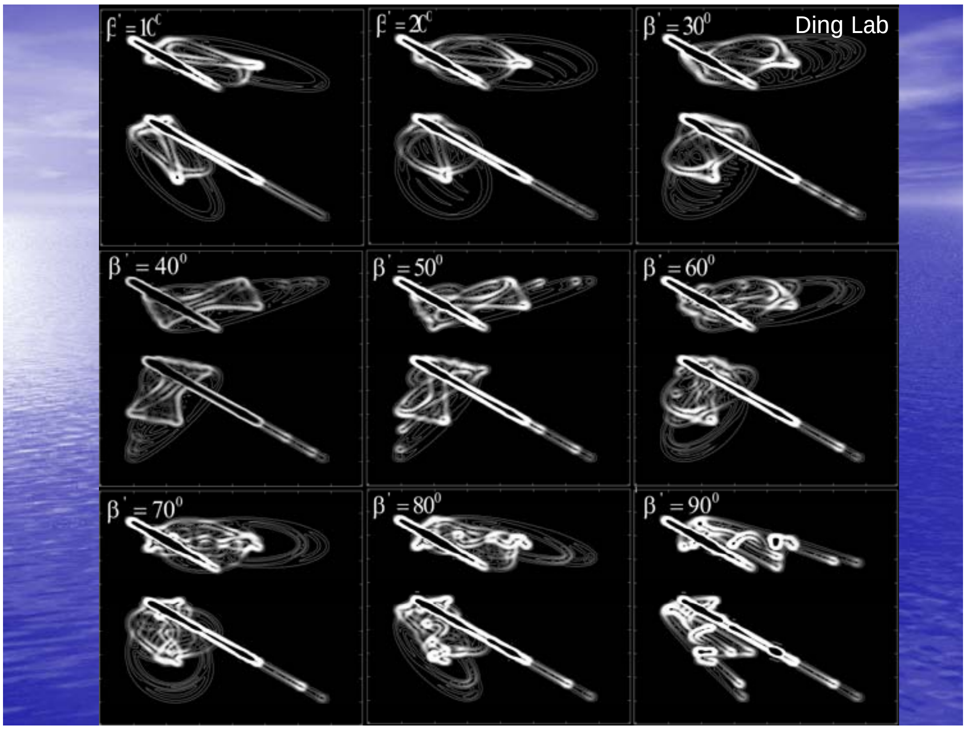

β' = 10°
β' = 20°
β' = 30°
Ding Lab
β' = 40°
β' = 50°
β' = 60°
β' = 70°
β' = 80°
β' = 90°

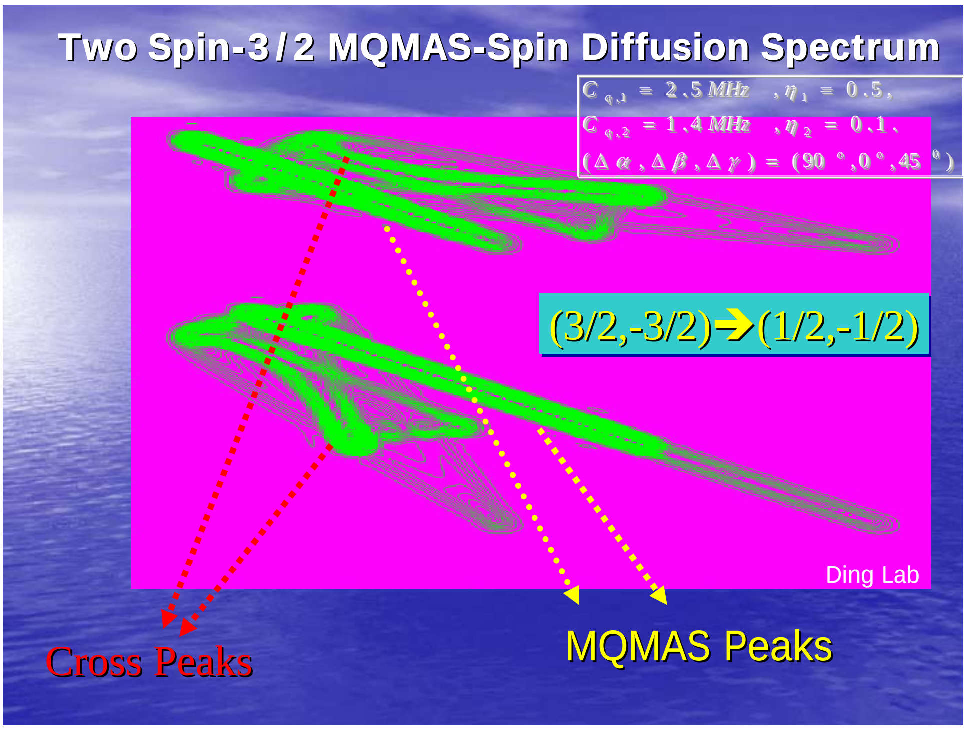

Two Spin-3/2 MQMAS-Spin Diffusion Spectrum
$C_{q,1} = 2.5\,MHz$, $\eta_1 = 0.5$,
$C_{q,2} = 1.4\,MHz$, $\eta_2 = 0.1$,
$(\Delta\alpha, \Delta\beta, \Delta\gamma) = (90°, 0°, 45°)$
(3/2,-3/2)➔(1/2,-1/2)
Ding Lab
Cross Peaks
MQMAS Peaks

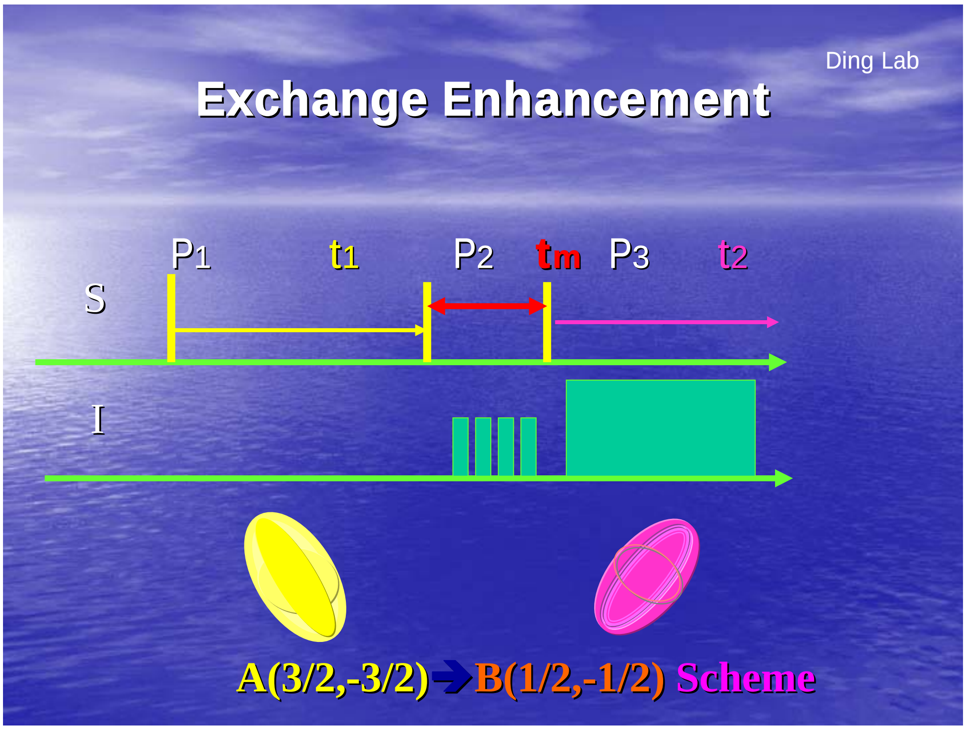
Ding Lab
Exchange Enhancement
P1
t1
P2
tm
P3
t2
S
I
A(3/2,-3/2)→B(1/2,-1/2) Scheme

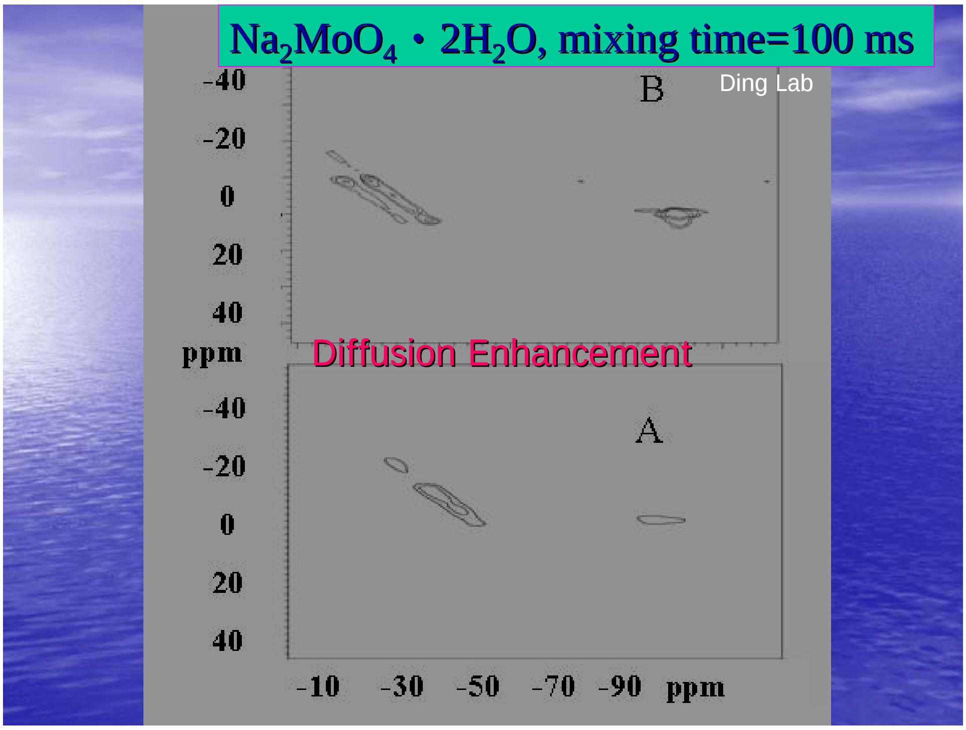
Na_2MoO_4 • $2H_2O$, mixing time=100 ms
B
Ding Lab
-40
-20
0
20
40
ppm
Diffusion Enhancement
-40
-20
0
20
40
A
-10 -30 -50 -70 -90 ppm

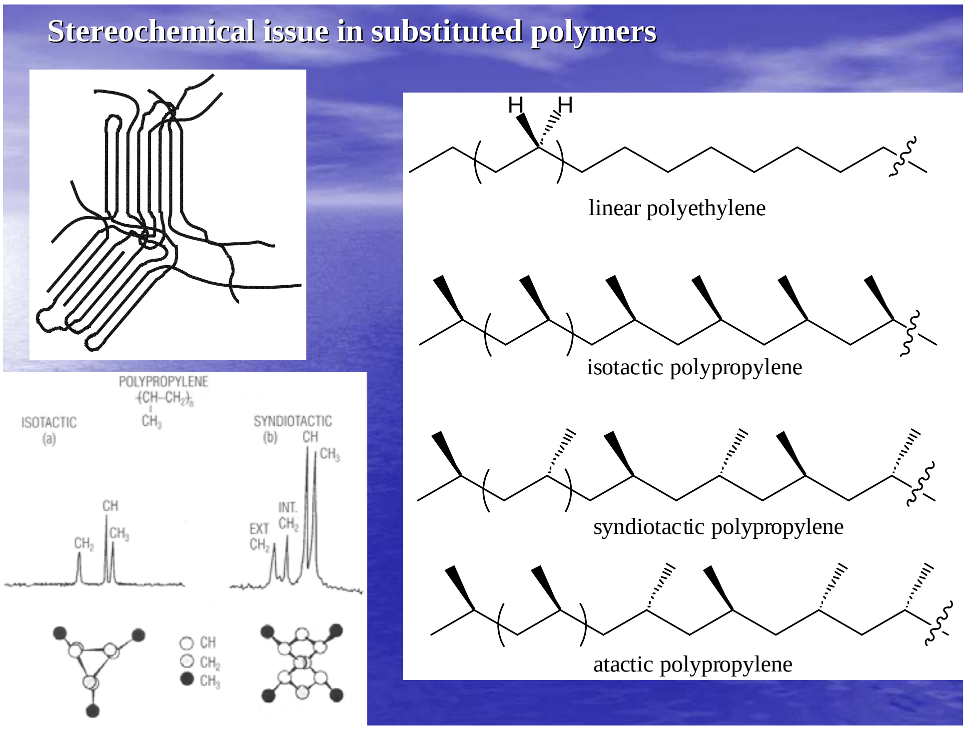
Stereochemical issue in substituted polymers
POLYPROPYLENE
ISOTACTIC (a)
SYNDIOTACTIC (b)
CH
CH2
CH3
EXT CH2
INT. CH2
H H
linear polyethylene
isotactic polypropylene
syndiotactic polypropylene
atactic polypropylene

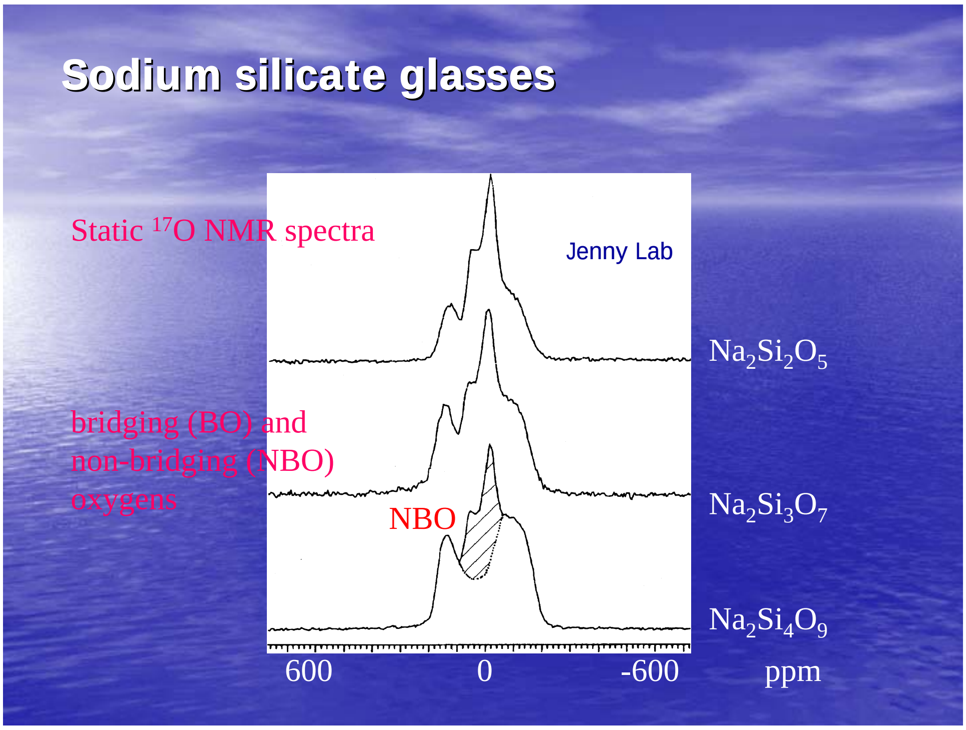
Sodium silicate glasses
Static 17O NMR spectra
Jenny Lab
bridging (BO) and non-bridging (NBO) oxygens
NBO
Na2Si2O5
Na2Si3O7
Na2Si4O9
600
0
-600
ppm

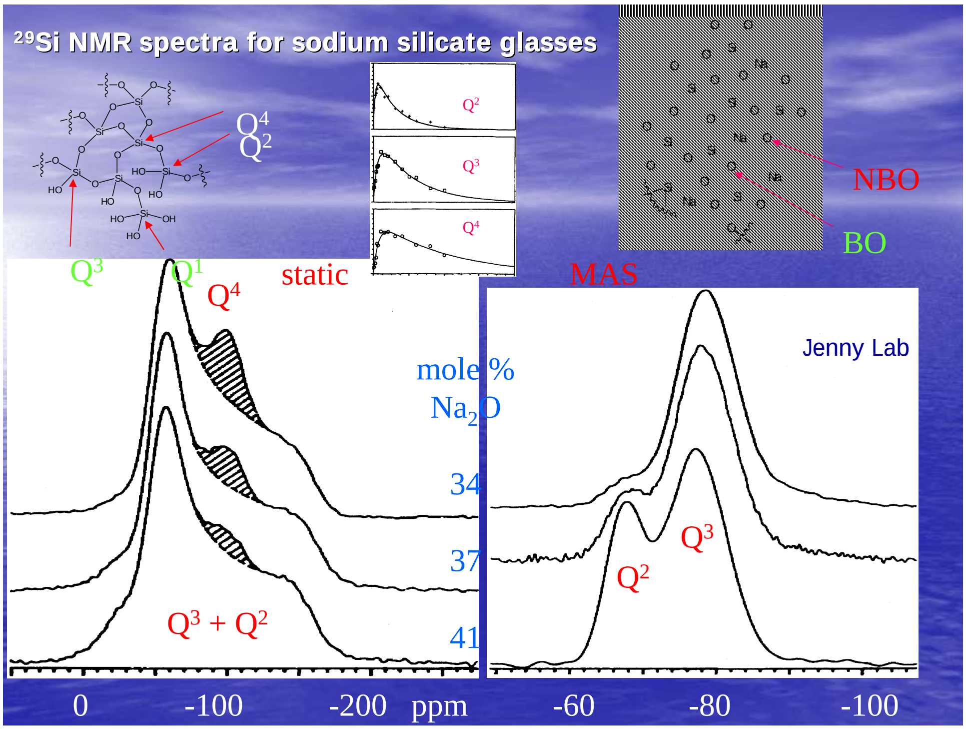

Macromolecules **2006**, *39*, 1029–1040

Multinuclear Solid-State NMR, Self-Diffusion Coefficients, Differential Scanning Calorimetry, and Ionic Conductivity of Solid Organic–Inorganic Hybrid Electrolytes Based on PPG–PEG–PPG Diamine, Siloxane, and Lithium Perchlorate

Hsien-Ming Kao,* Shih-Wei Chao, and Pai-Ching Chang

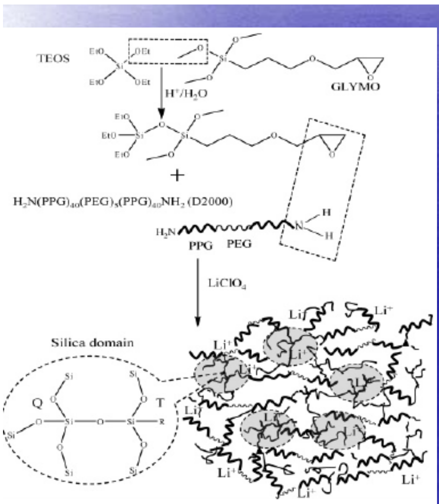

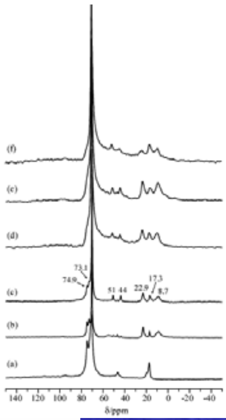

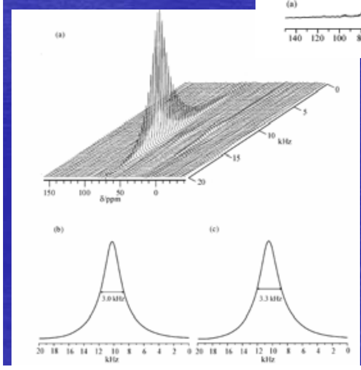

Pictorial description of the preferred connectivities in sodium aluminoborate glasses.

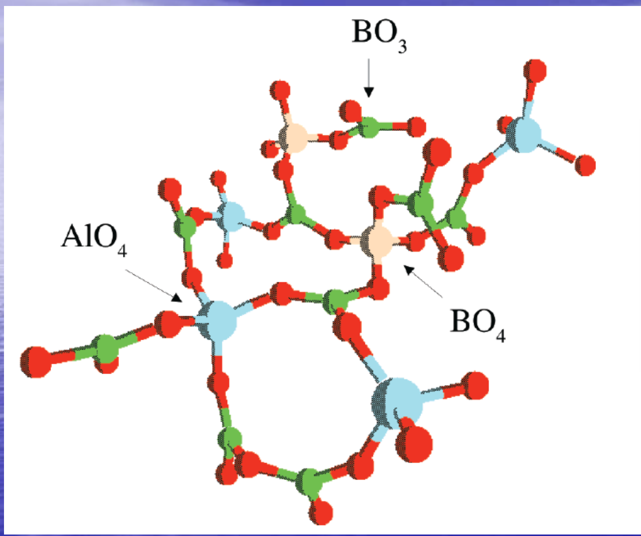

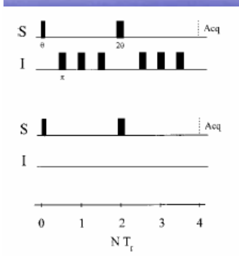

Marko Bertmer, Lars Zu1chner, Jerry C. C. Chan, and Hellmut Eckert, J Phys Chem B104, 6541(2000)

Mechanistic Study of Apatite Formation on Bioactive Glass Surface Using 31P Solid-State NMR Spectroscopy

Chan Lab

Chem. Mater. **2005,** *17,* 4493-4501

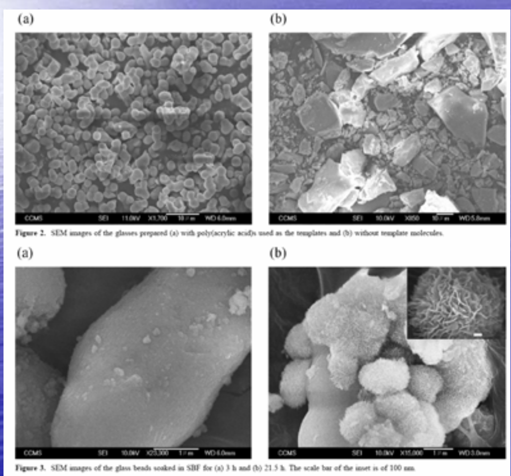

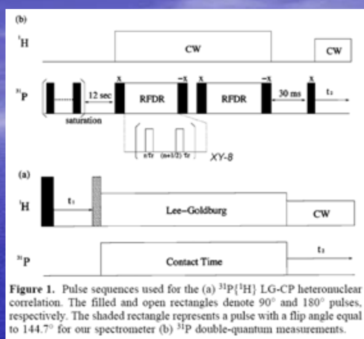

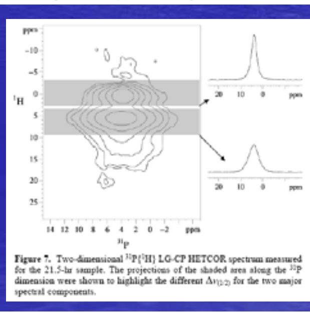

^{17}O 3QMAS NMR spectrum for a borosilicate

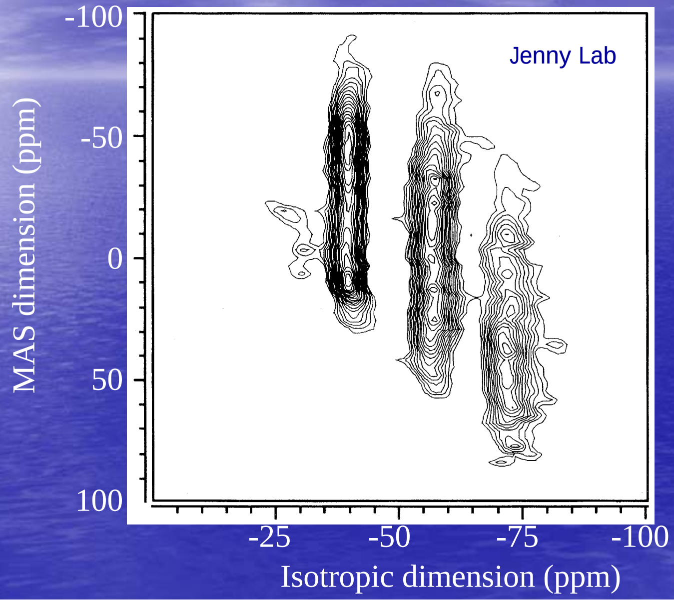

Porous materials

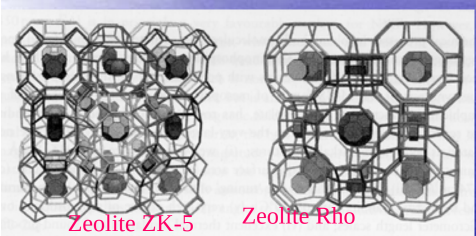

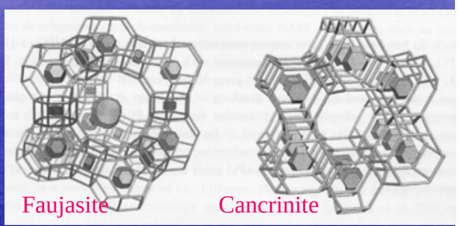

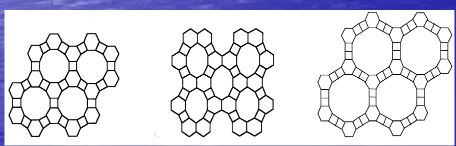

$AlPO_4$-5 along [001] $AlPO_4$-11 along [100]   VPI-5 along [001]

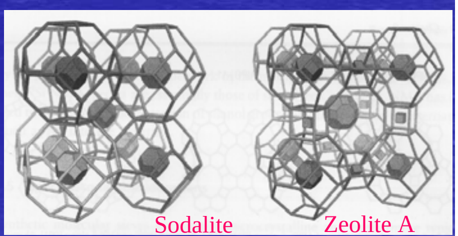

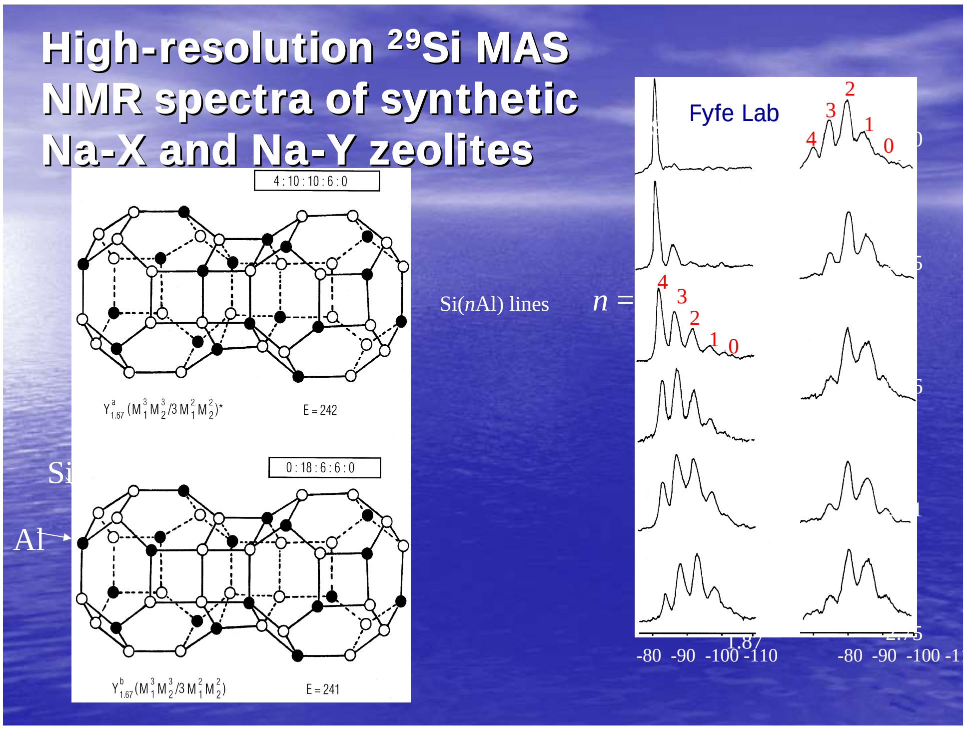
High-resolution ²⁹Si MAS NMR spectra of synthetic Na-X and Na-Y zeolites
Fyfe Lab
4 : 10 : 10 : 6 : 0
0 : 18 : 6 : 6 : 0
E = 242
E = 241
Si(nAl) lines
n =
4 3 2 1 0
Si
Al
1.87
2.75
-80 -90 -100 -110

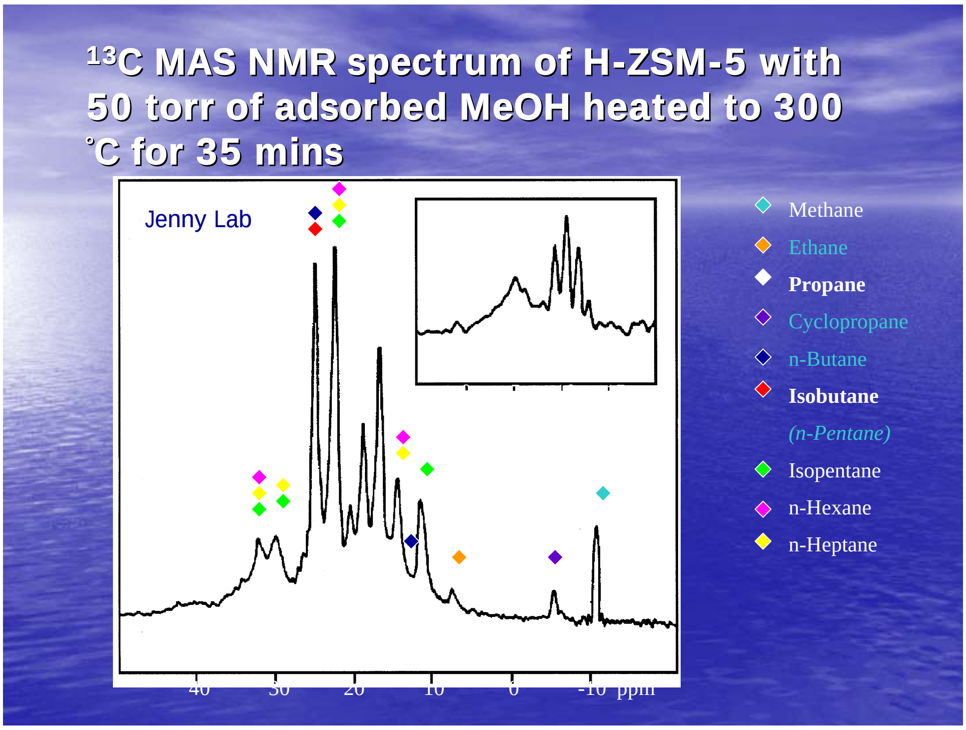
¹³C MAS NMR spectrum of H-ZSM-5 with 50 torr of adsorbed MeOH heated to 300 °C for 35 mins
Jenny Lab
Methane
Ethane
Propane
Cyclopropane
n-Butane
Isobutane
(n-Pentane)
Isopentane
n-Hexane
n-Heptane
40 30 20 10 0 -10 ppm

Methylated aromatic products

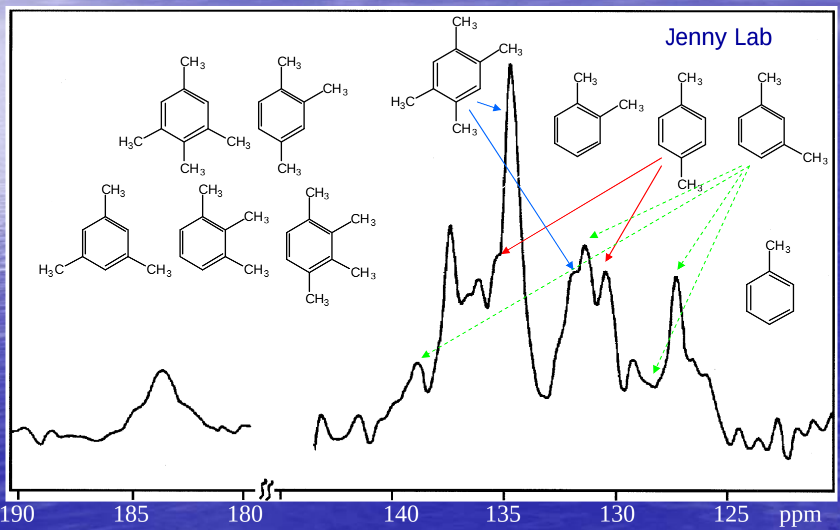

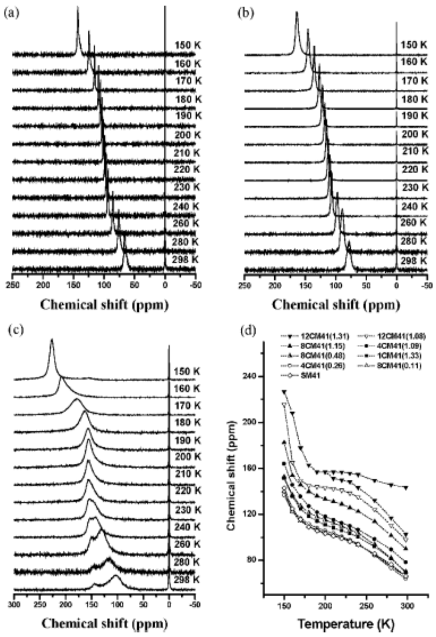

Figure 1. VT-HP ^{129}Xe NMR spectra of (a) SM41, (b) 4CM41(1.09), and (c) 12CM41(1.31). All spectra were obtained with a Xe partial pressure of about 15.2 Torr. (d) Variations of the ^{129}Xe CS with temperature for Xe adsorbed in parent and various silylated samples.

Liu Lab

Probing the Alkyl Ligands on Silylated Mesoporous MCM-41 Using Hyperpolarized ^{129}Xe NMR Spectroscopy

J. Phys Chem B, 2005, *109,* 681-684

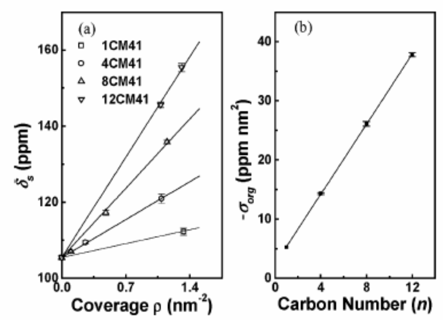

Figure 2. (a) Variations of δ_s with surface alkylsilane coverage. (b) Plot of shielding $-\sigma_{org}$ against carbon number of grafted alkylsilanes.

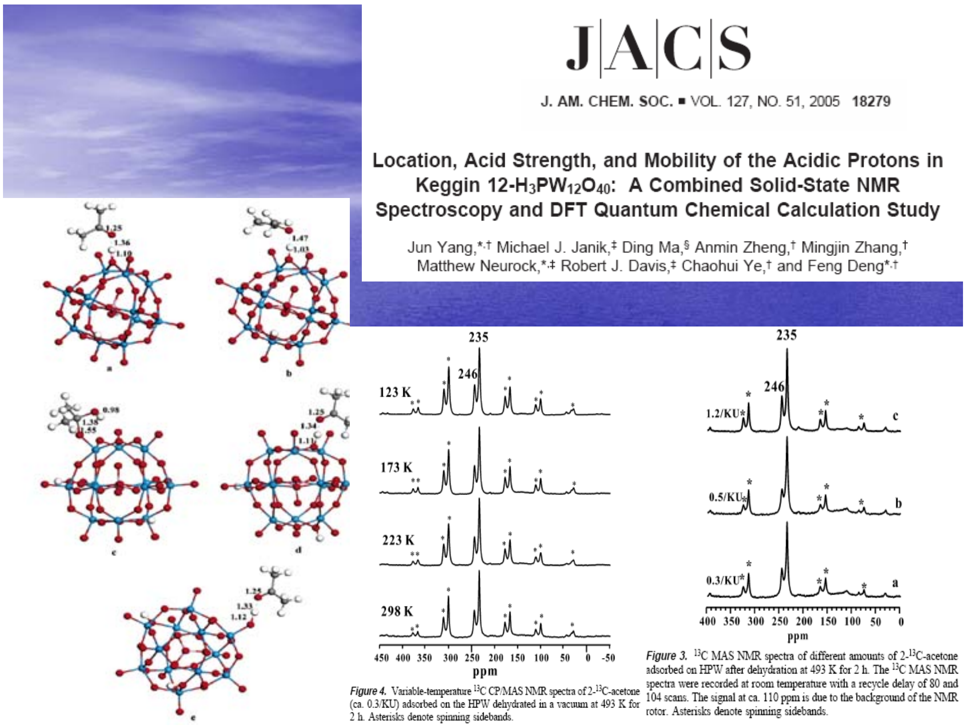

Static 2D exchange spectrum for polyethyleneoxide (PEO)

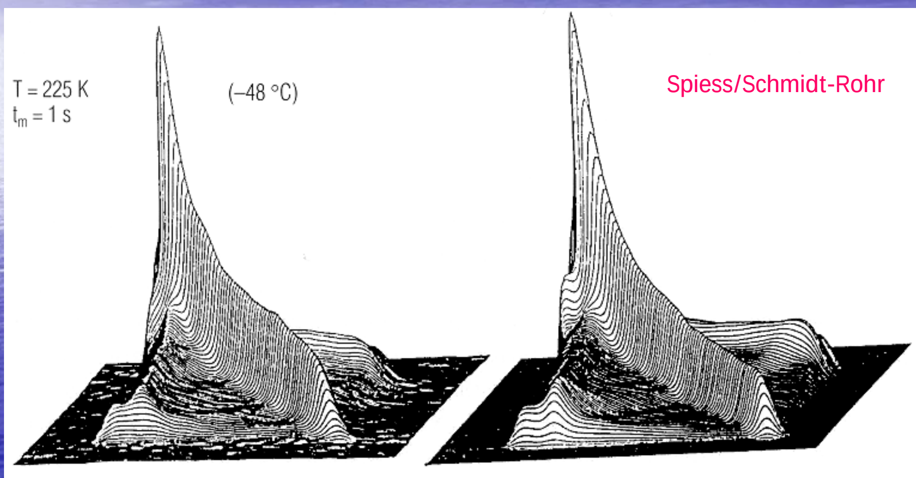

Experiment Simulation

3D static ^{13}C exchange spectra of polyethyleneoxide polyvinylacetate

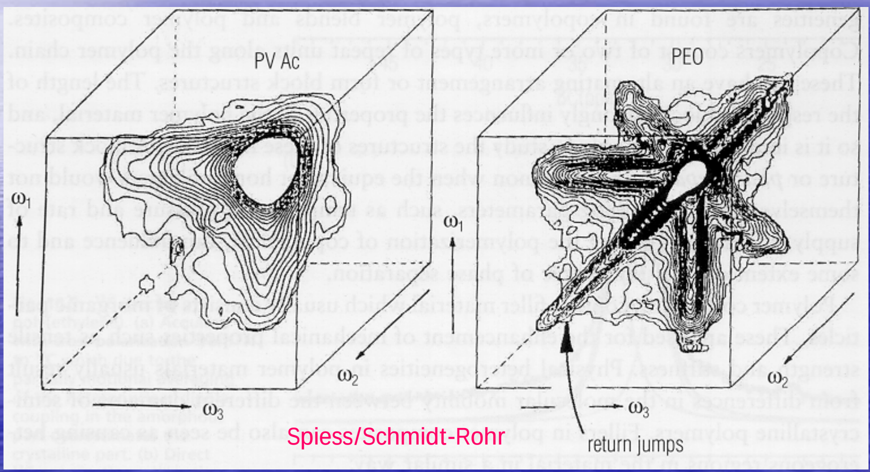

J. Phys. Chem. B **2001,** *105,* 5713−5721

Water Dynamics on the Surface of MCM-41 via ^2H Double Quantum Filtered NMR and Relaxation Measurements

Dennis W. Hwang, Anil K. Sinha, Chi-Yuan Cheng, Tsyr-Yan Yu, and Lian-Pin Hwang*

Department of Chemistry, National Taiwan University, and Institute of Atomic and Molecular Sciences, Academia Sinica, Taipei, Taiwan, R.O.C.

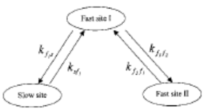

Figure 1. Schematic representation of three-site model for D_2O adsorption in MCM-41. The water molecules exchange between the site s and site f_1 independently of the exchange between site f_1 and site f_2. The population of water in site s, site f_1, and site f_2, is denoted by P_{f1}, P_{f2}, and P_s, respectively. k_{xy} is the microscopic rate constant for transfer from site x to site y.

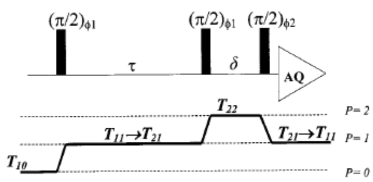

Figure 3. Pulse sequence and coherence-transfer pathway used in DQF experiment. T_{lq} represents the irreducible tensorial component with rank l and coherence q. τ is the DQ evolution time for double quantum coherence and δ was set at 10 μs.

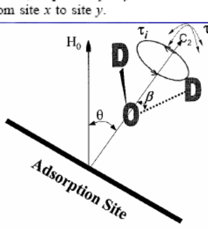

Figure 2. The modified cone model for D_2O molecule adsorption in site s used in the present studies. τ_w is correlation time of restricted wobbling motion, and τ_i^s is correlation time of internal rotation motion.

TABLE 1: Parameters Used in Simulation for Sample A

temp	P_{f1}/P_s	P_{f2}/P_s	$\tau_c^{f_1}$	$\tau_c^{f_2}$	τ_w	τ_i^s	$\tau_{ex}^{f_1 s}$	$\tau_{ex}^{f_1 f_2}$	S
200 K	*[a]	*	*	*	$>10^{-4}$	$1.5 \pm 0.1 \times 10^{-10}$	*	*	0.026 ± 0.001
210 K	*	*	*	*	$>10^{-4}$	$1.2 \pm 0.1 \times 10^{-10}$	*	*	0.026 ± 0.001
220 K	*	*	*	*	$2.5 \pm 0.5 \times 10^{-5}$	$9.5 \pm 0.5 \times 10^{-11}$	*	*	0.026 ± 0.001
230 K	*	*	*	*	$2.5 \pm 0.6 \times 10^{-5}$	$8.5 \pm 0.4 \times 10^{-11}$	*	*	0.025 ± 0.001
240 K	*	*	*	*	$2.3 \pm 0.3 \times 10^{-5}$	$7.5 \pm 0.3 \times 10^{-11}$	*	*	0.025 ± 0.001
250 K	<0.01	*	*	*	$3.2 \pm 0.8 \times 10^{-5}$	$3.8 \pm 0.2 \times 10^{-11}$	*	*	0.022 ± 0.001
260 K	0.01	*	*	*	$2.5 \pm 0.5 \times 10^{-5}$	$3.8 \pm 0.2 \times 10^{-11}$	$>10^{-3}$	*	0.020 ± 0.001
273 K	0.18	*	$4.0 \pm 0.2 \times 10^{-10}$	*	$4.0 \pm 0.4 \times 10^{-5}$	$2.0 \pm 0.1 \times 10^{-11}$	$1.5 \pm 0.1 \times 10^{-4}$	*	0.018 ± 0.001

[a] Asterisks (*) indicate the physical phenomenon of the represented parameter was not observed.

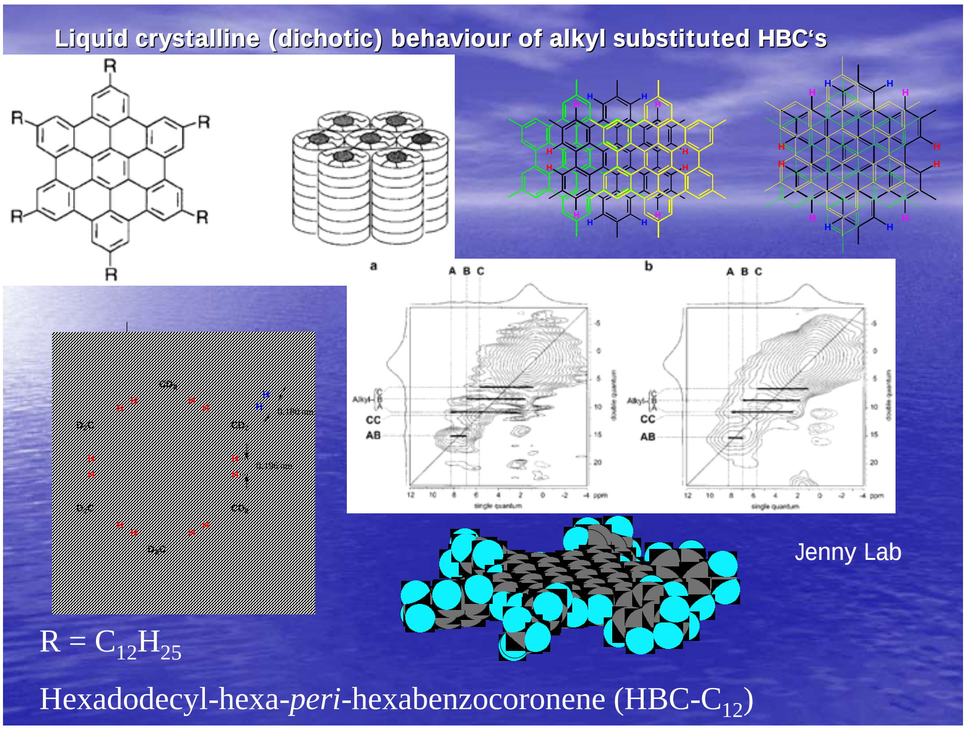
Liquid crystalline (dichotic) behaviour of alkyl substituted HBC's
R
a
b
A B C
Alkyl-
CC
AB
single quantum
double quantum
Jenny Lab
R = C12H25
Hexadodecyl-hexa-peri-hexabenzocoronene (HBC-C12)

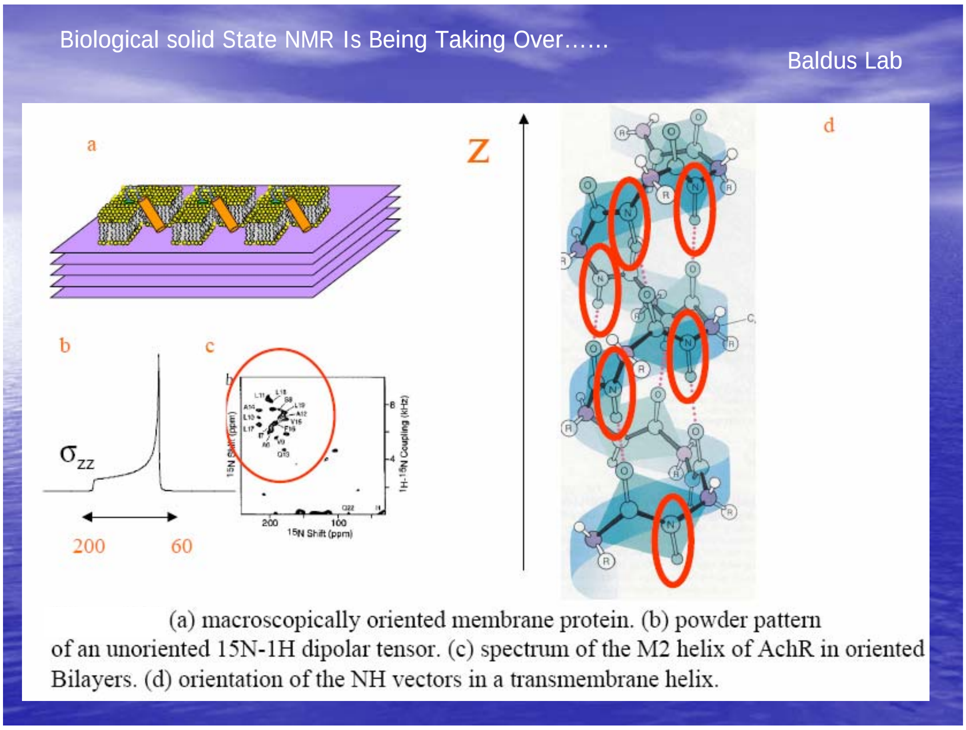
Biological solid State NMR Is Being Taking Over……
Baldus Lab
a
Z
d
b
c
σzz
200
60
15N Shift (ppm)
1H-15N Coupling (kHz)
(a) macroscopically oriented membrane protein. (b) powder pattern
of an unoriented 15N-1H dipolar tensor. (c) spectrum of the M2 helix of AchR in oriented
Bilayers. (d) orientation of the NH vectors in a transmembrane helix.

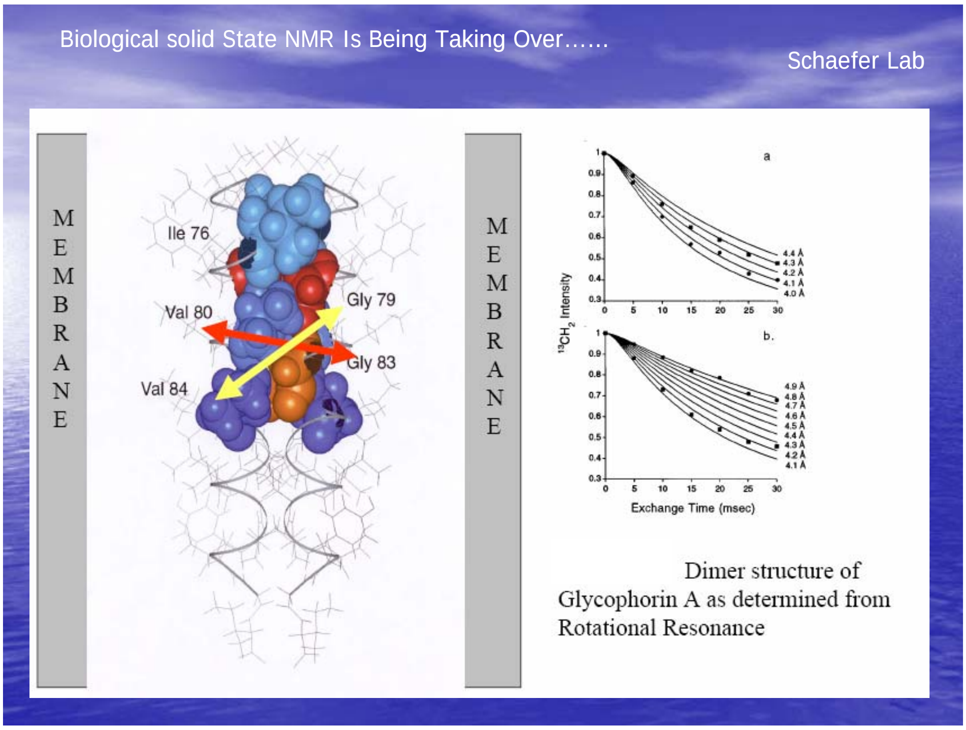
Biological solid State NMR Is Being Taking Over……
Schaefer Lab
MEMBRANE
Ile 76
Val 80
Gly 79
Gly 83
Val 84
MEMBRANE
13CH2 Intensity
Exchange Time (msec)
Dimer structure of Glycophorin A as determined from Rotational Resonance

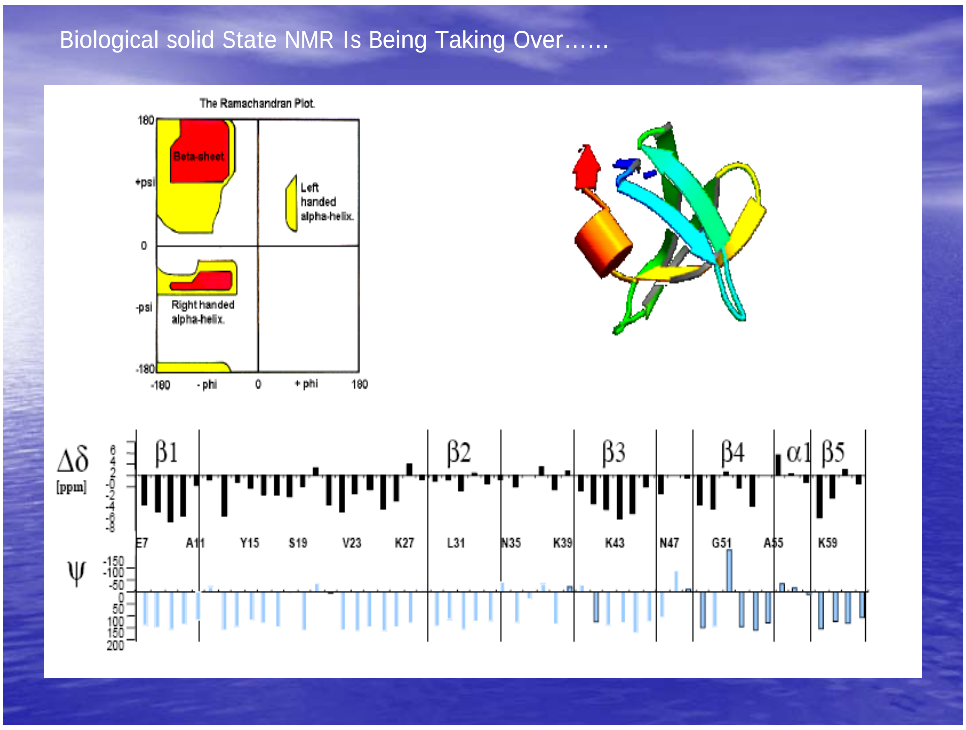
Biological solid State NMR Is Being Taking Over……
The Ramachandran Plot.
Beta-sheet
Left handed alpha-helix.
Right handed alpha-helix.
+psi
-psi
- phi
+ phi
Δδ [ppm]
ψ
β1
β2
β3
β4
α1
β5
E7
A11
Y15
S19
V23
K27
L31
N35
K39
K43
N47
G51
A55
K59

Biological solid State NMR Is Being Taking Over……

Schaefer Lab

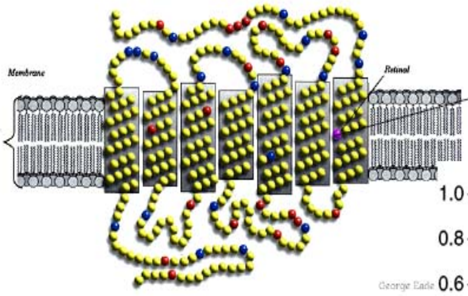

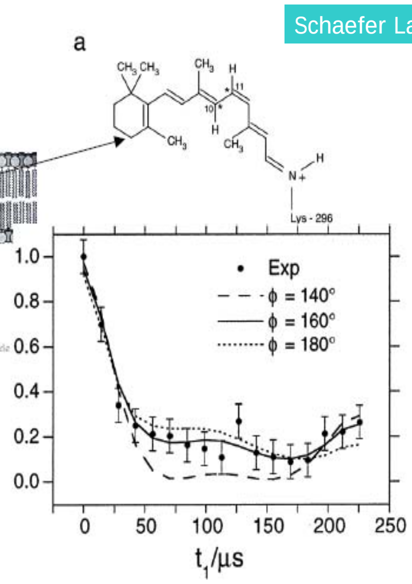

the membrane protein rhodopsin, retinal chromophore and the NMR torsion angle measurement

Biological solid State NMR Is Being Taking Over……

Tycko Lab

a

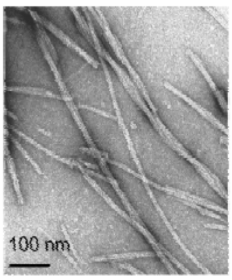

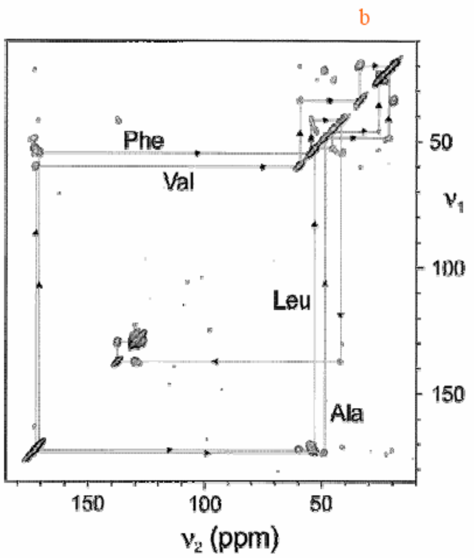

Transmission electron micrograph of the seven-residue peptide A16-22
(b) 2D on A16-22

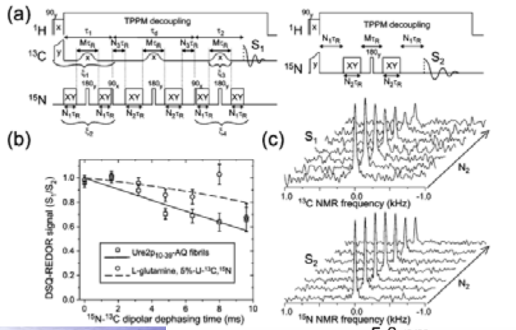

Jerry C. C. Chan, Nathan A. Oyler, Wai-Ming Yau, and Robert Tycko, Biochemistry 44, 10669(2005)

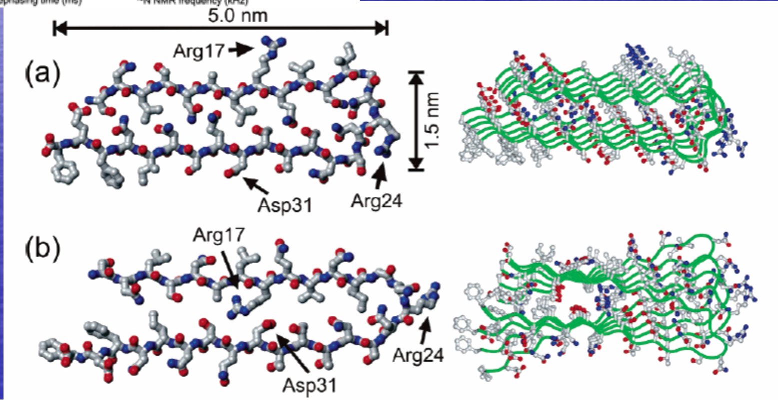

Biological solid State NMR Is Being Taking Over……

Griffin Lab

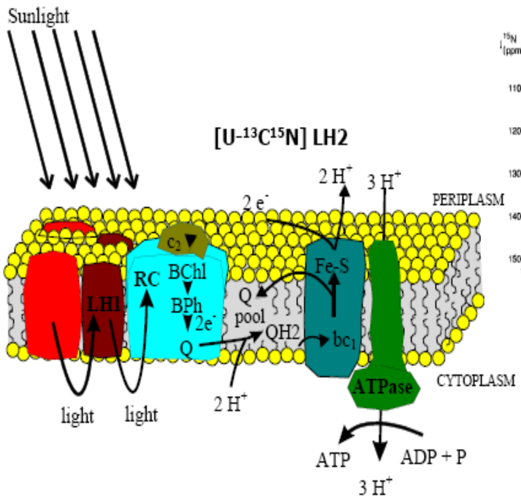

Membrane of the purple photosynthetic bacterium
Rhodopseudomonas acidophila 10050

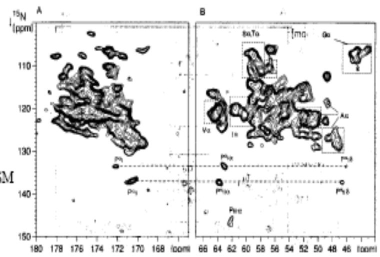

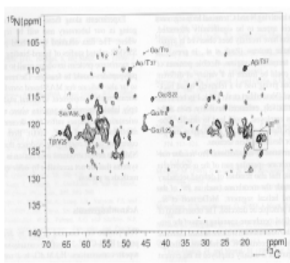

Biological solid State NMR Is Being Taking Over……

Cross Lab

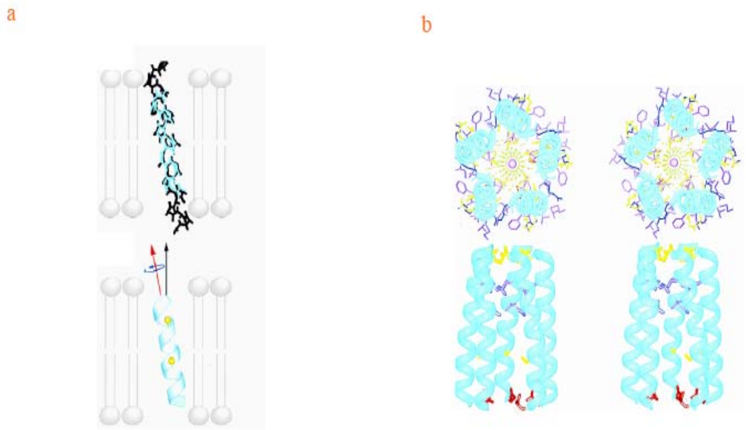

(a) M2 transmembrane helix structure as obtained from the Solid-state NMR data. (b) proposed molecular model of the pentrameric structure.

Structural studies of filamentous bacteriophage by NMR spectroscopy

David S. Thiriot, Ana Carolina Zeri, Lena Zagyanskiy,

Alexander A. Nevzorov, Michael Mesleh, Chin H. Wu and Stanley J. Opella

Department of Chemistry and Biochemistry

University of California-San Diego, La Jolla, CA, USA

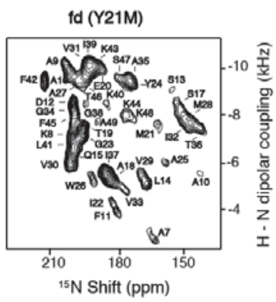

Experimental two dimensional 1H/15N PISEMA of uniformly labled Y21M fd (Zeri et al., 2002) bacterophage particles aligned in the magnetic field of the NMR spectrometer. Each resonance is characterized by the orientationally dependent frequencies associated with the 1H-15N heteronuclear dipolar coupling and 15N chemical shift.

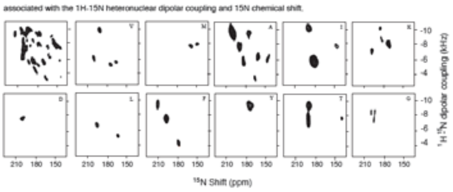

Experimental two dimensional 1H/15N PISEMA spectra of uniformly and selectively labled Y21M filamentous bacteriophage particles. The single letter abbreviations for the labled amino acids are indicated.

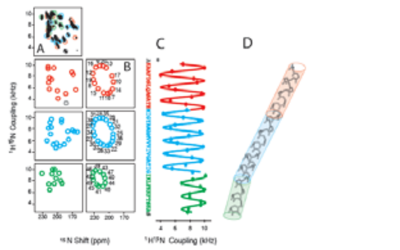

A) Experimental PISEMA spectrum of uniformly labled Y21M fd B) PISA wheels corresponding to the data in A C) Dipolar waves corresponding to the data in A D) Tube representaiton of fd coat protein and ribbon representation of an ideal helix in the predicted orientation

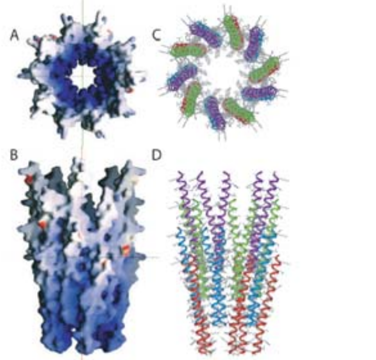

Model of a section of the Y21M fd filamentous bacteriphage capsid built from the structure determined by solid state NMR and the symmetry derived from fiber diffraction studies. A) and B) electrostatic potential on the molecule's surface of the virus (A is a bottom view and B is a side view along the virus axis) obtained using the program GRASP. C) and D) Views of the capsid structure shoing the arrangement of the coat proteins in pentamers and further assembly of the 2-fold helical structure obtained using the program Insight II.

Solid-State NMR Studies of the Structure, Dynamics, and Assembly of β-Sheet Membrane Peptides and α-Helical Membrane Proteins with Antibiotic Activities

Acct Chem Res 2006

MEI HONG
Department of Chemistry, Iowa State University, Ames, Iowa 50011

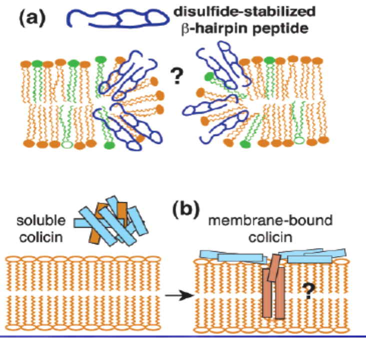

FIGURE 1. (a) Disulfide-stabilized *β*-hairpin antimicrobial peptides disrupt microbial cell membranes through mechanisms that are not well understood. The toroidal pore mechanism is illustrated here. (b) α-Helical channel-forming colicins spontaneously insert into lipid bilayers after undergoing large conformational changes. The membrane-bound structure is largely unknown.

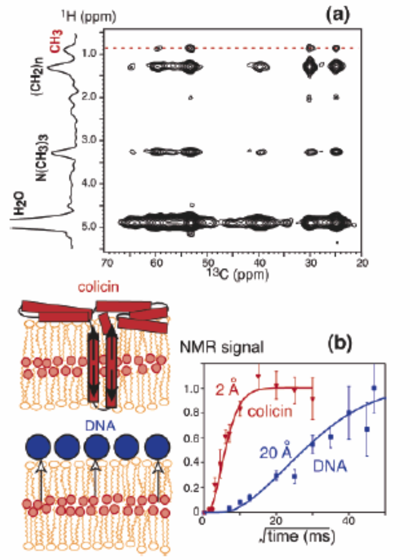

FIGURE 4. (a) Representative 2D ^{1}H−^{13}C correlation spectrum of membrane-bound colicin, highlighting the lipid methyl−protein cross-peaks (dashed line). (b) Magnetization buildup curves from the methyl protons to colicin (red) and DNA (blue). The buildup rates indicate that colicin has a transmembrane domain while DNA resides purely on the membrane surface.[28]

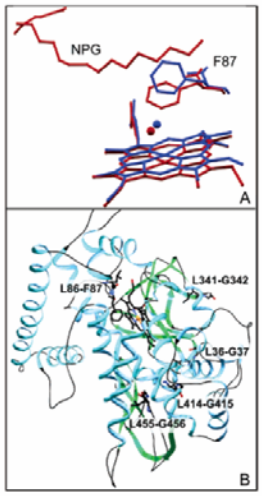

Figure 1. (A) Shift in the conformation of Phe87 residue and shift of the water ligand (red and blue balls) upon substrate binding; the PDB files 1BU7[36] (the resting state of the protein, in blue) and 1JPZ[26] (the NPG bound state of the protein, in red) were overlaid using 432 backbone atoms within conserved helices D, E, I, L, J, and K, employing Swiss PDB Viewer (SPDBV).[53] The RMS deviation for the backbone heavy atoms in this superposition was 0.60 Å. (B) Positions of the Leu-Phe and four Leu-Gly pairs in the heme domain of cytochrome P450 BM-3.[36] The unique Leu86-Phe87 pair is close to the heme iron and is involved in the binding pocket, but the Leu-Gly pairs are not. The figures were prepared with programs POV Ray (http://www.povray.org) and SPDBV.[53]

Ligand Binding Studied by SSNMR

T. Jovanovic, A. E. McDermott, JACS 2005

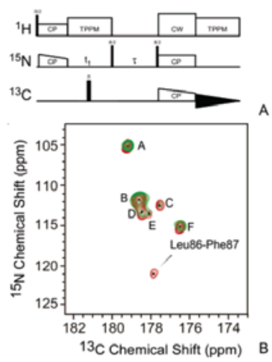

Figure 4. Pulse sequence (A), and 2D T_1 ^{15}N measurements on substrate-bound form of ^{13}CO−Leu, ^{15}N−Gly, ^{15}N−Phe (B). The SPECIFIC CP spectrum is in red, and the 2D T_1 ^{15}N filtered experiment for τ = 1 s is in green. The Leu86-Phe87 peak is much reduced in the filtered experiment, due to its more efficient relaxation.

Structure of a protein determined by solid-state magic-angle-spinning NMR spectroscopy

NATURE | VOL 420 | 7 NOVEMBER 2002 |

Federica Castellani, Barth van Rossum, Annette Diehl, Mario Schubert, Kristina Rehbein & Hartmut Oschkinat

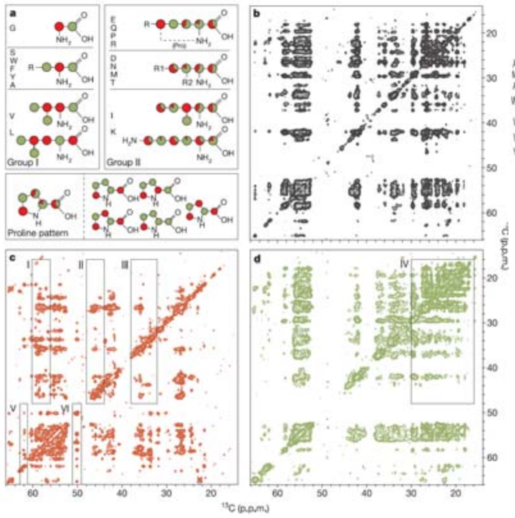

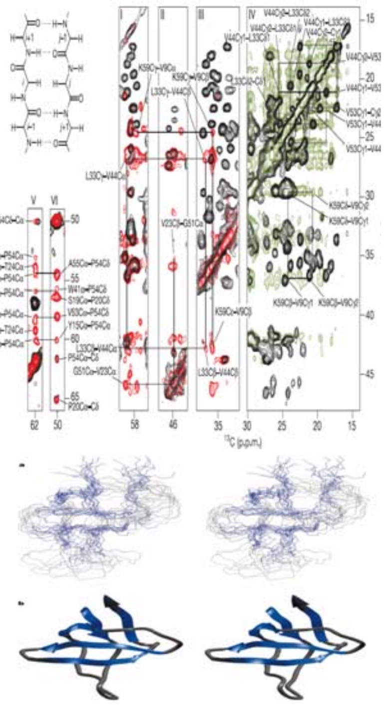

Toxin-induced conformational changes in a potassium channel revealed by solid-state NMR

Adam Lange[1], Karin Giller[1], Sönke Hornig[2], Marie-France Martin-Eauclaire[3], Olaf Pongs[2], Stefan Becker[1] & Marc Baldus[1]

Vol 440|13 April 2006|doi:10.1038/nature04649 nature

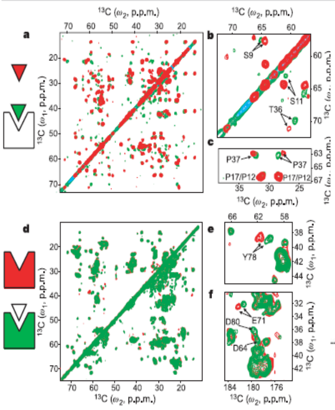

Figure 1 | Comparison of ssNMR data of KTX and KcsA-Kv1.3 in free and complex form. a–c, (^{13}C,^{13}C) Two-dimensional spin diffusion spectrum obtained on uniformly (U) [^{13}C,^{15}N]-labelled KTX in free, solid-phase form (red) and in complex with KcsA-Kv1.3 (green). KTX is symbolized by triangles at the left of the panel. **d–f**, Two-dimensional spin diffusion spectrum obtained on U-[^{13}C,^{15}N]KcsA-Kv1.3 (red) and KTX–U-[^{13}C,^{15}N]KcsA-Kv1.3 (green, see cartoon at the left of the panel). In both data sets, spectral regions are shown for specific residue types (**b**, **c** and **e**, **f**). Carbon resonance frequencies ω_1 and ω_2 are in p.p.m.

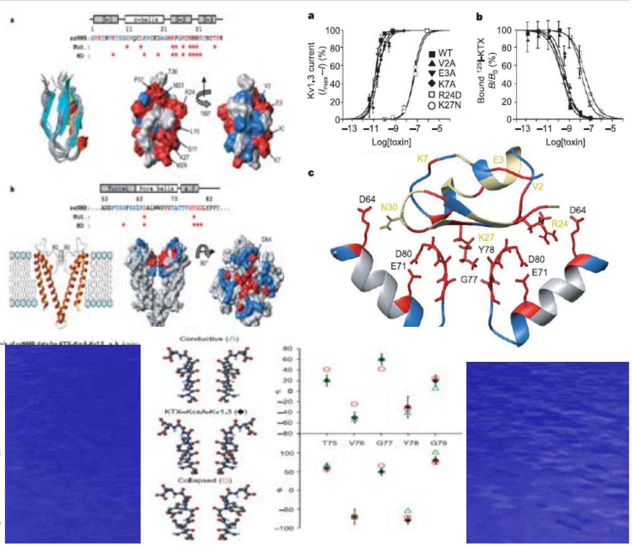

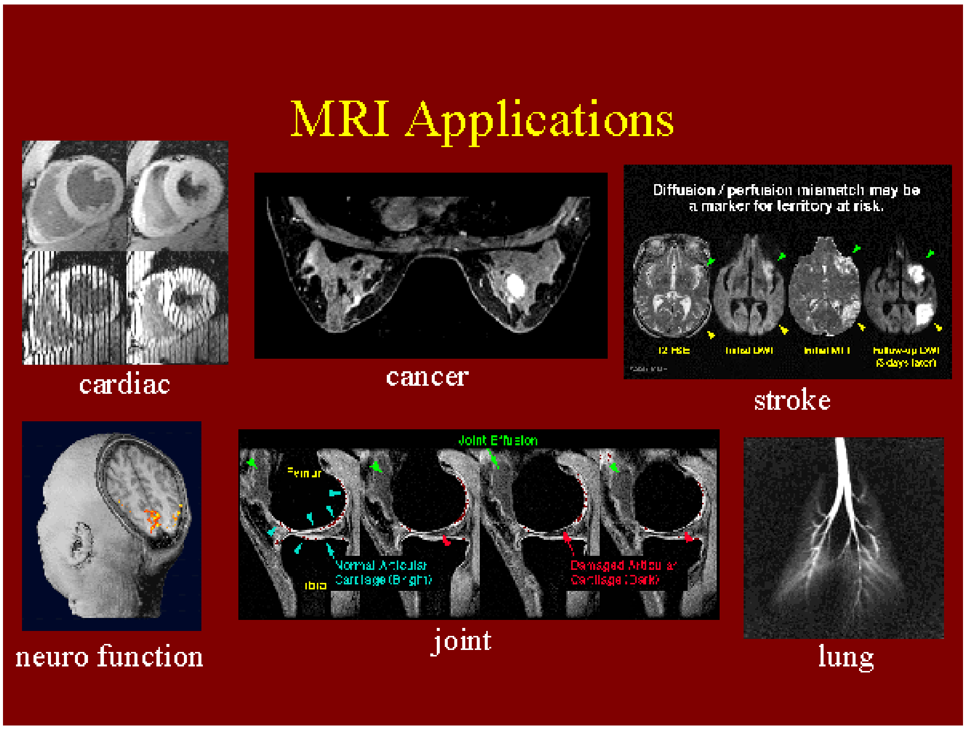
MRI Applications
cardiac
cancer
Diffusion / perfusion mismatch may be a marker for territory at risk.
stroke
Joint Effusion
neuro function
joint
lung

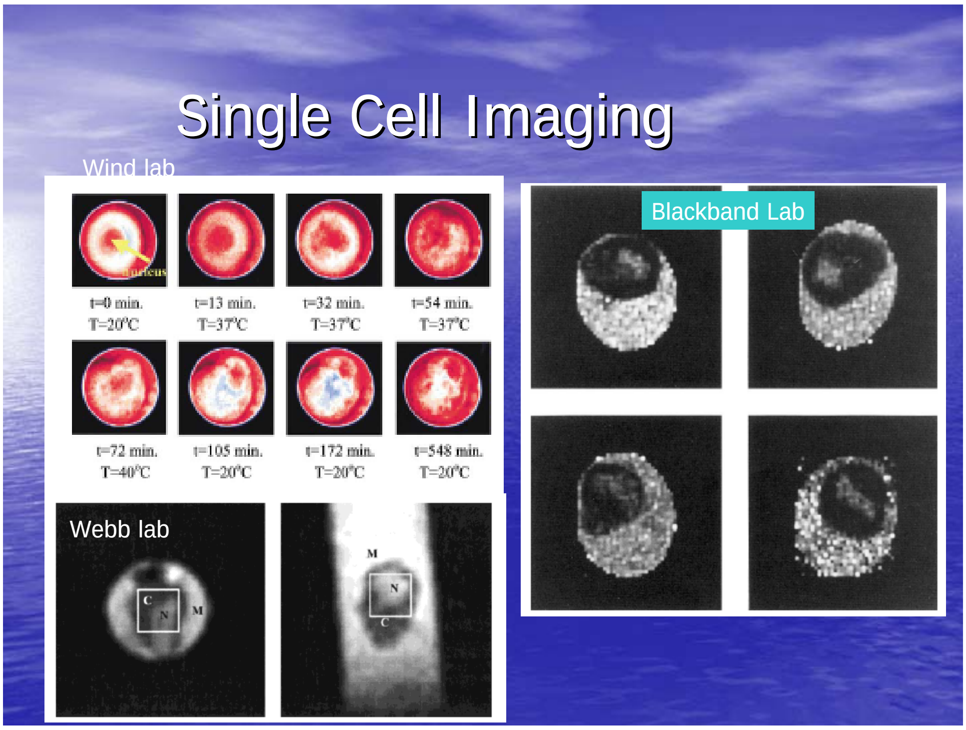
Single Cell Imaging
Wind lab
t=0 min. T=20°C
t=13 min. T=37°C
t=32 min. T=37°C
t=54 min. T=37°C
t=72 min. T=40°C
t=105 min. T=20°C
t=172 min. T=20°C
t=548 min. T=20°C
Webb lab
Blackband Lab

Imaging Gene Expression

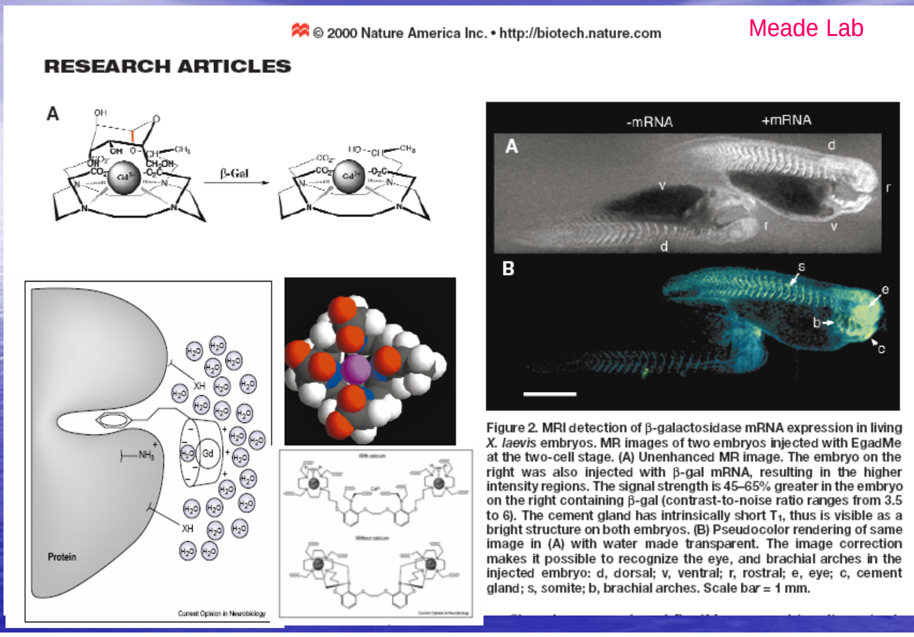

A-Z Applications of NMR Imaging

Xia Lab

- **A**uto industry: alternative fuel, new materials, ...
- **B**iologic science: growth activities, metabolic mapping, ...
- **C**hemistry: chemical shift selected imaging, ...
- **D**rug design: animal's response to new drugs, ...
- **E**ngineering : artificial joint, polymer flow, 'mouse', ...
- **F**ood industry: processing, packaging, storage, ...
- **G**eology: fossil characterization, ...
- **H**ealth science: osteoarthritis, stroke, cataracts, ...
- **I**mage process: pattern recognition, ...
- **J**-coupling: structure of molecules, ...
- **K**-space: new algorithm of image reconstruction, ...
- **L**ocalization: localized spectroscopy, zoom imaging, ...
- **M**athematics: maximum entropy post-processing, ...

A-Z Applications of Solid State NMR

A-Z Applications of NMR Imaging

Xia Lab

- **N**euroscience: neuron activity (functional MRI), …
- **O**il industry: oil/water separation in porous media, …
- **P**hysics: polymer dynamics, solid state physics, …
- **Q**uality control: on-line process control, …
- **R**heology: fluid flow in complex geometries, …
- **S**port health: sport injuries of knee and spinal cord, …
- **T**umor surgery: MR-guided brain surgery, …
- **U**ltrafast imaging: FLASH, EPI, snap-shot, …
- **V**eterinary: pet care and surgery, …
- **W**ood industry: forest research, lignin characterization, …
- **X**enon imaging: hyperpolarized 129Xe imaging, …
- **Y**ields in crop: transportation of water and nutrients, …
- **Z**oology: non-invasive anatomic structure, …

A-Z Applications of Solid State NMR

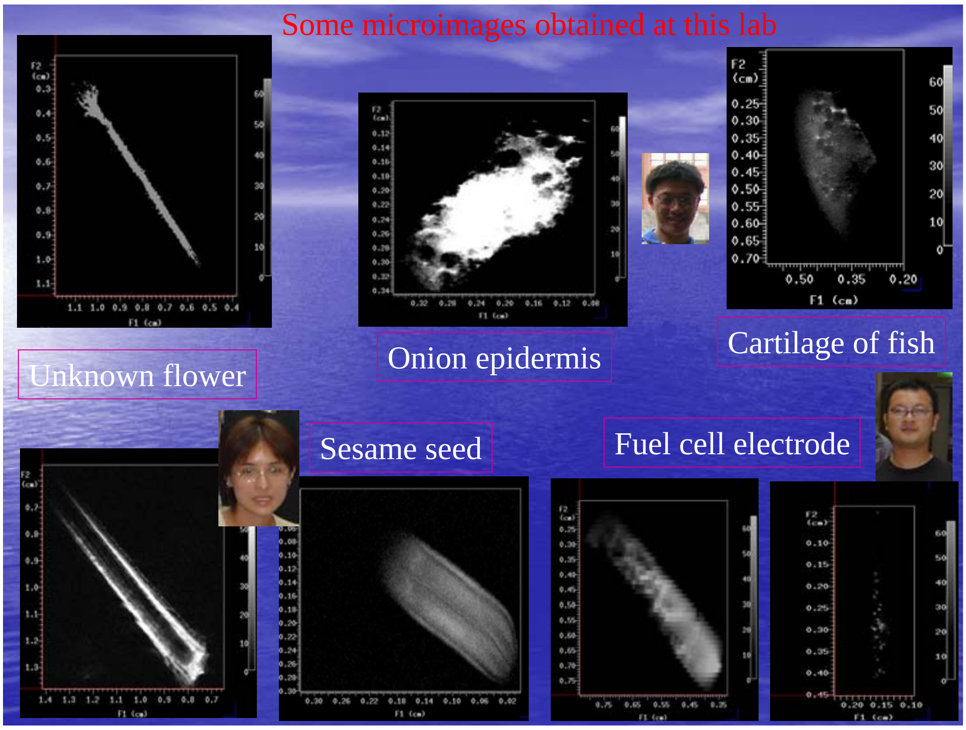

The Structure of DMFC (DMFC： Direct Methanol Fuel Cell).

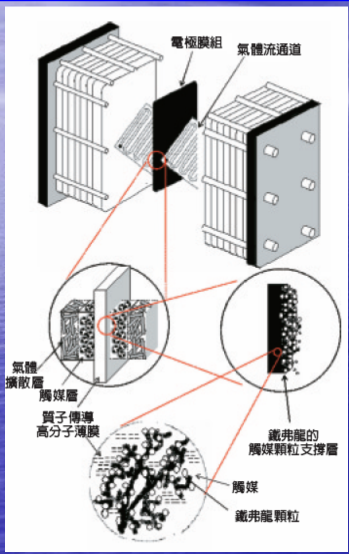

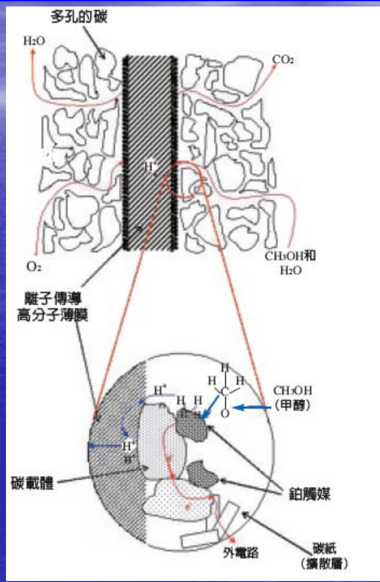

Images of Fuel Cell

Chu and Ding Labs

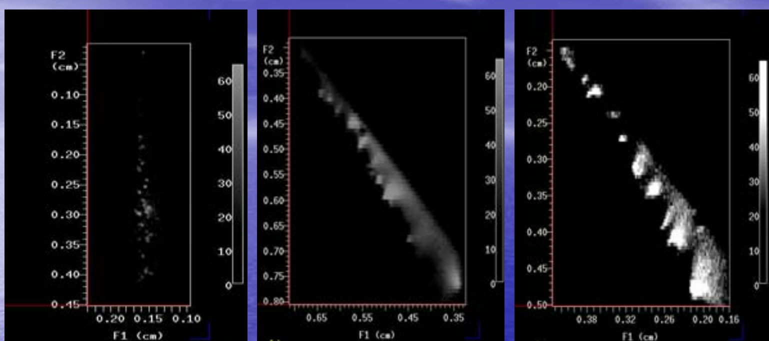

The microimages of a fuel cell material with spatial resolutions of 6 (left) , 15 (center) and 9 micrometers, the highest resolution achieved on this system.

JACS COMMUNICATIONS

Wasylishen Lab

Published on Web 08/28/2004

In Situ Observations of Water Production and Distribution in an Operating H_2/O_2 PEM Fuel Cell Assembly Using [1]H NMR Microscopy

Kirk W. Feindel, Logan P.-A. LaRocque, Dieter Starke, Steven H. Bergens,* and Roderick E. Wasylishen*

Department of Chemistry, University of Alberta, Edmonton, Alberta, Canada T6G 2G2

Received June 30, 2004; E-mail: steve.bergens@ualberta.ca; roderick.wasylishen@ualberta.ca

0.7 mm slice, pixel size = 164 × 234 μm,

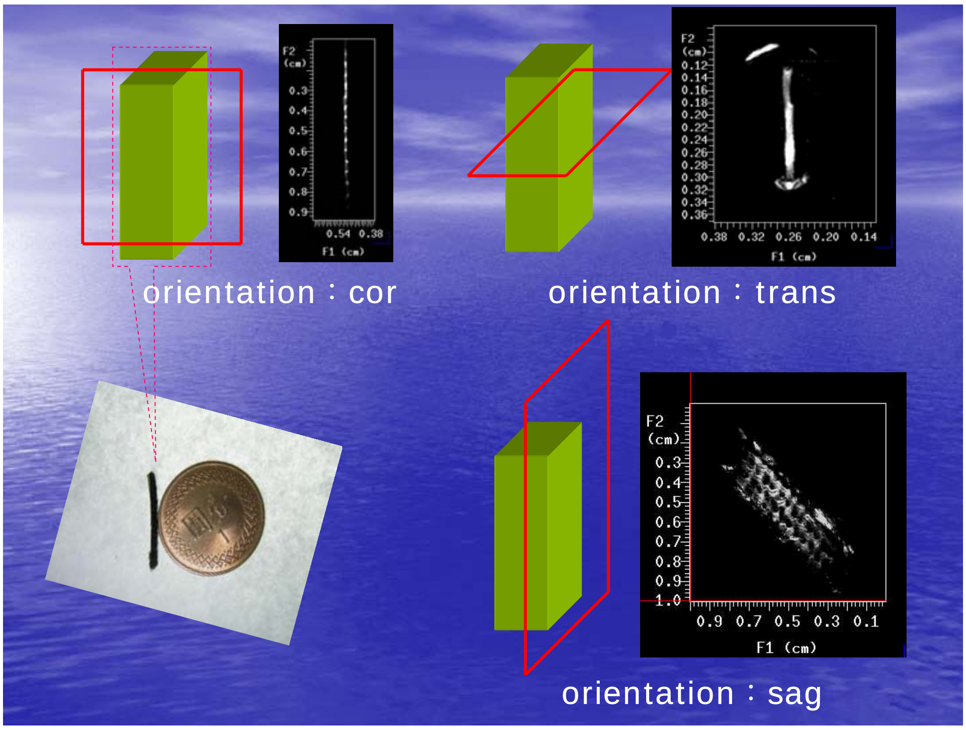
orientation：cor
orientation：trans
orientation：sag

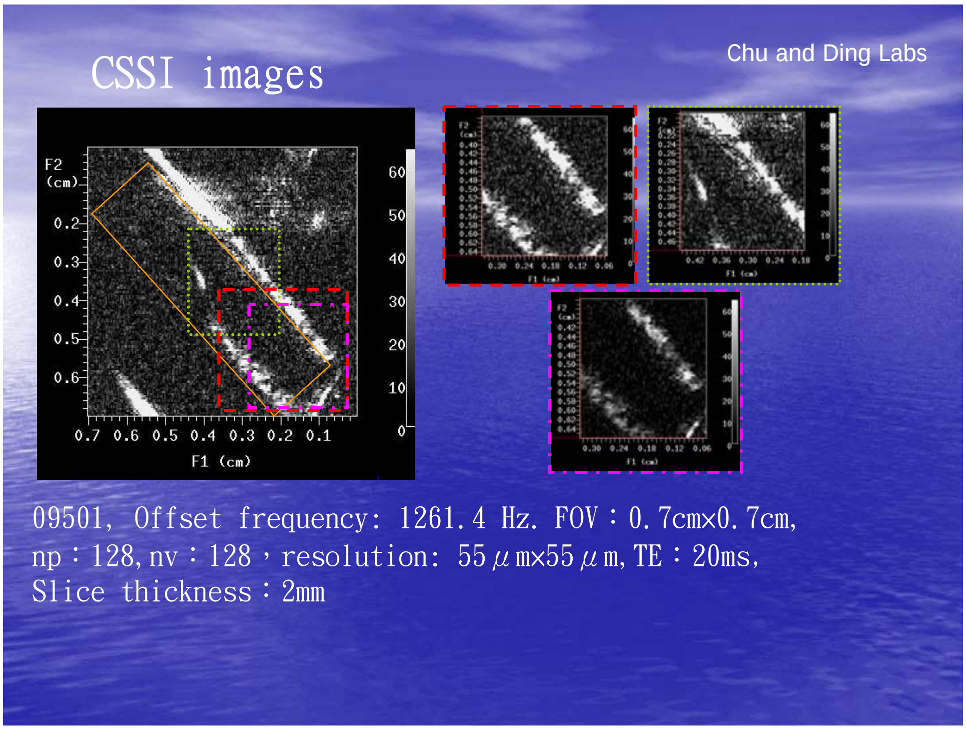
CSSI images
Chu and Ding Labs
09501, Offset frequency: 1261.4 Hz. FOV：0.7cmx0.7cm,
np：128,nv：128，resolution: 55μmx55μm,TE：20ms,
Slice thickness：2mm

CSSI images

Chu and Ding Labs

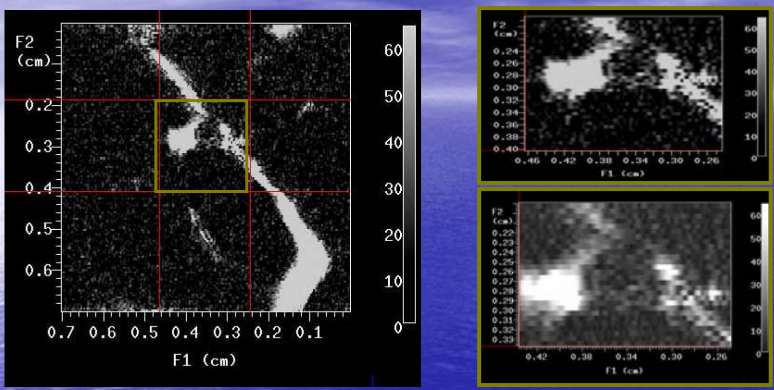

09501, Offset frequency: 1993 Hz. FOV：0.7cmx0.7cm,
np：128,nv：128，resolution: 55μmx55μm,TE：20ms,
Slice thickness：2mm

T_2 weighted images

Chu and Ding Labs

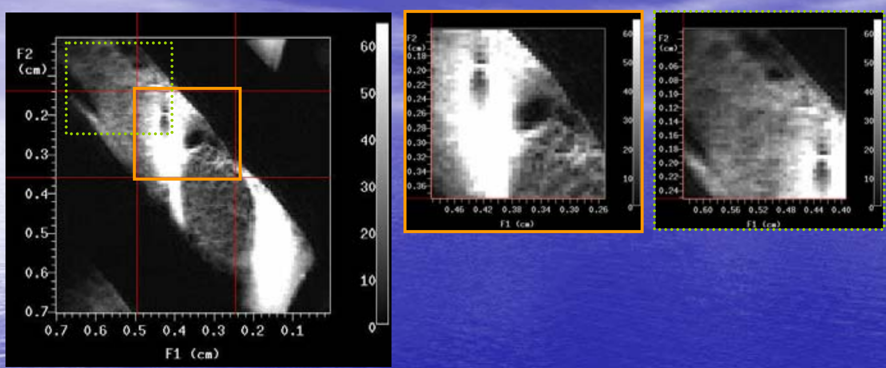

09501, SEMS,FOV：0.7cmx0.7cm,
np：128,nv：128，resolution: 55μmx55μm,TE：10ms,
Slice thickness：2mm.
Bright regions correspond to short T2. Porous regions correspond to where electrode cracks.

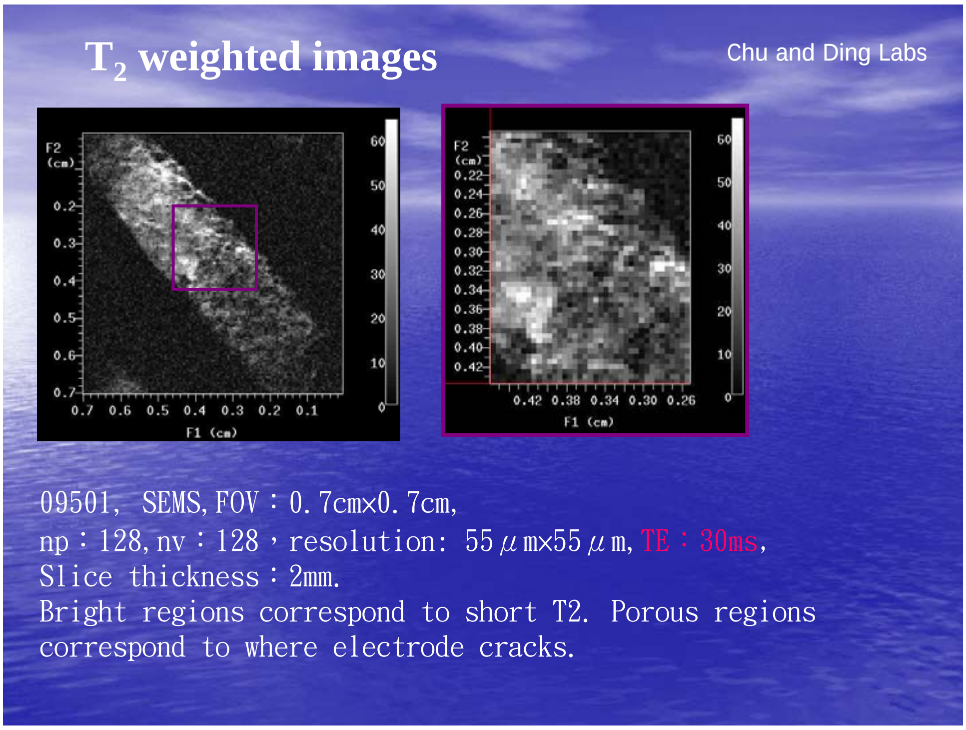
T2 weighted images
Chu and Ding Labs
F2 (cm)
F1 (cm)
09501, SEMS, FOV：0.7cmx0.7cm,
np：128, nv：128，resolution: 55μmx55μm, TE：30ms,
Slice thickness：2mm.
Bright regions correspond to short T2. Porous regions correspond to where electrode cracks.

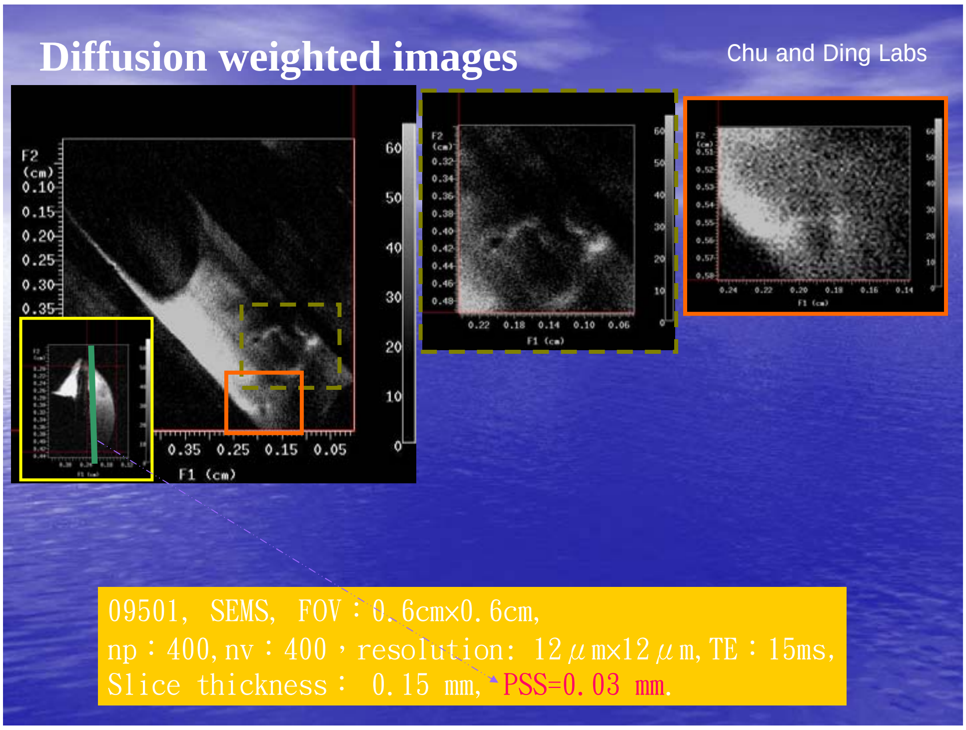
Diffusion weighted images
Chu and Ding Labs
F2 (cm)
F1 (cm)
09501, SEMS, FOV：0.6cmx0.6cm,
np：400, nv：400，resolution: 12μmx12μm, TE：15ms,
Slice thickness： 0.15 mm, PSS=0.03 mm.

Diffusion weighted images

Chu and Ding Labs

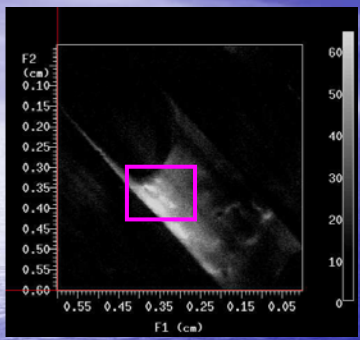

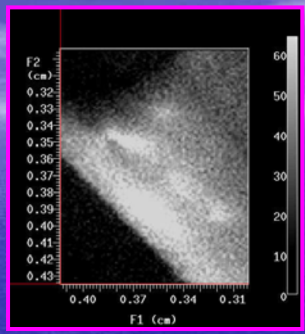

Same as the previous image.
09501, SEMS, FOV : 0.6cm×0.6cm,
np : 400, nv : 400, resolution: 12μm×12μm, TE : 15ms,
Slice thickness : 0.15 mm, PSS=0.03 mm.

Diffusion Tensor Imaging

Ding Lab

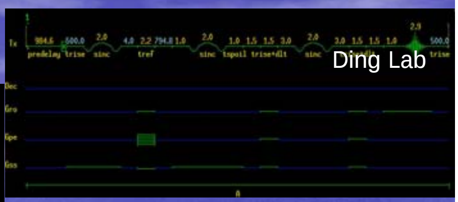

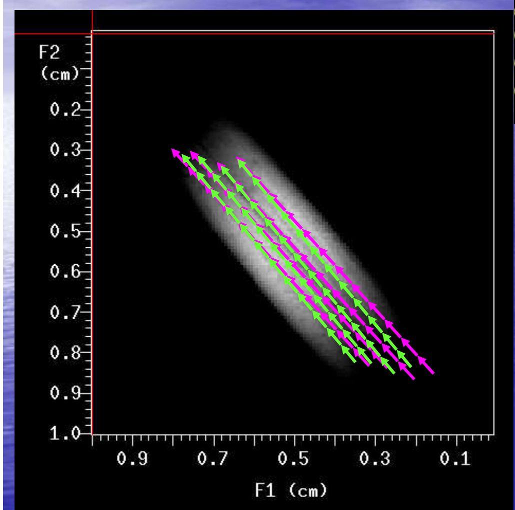

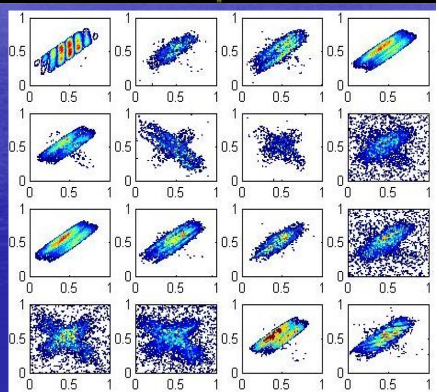

Diffusion field constructed by showing the z-axis of the diffusion tensor in the "moving" principal axis system.

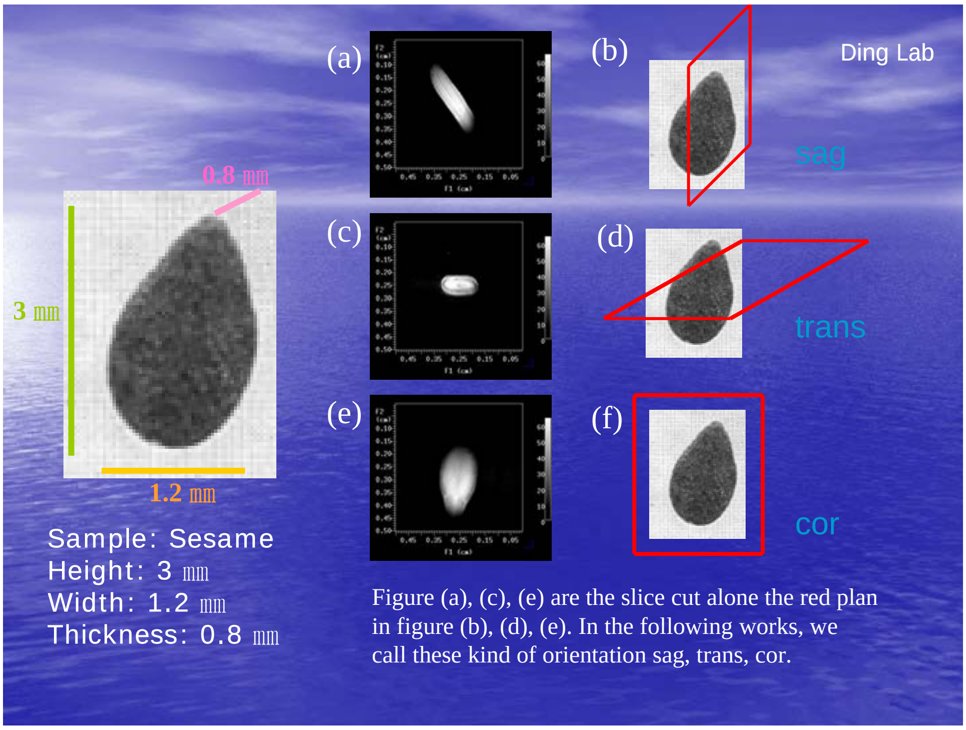
Ding Lab
(a)
(b)
sag
(c)
(d)
trans
(e)
(f)
cor
0.8 ㎜
3 ㎜
1.2 ㎜
Sample: Sesame
Height: 3 ㎜
Width: 1.2 ㎜
Thickness: 0.8 ㎜
Figure (a), (c), (e) are the slice cut alone the red plan in figure (b), (d), (e). In the following works, we call these kind of orientation sag, trans, cor.

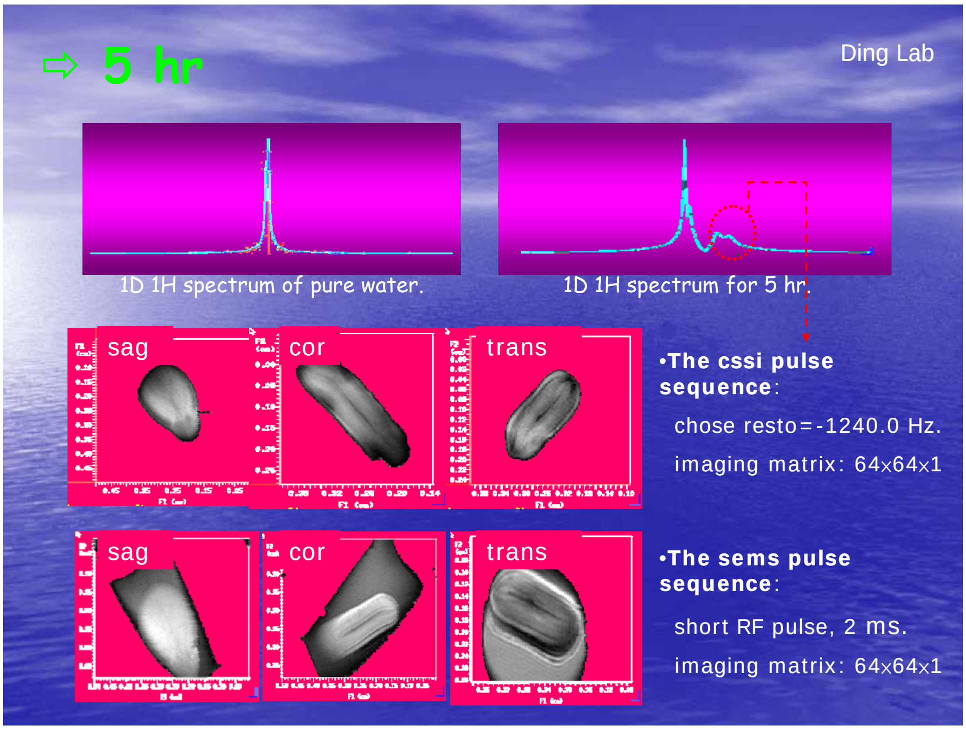
5 hr
Ding Lab
1D 1H spectrum of pure water.
1D 1H spectrum for 5 hr.
sag
cor
trans
•The cssi pulse sequence:
chose resto=-1240.0 Hz.
imaging matrix: 64x64x1
sag
cor
trans
•The sems pulse sequence:
short RF pulse, 2 ms.
imaging matrix: 64x64x1

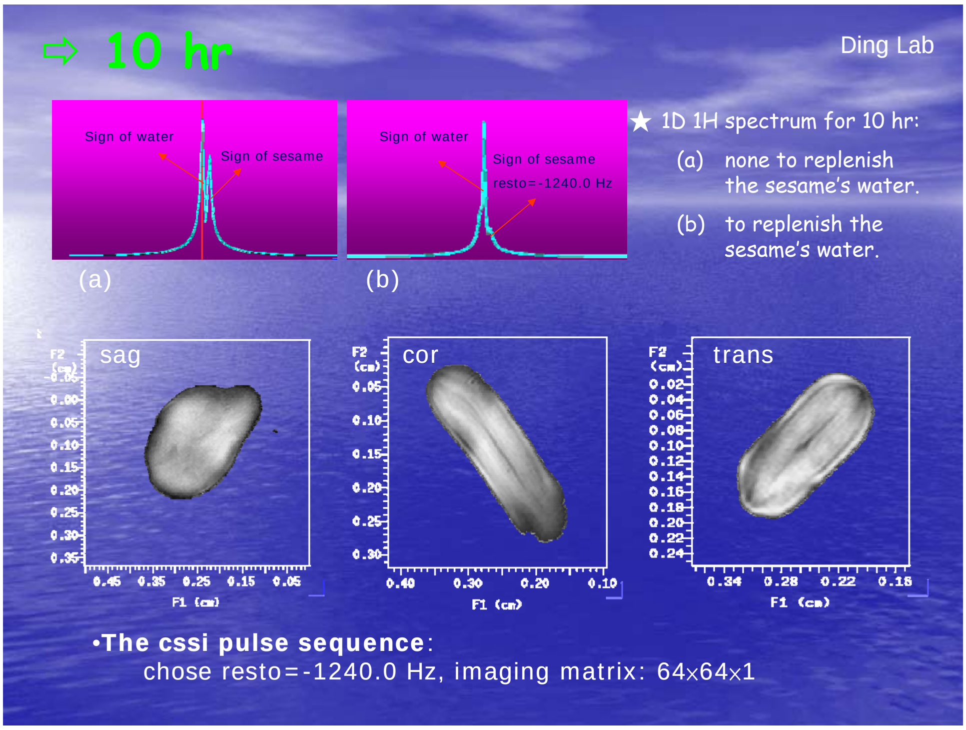

⇨ 10 hr
Ding Lab
Sign of water
Sign of sesame
Sign of water
Sign of sesame
resto=-1240.0 Hz
(a)
(b)
★ 1D 1H spectrum for 10 hr:
(a) none to replenish the sesame's water.
(b) to replenish the sesame's water.
sag
cor
trans
F1 (cm)
F2 (cm)
•The cssi pulse sequence:
chose resto=-1240.0 Hz, imaging matrix: 64x64x1

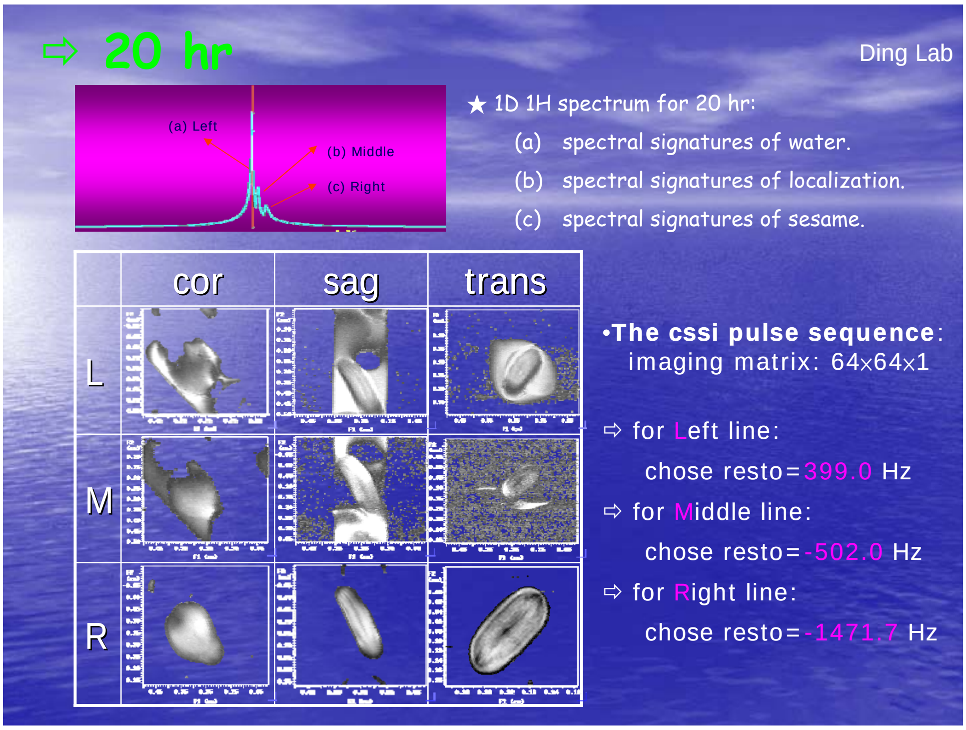

⇨ 20 hr
Ding Lab
(a) Left
(b) Middle
(c) Right
★ 1D 1H spectrum for 20 hr:
(a) spectral signatures of water.
(b) spectral signatures of localization.
(c) spectral signatures of sesame.
cor
sag
trans
L
M
R
•The cssi pulse sequence:
imaging matrix: 64x64x1
⇨ for Left line:
chose resto=399.0 Hz
⇨ for Middle line:
chose resto=-502.0 Hz
⇨ for Right line:
chose resto=-1471.7 Hz

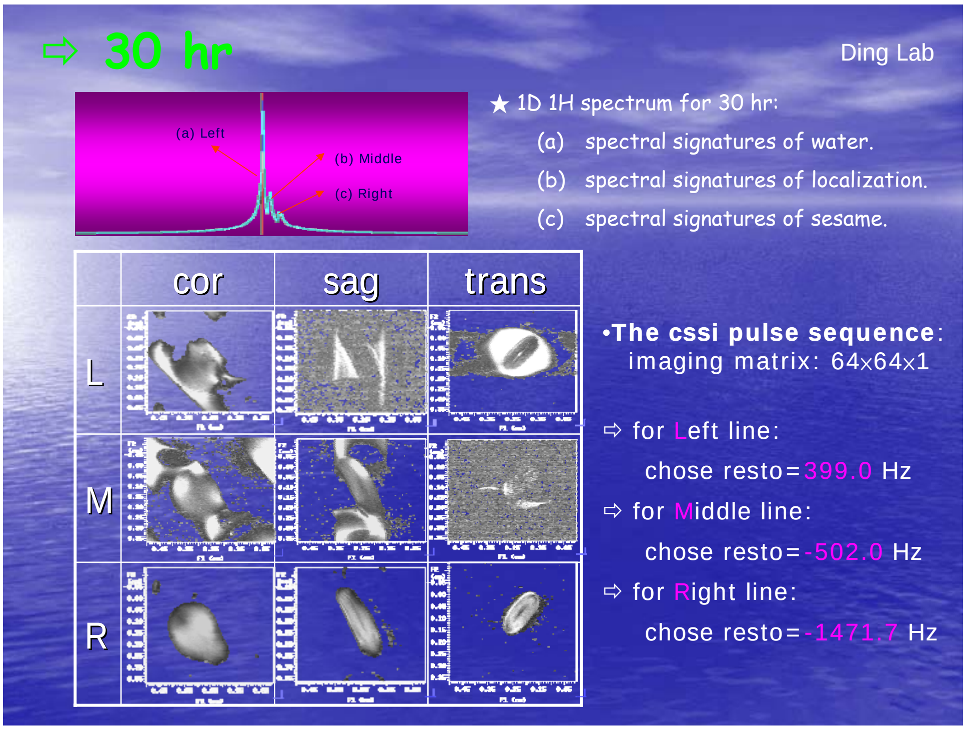
⇨ 30 hr
Ding Lab
(a) Left
(b) Middle
(c) Right
★ 1D 1H spectrum for 30 hr:
(a) spectral signatures of water.
(b) spectral signatures of localization.
(c) spectral signatures of sesame.
cor
sag
trans
L
M
R
•The cssi pulse sequence:
imaging matrix: 64x64x1
⇨ for Left line:
chose resto=399.0 Hz
⇨ for Middle line:
chose resto=-502.0 Hz
⇨ for Right line:
chose resto=-1471.7 Hz

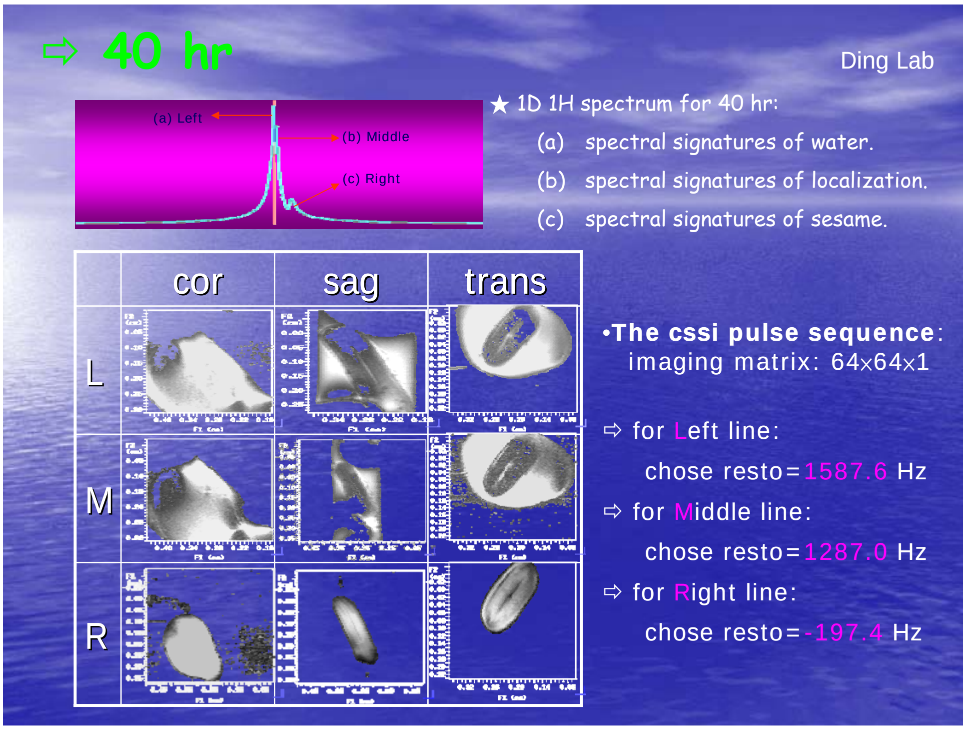
⇨ 40 hr
Ding Lab
(a) Left
(b) Middle
(c) Right
★ 1D 1H spectrum for 40 hr:
(a) spectral signatures of water.
(b) spectral signatures of localization.
(c) spectral signatures of sesame.
cor
sag
trans
L
M
R
•The cssi pulse sequence:
imaging matrix: 64x64x1
⇨ for Left line:
chose resto=1587.6 Hz
⇨ for Middle line:
chose resto=1287.0 Hz
⇨ for Right line:
chose resto=-197.4 Hz

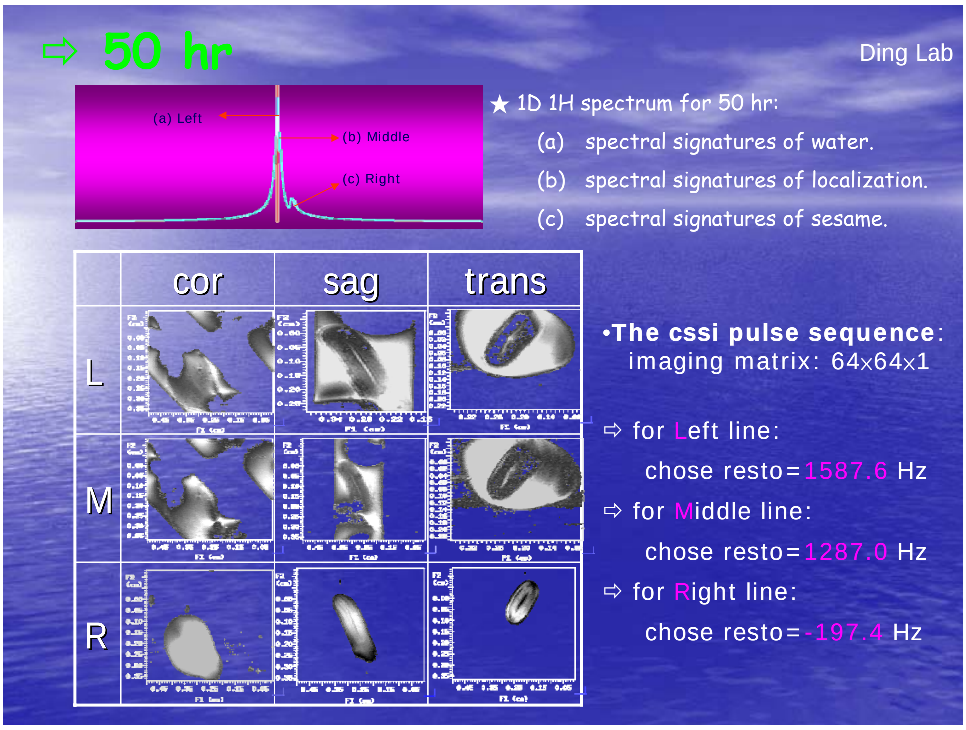
⇨ 50 hr
Ding Lab
(a) Left
(b) Middle
(c) Right
★ 1D 1H spectrum for 50 hr:
(a) spectral signatures of water.
(b) spectral signatures of localization.
(c) spectral signatures of sesame.
cor
sag
trans
L
M
R
•The cssi pulse sequence:
imaging matrix: 64x64x1
⇨ for Left line:
chose resto=1587.6 Hz
⇨ for Middle line:
chose resto=1287.0 Hz
⇨ for Right line:
chose resto=-197.4 Hz

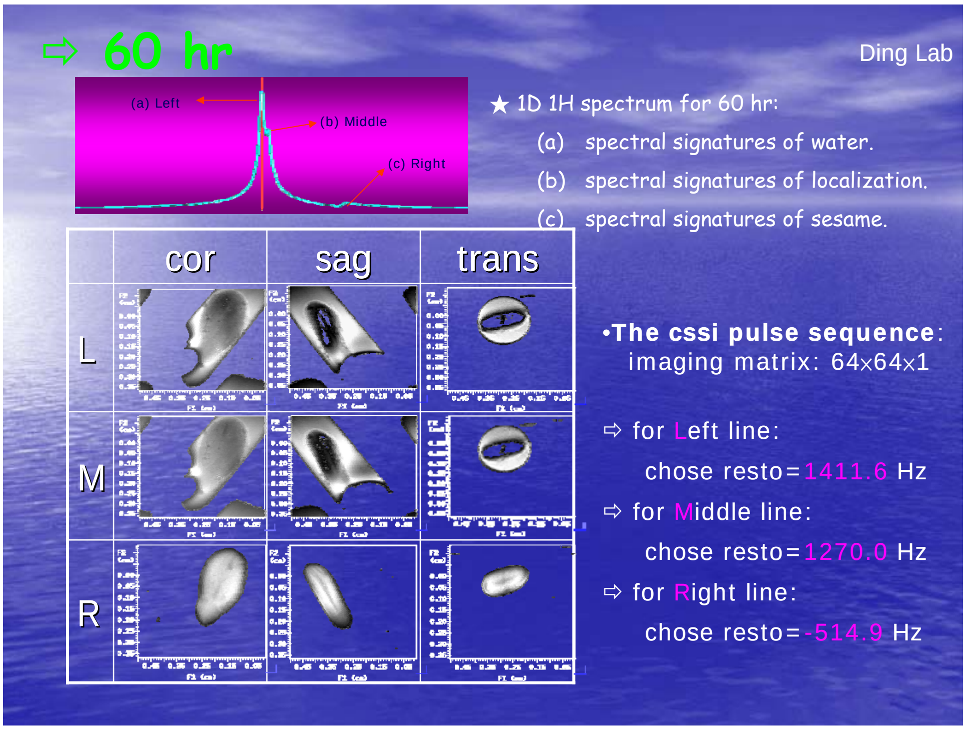
⇨ 60 hr
Ding Lab
(a) Left
(b) Middle
(c) Right
★ 1D 1H spectrum for 60 hr:
(a) spectral signatures of water.
(b) spectral signatures of localization.
(c) spectral signatures of sesame.
cor
sag
trans
L
M
R
•The cssi pulse sequence:
imaging matrix: 64x64x1
⇨ for Left line:
chose resto=1411.6 Hz
⇨ for Middle line:
chose resto=1270.0 Hz
⇨ for Right line:
chose resto=-514.9 Hz

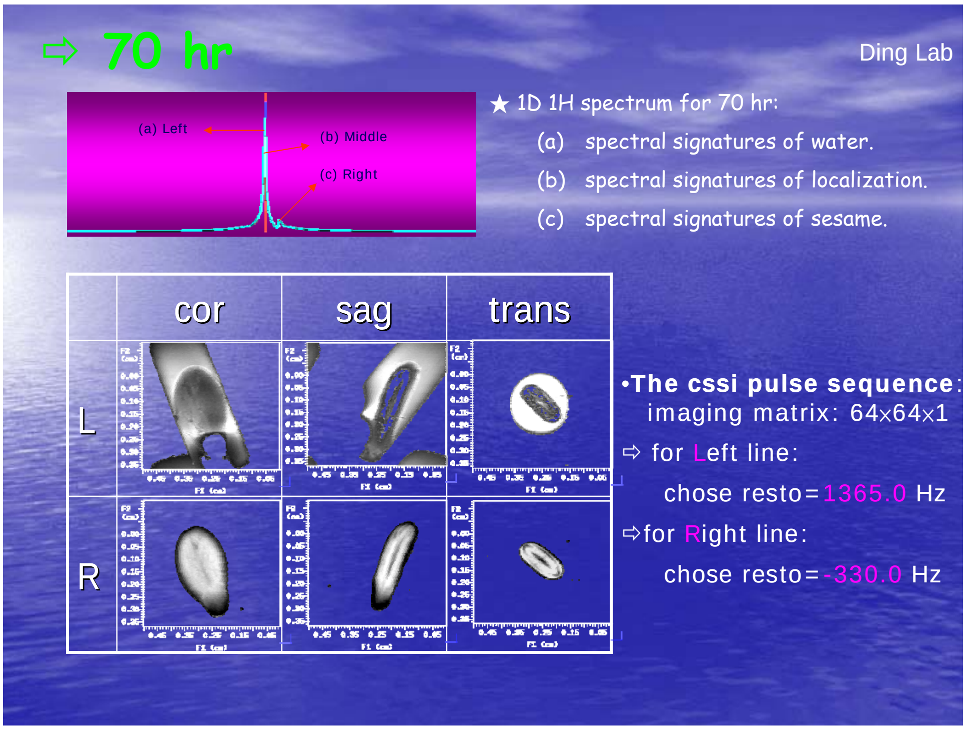

⇨ 70 hr
Ding Lab
(a) Left
(b) Middle
(c) Right
★ 1D 1H spectrum for 70 hr:
(a) spectral signatures of water.
(b) spectral signatures of localization.
(c) spectral signatures of sesame.
cor
sag
trans
L
R
•The cssi pulse sequence:
imaging matrix: 64x64x1
⇨ for Left line:
chose resto=1365.0 Hz
⇨for Right line:
chose resto=-330.0 Hz

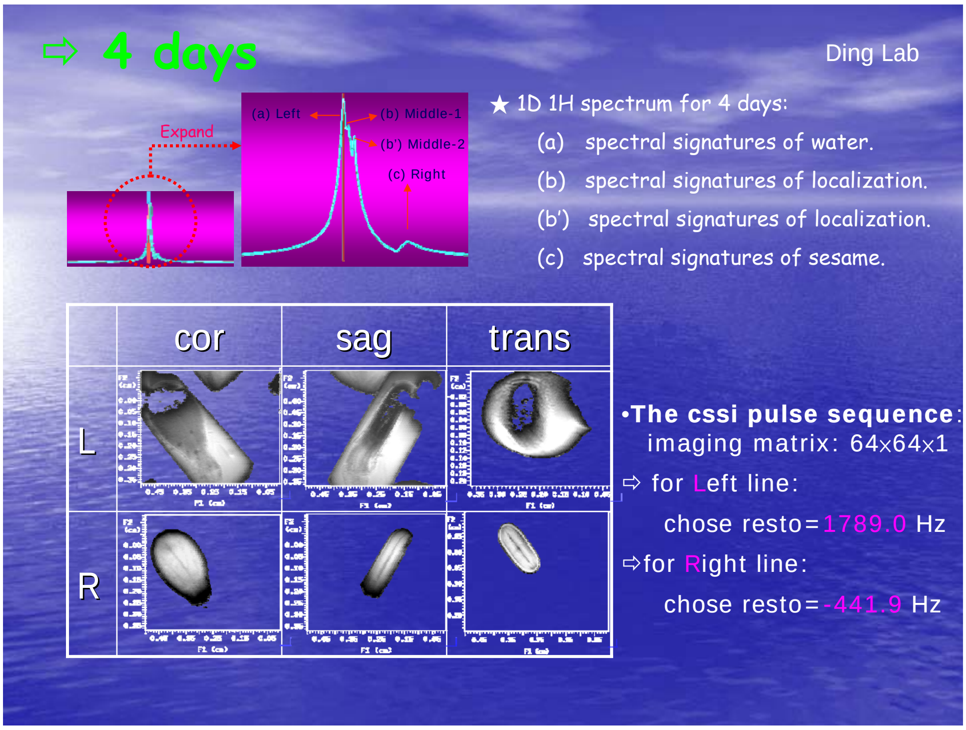

⇨ 4 days
Ding Lab
Expand
(a) Left
(b) Middle-1
(b') Middle-2
(c) Right
★ 1D 1H spectrum for 4 days:
(a) spectral signatures of water.
(b) spectral signatures of localization.
(b') spectral signatures of localization.
(c) spectral signatures of sesame.
cor
sag
trans
L
R
•The cssi pulse sequence:
imaging matrix: 64x64x1
⇨ for Left line:
chose resto=1789.0 Hz
⇨for Right line:
chose resto=-441.9 Hz

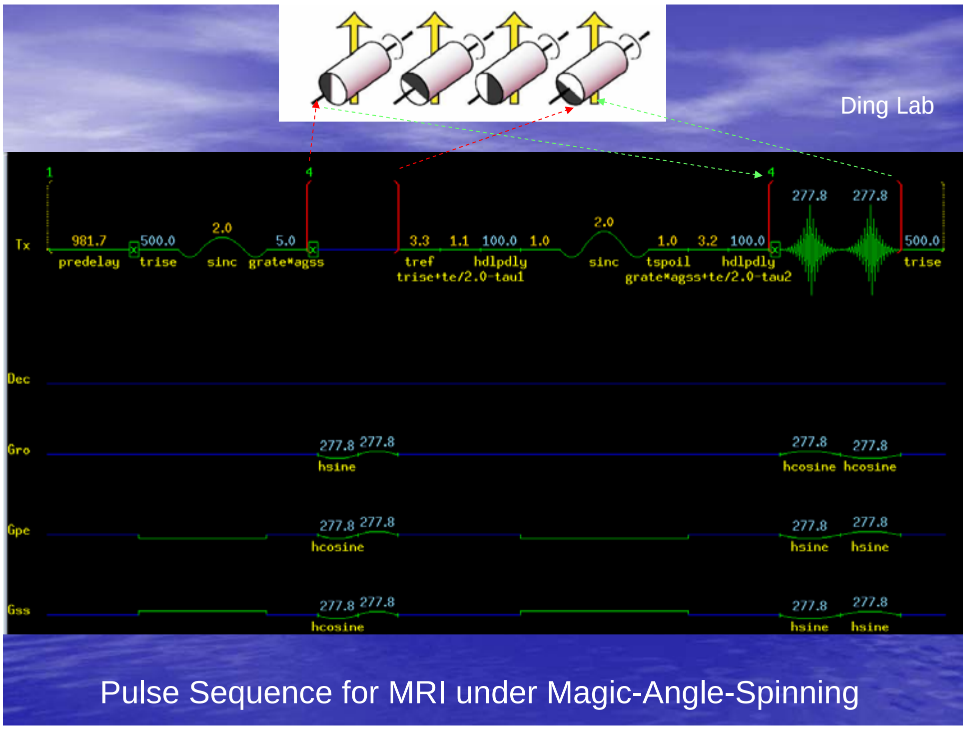
Ding Lab
Tx
Dec
Gro
Gpe
Gss
981.7 predelay
500.0 trise
2.0 sinc
5.0 grate*agss
3.3 tref
trise+te/2.0-tau1
1.1 100.0 hdlpdly
1.0
2.0 sinc
1.0 tspoil
3.2 100.0 hdlpdly
grate*agss+te/2.0-tau2
277.8 277.8
500.0 trise
hsine
hcosine
Pulse Sequence for MRI under Magic-Angle-Spinning

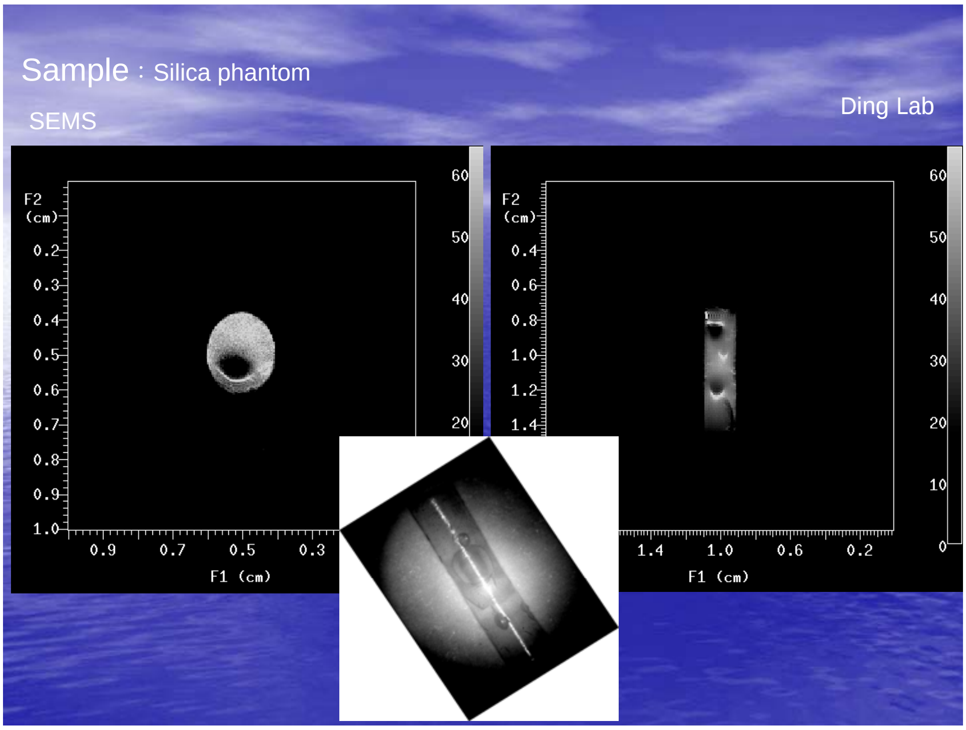
Sample : Silica phantom
SEMS
Ding Lab
F2 (cm)
F1 (cm)

Ding Lab

np : 256
nv : 128
FOV : 0.8 x 0.8 (㎝)
thk : 4 (㎜)
Spin rate :1800 Hz
Pulse sequence : Spiess
nc1 : 8
nc2 : 8
cge : 0.6

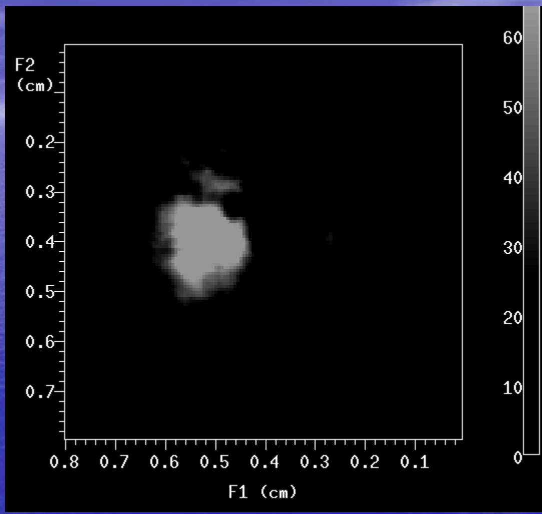

Concluding Remarks

- Solid state NMR has been a powerful methodology benefiting a large number of disciplines from physics, chemistry, materials science and biology to medicine and social sciences.
- Solid state NMR is still in fast development, driven by, in particular, advanced materials and biological systems. New pulse sequences keep emerging while old ones find new applications.
- Micro-imaging is relatively underdeveloped, numerous SSNMR pulse sequences are to be employed.
- VARIAN has played a crucial role and continues to be a major driving force.

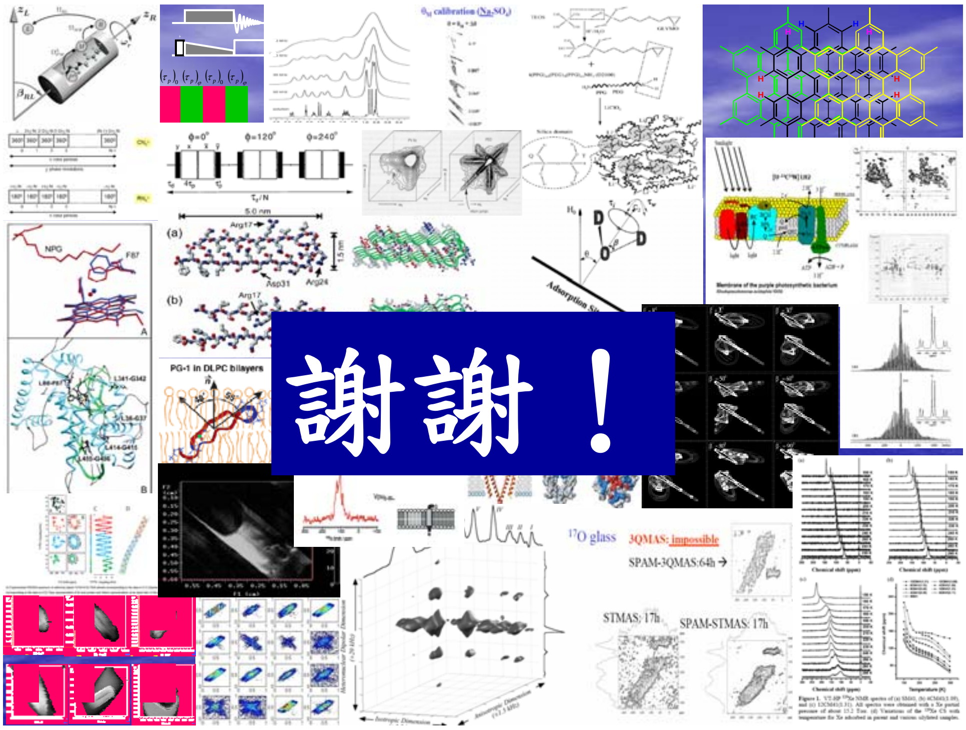
謝謝 ！
PG-1 in DLPC bilayers
^{17}O glass
3QMAS: impossible
SPAM-3QMAS:64h →
STMAS: 17h
SPAM-STMAS: 17h